

**DOCKET NO: A-93-02  
V-B-17**

**TECHNICAL SUPPORT DOCUMENT FOR SECTION 194.24:  
EPA's EVALUATION OF DOE'S ACTINIDE SOURCE TERM**

**U. S. ENVIRONMENTAL PROTECTION AGENCY  
Office of Radiation and Indoor Air  
Center for the Waste Isolation Pilot Plant  
401 M. Street, S. W.  
Washington, DC 20460**

**MAY 1998**

## Table of Contents

### Executive Summary and Report Outline

1.0	Introduction .....	1
2.0	Solubility and Actinide Oxidation States .....	2
3.0	Effects of the Magnesium Carbonates on Predicted Repository Conditions Due to MgO Backfill .....	6
4.0	FMT Modeling Results .....	12
5.0	Review of the Uranium(VI) Solubility .....	29
6.0	Actinide Solubility Uncertainty Range .....	34
7.0	Influence of Ligands and Complexants on Actinide Migration .....	37
8.0	Microbial Effects .....	60
9.0	Conclusions and Key Issues .....	71
10.0	References .....	73

## Executive Summary and Report Outline

This report discusses issues important to the modeling of the actinide source term in the WIPP performance assessment as presented in DOE's Compliance Certification Application (CCA) (A-93-02, II-G-1) and supplemental information provided by DOE since the submission of the CCA. The primary document reviewed was the SOTERM appendix to the CCA. Other relevant information obtained after the CCA was submitted from DOE and its contractors was also utilized during the review process. Such information was obtained through either earlier reports referenced in the CCA, new reports provided by DOE, and reports found in Sandia National Laboratory's WIPP Records Center. Examples of such information were DOE's responses to questions raised during the SOTERM review and corrections to errors which were occasionally detected.

40 CFR 194.24(b) states that both waste characteristics and waste components need to be analyzed and the results submitted as part of the compliance certification application. Those waste characteristics and components that affect releases need to be incorporated into performance assessment (194.32(a)). DOE has identified actinide solubility as a major characteristic of the waste that needs to be considered. Other examples that DOE included are, colloids, gas production, and physical properties. Waste components are those constituents of the waste which could influence the waste characteristics and thereby affect the performance of the disposal system. Examples provided include metals, cellulose, chelating agents, and water. In addition to radioactivity, DOE has identified four waste components requiring limits (Appendix WCL, Table WCL-1): ferrous metals, cellulose/plastics/rubbers (microbial substrates), free water, and nonferrous metals.

Issues addressed in this document include EPA's evaluation of: actinide solubility and oxidation states, the overall effect of magnesium oxide (MgO) backfill material on the actinide source term, FMT chemistry modeling results and assumptions, the U(VI) solubility model, the approach used to determine uncertainties in the actinide solubility results, the potential impact of ligands and humic complexants on actinide mobility, and possible microbial effects on actinide migration and gas generation.

Section 1 provides a perspective on discussion of the actinide source term and its contribution to radionuclide releases. Section 2 describes actinide solubility and oxidation states. Actinides can exist in oxidation states ranging from +3 to +6, depending on the specific actinide under consideration and prevailing redox conditions. After closure, the repository is expected to become anoxic relatively rapidly. The assumption of reducing conditions after closure is reasonable because of the interaction of the iron and brine. DOE presents the experimental and chemical reasoning for the determination of the specific oxidation states for each actinide expected to be predominant in the repository and identifies the expected oxidation states for thorium, uranium, neptunium, americium, curium, and plutonium.

Section 3 discusses the effects of magnesium carbonates on predicted repository conditions due to MgO backfill. DOE's determination of which magnesium carbonate mineral phase will dominate in the repository was investigated and EPA believes that metastable, hydrated magnesium carbonate phases (probably hydromagnesite) are more likely to be present than magnesite, as suggested by DOE in Appendix SOTERM. This is important because these hydrated phases can be

shown to change the actinide solubilities from that modeled in the CCA performance assessment (PA). The presence of the hydromagnesite acts to reduce the solubility while the short-lived nesquehonite phase increases actinide solubility. EPA believes that hydromagnesite will be the metastable hydrated magnesium carbonate phase and nesquehonite will be an intermediate phase. DOE has accepted that a hydrated magnesium carbonate phase will be the dominant alteration product of reactions between magnesium oxide backfill material and brines under expected repository conditions. As a result of this difference in the expected hydrated magnesium mineral phase, the EPA mandated performance assessment verification test used the recalculated actinide solubilities of the +III, +IV, and +V actinide oxidation states.

In section 4, the Fracture-Matrix Transport (FMT) geochemical model was reviewed and EPA determined that the thermodynamic model was appropriate for calculating the actinide solubilities of the +III, +IV, and +V actinide oxidation states. It was concluded that by following the methodologies documented in the CCA, the results provided in the CCA can be verified. This was determined after errors in the database were discovered, communicated to DOE, corrected by DOE, and the runs redone by EPA.

In contrast to the +III, +IV, and +V actinide oxidation states, the FMT thermodynamic database contains no data for uranium (+VI) so its solubility was estimated by an alternative method. This different approach was reviewed and discussed in Section 5. EPA believes that the evidence provided by DOE in the CCA and in supplemental information indicates that the CCA uranium (+VI) solubility values are adequate for use in the performance assessment.

In the CCA, DOE uses point estimates for the actinide solubility and has estimated an uncertainty range around the point estimates. The uncertainty range developed by DOE used data from 150 measurements of differences between measured and predicted concentrations to develop an uncertainty range that adequately captures actinide uncertainty. EPA's review of DOE's actinide solubility uncertainty range is discussed in Section 6.

Actinide mobility is a broad concept that includes all mechanisms which could lead to actinide migration in the aqueous phase. Complexation by ligands and humic materials could enhance the mobility of the actinides beyond that predicted by solubility experiments and related solubility modeling. Section 7 discusses EPA's review of the influence of ligands and complexants on actinide migration. EPA reviewed DOE's documentation and conducted independent calculations and concludes that while organic ligands will be present, they are not expected to have appreciable effect on actinide solubilities. A review of DOE's presentation of humic materials finds that there are uncertainties associated with DOE's characterization of humic materials, but EPA believes that humic materials are unlikely to cause excessive actinide mobility under WIPP conditions. EPA concludes that the incorporation of the humic materials is adequate for performance assessment.

Microbiological issues that are important to a review of the Actinide Source Term in DOE's WIPP CCA fall into two categories: the potential magnitude of microbially-mediated radionuclide mobilization and the potential for, and rate of, microbial gas generation. EPA finds that, even though there are uncertainties with DOE's characterization of microbial issues, DOE's approach in the performance assessment is reasonable relative to gas generation and actinide microbial binding parameters. EPA's review of microbial effects are discussed in Section 8.

Although there were uncertainties in DOE's characterization of some issues, EPA has concluded that, generally, the technical approach used by DOE for establishing the actinide source term was scientifically valid and adequate for use in the CCA performance assessment calculations.

## 1.0 Introduction

The modes of radionuclide releases at WIPP are 1) cuttings and cavings, 2) spillings, 3) direct brine release, and 4) long-term brine releases. Of these four release mechanisms, the actinide source term plays a role in long-term brine releases and direct brine release. Long-term brine releases occur through the Culebra dolomite and the Salado anhydrite markerbeds. Again, the driving forces in releases from this mechanism are pressure and saturation in the repository. Performance assessment results indicate that limited brine flows through the Salado markerbeds to the accessible environment; therefore, the actinide source term plays almost no role in this pathway. The actinide source term does affect the amount of actinides that reach the Culebra, however, the Culebra tends to filter the colloids so that they contribute little to transport in the Culebra. In addition, physical and chemical retardation are expected to occur and be highly effective in reducing transport of radionuclides through the Culebra. Direct brine releases are short-term releases that happen immediately after an intrusion event. Direct brine releases are controlled by the volume of brine released as well as the solubility. Direct brine releases require saturated repository conditions and high repository pressure (> 8 Megapascals). Many CCA realizations have conditions which are not saturated and which do not contribute to releases. Some low probability direct brine releases do occur that contribute to releases, although the releases do not come close to the radioactive waste disposal standard (see the Technical Support Document: Overview of Major Performance Assessment Issues, A-93-02, V-B-5).

This report discusses issues important to the modeling of the actinide source term in the WIPP performance assessment as presented in DOE's Compliance Certification Application (CCA) (A-93-02, II-G-1) and supplemental information provided by DOE since the submission of the CCA. The primary document reviewed was the SOTERM appendix to the CCA. Other relevant information obtained after the CCA was submitted from DOE and its contractors was also utilized during the review process. Such information was obtained through either earlier reports referenced in the CCA, new reports provided by DOE, and reports found in Sandia National Laboratory's WIPP Records Center. Examples of such information were DOE's responses to questions raised during the SOTERM review and corrections to errors which were occasionally detected.

In the comments on EPA's proposed rule, commenters raised concerns about the processes related to the magnesium oxide backfill. Many of the comments stated that nesquehonite would be the controlling form of the magnesium carbonate in the repository. In the CCA, DOE believed magnesite would be the dominant species of magnesium carbonate, but EPA's review identified that hydromagnesite would be the expected form. The use of the oxidation analogy also drew many comments. These issues and others are addressed in this document.

## 2.0 Solubility and Actinide Oxidation States

A conceptualization of the redox environment within the repository is important to predicting the solubilities of probable solids incorporating actinide species. Actinides can exist in oxidation states ranging from +3 to +6, depending on the specific actinide under consideration and prevailing redox conditions. After closure, the repository is expected to become anoxic relatively rapidly because of reactions between any available oxygen and iron metal and aerobic biodegradation of organic material (SOTERM 2.2.3). Both organic materials and iron metal are expected to be major components of the waste inventory. According to DOE (SOTERM 4.6) "each drum contains about 170 moles of iron in the container... The reaction rate of iron with the brine is very fast (Appendix PAR, Parameter 1). Therefore, as any brine moves into the repository it will react with the iron and establish a highly reducing environment." Additionally, the production of hydrogen by metal corrosion reactions is expected to contribute to creating reducing conditions in the repository. The assumption of reducing conditions after closure is reasonable because of the interaction of the iron and brine. Because of these reactions, oxidizing conditions are expected to last only a short while after closure. EPA therefore concurs with DOE that reducing conditions will prevail in the repository after closure.

The FMT model (A-93-02, II-G-3, Volume 6--FMT Quality Assurance Package), which was used by DOE to calculate solubilities of actinide solids, does not include representations of redox processes, hence actinides must be designated as being present entirely in a single oxidation state. This treatment requires that a conceptualization of the redox conditions in the repository be developed based on available information on the inventory and knowledge of relevant redox reactions. The FMT code is discussed in this document (section 4) and in the Technical Support Document for Section 194.23: Models and Computer Codes (A-93-02, V-B-6, Appendix A).

DOE presents the experimental and chemical reasoning for the determination of the specific oxidation states for each actinide expected to be predominant in the repository (Appendix SOTERM 4; CCA Reference 479). DOE provides a summary of the literature and a discussion of experimental results for thorium, uranium, neptunium, americium, curium, and plutonium. Consideration of actinide chemistry indicates that specific oxidation states can be expected under reducing conditions (CCA Chapter 6.4.3.5; Appendix SOTERM 4). Thorium will be present in the +4 oxidation state, which is the only one stable in the natural environment. Americium is expected to be present in primarily the +3 oxidation state. Higher oxidation of Am(+5) and Am(+6) can occur under oxidizing conditions, but are rapidly reduced by naturally occurring reductants and in brines at pH greater than 9 (Felmy et al. 1990). Plutonium is expected to be present as either Pu(+3) or Pu(+4). Higher oxidation states of Pu (i.e., +5 and +6) can exist under oxidizing conditions, but have been reported to be reduced rapidly by metallic iron (presentation by Ruth Weiner, Technical Exchange Meeting, SNL, June 27, 1996, in Bynum, 1996). Consequently, Pu(+5) and Pu(+6) are not expected to be dominant oxidation states for Pu under the reducing conditions of the repository and abundance of metallic iron. Uranium is expected to exist in both the +4 and +6 oxidation states; the predominance of which could not be ascertained based on current knowledge or uranium chemistry. The predominance of U(+4) requires extremely reducing conditions, that while possible for the repository, cannot be predicted with certainty. Consequently, for the PA, uranium is designated as being present as U(+4) in 50% of the runs and as U(+6) in the

other 50%. Likewise, neptunium is expected to be present as either Np(+4) and/or Np(+5), because the designation of a predominant form could not be made with complete certainty for the repository conditions.

Questions have been raised by stakeholders who believe that Pu(VI) will be present in the WIPP repository. In their description of the actinide source in Appendix SOTERM of the CCA, DOE determined that the any plutonium that might be dissolved in brines that infiltrate into the repository would exist as either Pu(III) or Pu(IV). As described in Appendix SOTERM of the CCA, Pu(V) and Pu(VI) are not expected to be important oxidation state for plutonium under the expected repository conditions. The issue is potentially important because the solids that incorporate Pu(V) and Pu(VI) tend to have higher solubilities than the solids that incorporate Pu(III) and Pu(IV).. Experiments by Reed et al. (1996) indicated that Pu(+6) is stable at a pH of 8 to 10 under oxidizing conditions and in the presence of high carbonate concentrations.

Stakeholders imply that the dominant oxidation for plutonium will be Pu(VI) based on an interpretation of some experimental work conducted by Reed et al. (1996) that were conducted at a pH of 8 to 10 under oxidizing conditions and in the presence of high carbonate concentrations. However, this interpretation of the Reed et al. (1996), as applied to the repository is incorrect because the experimental conditions used by Reed et al. (1996) are not representative of these expected for the repository. The repository inventory includes large quantities of reducing agents in the form of metallic iron, organic matter, and organic chemicals. These reductants are expected to rapidly consume any available oxygen present in the repository atmosphere shortly after closure, producing anaerobic or reducing conditions. Under reducing conditions, plutonium is expected to be stable in either the +3 or +4 oxidation states based on both experimental studies and chemical equilibrium calculations.

The experimental studies considered by DOE in developing their conceptual model for plutonium includes those conducted at SNL by R. Weiner and coworkers (Weiner, 1996). These studies clearly show that Pu(VI) is reduced by iron in both soluble (i.e.,  $\text{Fe}^{2+}$ ) and metallic (i.e., iron powder) forms. In experimental studies of the solubilities of plutonium and other actinides, iron powder is used to maintain reducing conditions, thereby preventing Pu(III) and Pu(IV) from oxidizing to Pu(V) and Pu(VI) (Felmy et al. 1989, p. 30; Rai and Ryan, 1985, p. 248). Other studies have shown that Pu(VI) and Pu(V) are reduced by humic acids even under the oxidizing conditions of seawater (Choppin, 1991, p. 113, 114). Humic acids and other organic acids are expected to be present in the repository from the degradation of cellulosic waste materials. These empirical observations show that Pu(VI) and Pu(V) will not persist in the presence of reductants, such as iron and organics, that will be present in the repository environment.

Also, it is important to note that the conceptual model that was developed to describe the actinide source term is based on conditions of chemical equilibrium. Under the reducing conditions that will be created by the presence of metallic iron, the stable oxidation states for plutonium are Pu(III) and/or Pu(IV). This conclusion is based on a comparison of the redox conditions (i.e., the Eh or pe) imposed by equilibrium between  $\text{Fe}^{2+}$  and  $\text{Fe}(\text{OH})_3(\text{s})$  and the Eh-pH conditions relevant to aqueous plutonium species (Brookins, 1988, p. 73-76, 144-145; Choppin, 1991, p. 110; Rai et al. 1980, p. 417). The  $\text{Fe}^{2+}/\text{Fe}(\text{OH})_3$  stability line in Eh-pH space intersects the Pu(III) and Pu(IV) fields, indicating these are the stable oxidation states for plutonium in the presence of iron. The redox conditions imposed by organic materials are lower than for the iron species (Scott and



Morgan, 1990, p. 371-374; Stumm and Morgan, 1996, p. 467-477), providing more information that leads to the conclusion that Pu(VI) will not persist under the expected repository conditions.

In consideration of the extensive empirical and theoretical information that indicates that Pu(III) and Pu(IV) are the stable oxidation states of dissolved plutonium under reducing conditions, the EPA concludes that it would be unreasonable to expect that the higher oxidation states of plutonium [i.e., Pu(V) and Pu(VI)] would persist in the repository environment. EPA agrees with DOE's approach of including Pu(III) and Pu(IV) as the predominant oxidation states for plutonium in actinide source term modeling and PA calculations.

The thermodynamic database for the FMT model contains information for three actinides oxidation states, i.e., Am(III), Th(IV), and Np(V). The solubilities predicted for the Th(IV) solids were used in the CCA also to represent soluble U(IV), Np(IV), and Pu(IV); an approach referred to in Appendix SOTERM as the oxidation state analogy. The oxidation state analogy is based on standard inorganic chemistry principles. In short, the actinide oxidation analogy means that actinides of the same oxidation state tend to have similar chemical properties under similar conditions. This generalization can be made because chemical reactions involving ionic species are related primarily to the charge densities of the reacting species (CCA, Appendix SOTERM). Actinides with the same oxidation state have the same core electronic structure (Silva and Nitsche, 1995, p. 379); hence have similar ionic radii and charge densities, which in turn leads to analogous chemical behavior in solubility and aqueous speciation reactions. Also, as stated by (Silva and Nitsche, 1995, p. 379): "Because of the similarities and the fact that actinide ions in the same oxidation state have essentially the same core structure, actinides ions in the same oxidation state will tend to have similar chemical properties". A similar phenomenon occurs for the lanthanide group elements (i.e., rare-earth elements of atomic numbers 57 through 71), which have the same core electronic structure for ionic species. (Silva and Nitsche, 1995, p. 379). In addition to the theoretical basis, DOE conducted experimental studies and analyses that confirmed the validity of the oxidation state analogy, and subsequently employed it in their representation of the solubilities of actinides (CCA, Appendix SOTERM).

This approach is reasonable in that it is recognized that actinides with the same oxidation state have similar chemical properties (Allard, 1981; Allard et al., 1980; Jensen, 1980). Also, ThO<sub>2</sub>(am), which was used to represent Th(+4), is generally expected to be more soluble than solid forms of U(+4), Np(+4), and Pu(+4), that might be expected to form under repository conditions, (Felmy et al. 1996; Novak and Moore, 1996; Novak et al. 1996a, Novak et al. 1996b), making it a conservative choice as the basis for the +4 actinide analogy.

The application of the actinide analogy to the +IV actinides is a good example of its appropriate application to the actinide source term. Besides the oxidation state analogy, another generalization that can be made is that there is an decreasing trend in the solubilities of actinide solid phases across the actinide series (DOE, 1998, p. 5). This generalization is based on the fact that ionic radii of the lanthanides and actinides decrease with increasing atomic number. With decreasing radii, the stabilities of actinide-oxide and actinide-hydroxide bonds are increased, leading to decreased solubility products, which is a direct indication of solubility, for similar compounds (DOE, 1998, p. 5). This effect is exemplified by the decrease in the solubility products of both hydrous actinide dioxides and crystalline actinide dioxides with increasing atomic number as shown by Rai et al. (1987, p.40). The data from Rai et al. (1987, p.40) show that the solubility

product for Th(IV) dioxides, which is the actinide with the lowest atomic number, is about 8 orders of magnitude greater than for U(IV) dioxides, about 9 orders of magnitude greater than for Np(IV) dioxides, and about 10 orders of magnitude greater than for Pu(IV) dioxides. These experiments confirm the validity of the actinide analogy for the +IV actinides in that Th(IV) solids are more soluble than U(IV), Np(IV), and Pu(IV) oxide solids. The data compiled by Rai et al. (1987, p.40) are most relevant to low ionic strength conditions. However, more recent experimental data from Rai et al. (1997, pp. 242-243,245) show that the actinide analogy for the order of solubilities of +IV actinides is also relevant to high ionic strength conditions expected for the WIPP. Rai et al. (1997, p. 239) indicate that the solubility products for ThO<sub>2</sub>(am) is about 8 orders of magnitude greater than for UO<sub>2</sub>(am) in concentrated NaCl and MgCl<sub>2</sub> solutions, consistent with the earlier data discussed above. Based on these established trends for the +IV actinides, DOE used the solubility of ThO<sub>2</sub>(am) to represent the concentrations of the other +IV actinides [i.e., U(IV), Np(IV), and Pu(IV)] under the expected repository conditions. The experimental evidence provided by Rai et al. (1997, p. 239) and Rai et al. (1987, p.40) clearly indicate that ThO<sub>2</sub>(am) is more soluble than the other +IV actinides as indicated by the solubility products determined for the various solids in the following table (Note: higher solubility products indicate higher solubilities for the same chemical conditions).

The FMT model contains no data for U(+6), hence, it was estimated by an alternative method. Table 2-1 lists the actinides and their expected oxidation states which were used in the CCA performance assessment calculations.

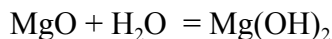
In summary, EPA concurred that repository conditions will likely be reducing, and consideration of two oxidation states for Pu (+3 and +4) and U (+6 and +4) is appropriate. The oxidation state analogy approach to assigning solubilities is a reasonable methodology for the purposes of PA, and EPA also agrees that chemical equilibrium models are appropriate for predicting the solubilities and subsequent concentrations of actinides in WIPP brines.

Table 2-1  
Predominant oxidation states for actinides expected to exist in the repository  
(from Table SOTERM-3)

<u>Actinide</u>	<u>Expected Oxidation State</u>
Thorium	+IV
Neptunium	+IV, +V
Americium	+III
Uranium	+IV, +VI
Plutonium	+III, +IV

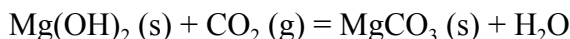
### 3.0 Effects of the Magnesium Carbonates on Predicted Repository Conditions Due to MgO Backfill

The use of an MgO backfill in the repository offers the potential for limiting the chemical conditions [i.e., pH and CO<sub>2</sub>(g) partial pressure] in the repository to a relatively narrow range, as described in Appendix SOTERM of the CCA. As brines infiltrate into the repository and encounter the MgO backfill, the initial reaction that is expected to occur is the hydration of the MgO to form brucite [Mg(OH)<sub>2</sub>]; a reaction that removes water from the brine in the solid phase, i.e.,

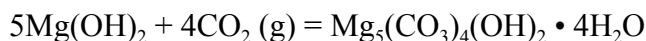


In the repository, the degradation of organic material will generate CO<sub>2</sub>(g). As the partial pressure of CO<sub>2</sub>(g) builds up, the Mg(OH)<sub>2</sub> thus formed will, in turn, react with the CO<sub>2</sub>(g) to form hydrated magnesium carbonates.

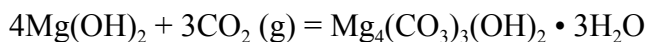
The calculations of chemical conditions for the repository described in the CCA are based on the assumption that the stable end-point assemblage that would result from MgO hydrolysis and carbonation would include brucite [Mg(OH)<sub>2</sub>(s)] and magnesite [MgCO<sub>3</sub>(s)], i.e.,



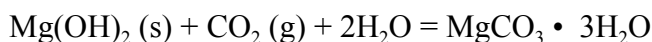
Magnesite is the phase that would be predicted to form based only on consideration of chemical equilibria. However, in aqueous systems Mg<sup>+2</sup> carbonation will initially result in the formation of hydrated carbonate phases, such as hydromagnesite, i.e.,



and



These two formulas for hydromagnesite have been reported in the literature (Novak, 1997). Another, hydrated magnesium carbonate called nesquehonite may also form, i.e.,



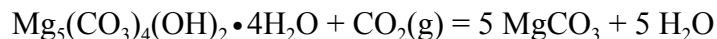
The nesquehonite formed by the above reaction is metastable according to experimental results (discussed below) and will convert relatively rapidly to hydromagnesite by reactions such as:



As is indicated by the reactions above, the direct formation of MgCO<sub>3</sub> from low-temperature solutions does not occur. Instead, hydrated magnesium carbonates form. The reason for the initial formation of the hydrated magnesium carbonates is related to the high energy of hydrolysis of the Mg<sup>2+</sup> ion, that makes it difficult to separate the waters of hydration from the ion during solid formation (Doner and Lynn, 1977; Lippman, 1973, p. 79, 83; Morse and Mackenzie 1990). Consequently, the Mg<sup>2+</sup> tends to form hydrated carbonates in which the Mg<sup>2+</sup> ions are still surrounded by their waters of hydration. In an analogous system, the Ca<sup>2+</sup> ion, which has a comparatively lower energy of hydrolysis than the Mg<sup>2+</sup> ion, precipitates directly from low-temperature carbonate solutions as CaCO<sub>3</sub>, i.e., calcite.

However, the hydrated magnesium carbonates (e.g., nesquehonite, hydromagnesite, other

forms) are not thermodynamically stable under the chemical conditions expected for the repository. Consequently, after some period of time, the hydrated magnesium carbonates (e.g., hydromagnesite) can be expected to dehydrate to produce magnesite [MgCO<sub>3</sub>], i.e.,



This dehydration step, if it proceeds to completion, would produce the thermodynamically stable assemblage of solids for the expected repository conditions, that is the assemblage with the lowest potential energy for the existent chemical conditions. The dehydration step is promoted by elevated temperatures and low activities of water, such as in brine solutions. This sequence of reactions has been observed in both experimental and natural systems, as discussed below, and is consistent with the chemical properties of the Mg<sup>2+</sup> ion and thermodynamic constraints.

Researchers at Sandia National Laboratory (SNL) conducted a series of scoping and crystal growth experiments to determine the types of magnesium carbonate solids that would precipitate from solution by reactions between brines and MgO backfill material. Overall, the results of these experimental studies are consistent with the above sequence of reactions, except that the final step of magnesite formation was not observed (see the SNL report of 4/23/97). In the SNL crystal growth experiments, an initial rapid hydrolysis of the MgO was observed and resulted in an increase in the solution pH. Next, a precipitate of nesquehonite was observed to form on the MgO pellets used in the experiments. The nesquehonite was characterized by acicular, blunt tipped, pseudo hexagonal crystals, and also identified by powder x-ray diffraction analyses.

The nesquehonite was then observed to alter to an intermediate solid with a formula of MgCO<sub>3</sub> • MgCl(OH) • 3H<sub>2</sub>O that is similar in composition to protohydromagnesite [(MgCO<sub>3</sub>)<sub>4</sub> • Mg(OH)<sub>2</sub> • 4H<sub>2</sub>O], being comprised of a mixture of magnesium carbonate, magnesium hydroxide, and waters of hydration. The magnesium hydroxide component is not present in nesquehonite. (There are a number of hydrated magnesium carbonates with stoichiometries intermediate between nesquehonite and hydromagnesite, including dypingite and protohydromagnesite, see Table 4-1 of the SNL report of 4/23/97.) The formation of the intermediate protohydromagnesite was clearly evident from a change in morphology of the acicular, blunt tipped, pseudo hexagonal crystals characteristic of the original nesquehonite to fine-grained flaky to platy crystals characteristic of protohydromagnesite (e.g., Davies and Bubela, 1973, p. 291). If the intermediate solid actually had a structure similar to nesquehonite, as some stakeholders have suggested, then it would not change its crystal morphology in response to continued reaction. The change in crystal morphology and resultant composition clearly indicates that the nesquehonite had altered to a protohydromagnesite-like phase, as they have been described by Davies and Bubela (1973, p. 291, 296). Although an absolutely pure precipitate of hydromagnesite was not identified in these crystal growth experiments, hydromagnesite was identified by x-ray diffraction analysis of products from scoping experiments (see page 7 of the SNL 4/23/97 report), indicating that is a primary reaction product.

In summary, the laboratory experiments described in Chemical Conditions Model: Results of the MgO Backfill Efficacy Investigation [A-93-02, II-A-39], the reaction of MgO with brines was observed to result in the rapid formation of nesquehonite, which then converted to

hydromagnesite within days. This result is consistent with previous studies that have shown that nesquehonite converts to hydromagnesite rapidly (Davies and Bubela, 1973). Consequently, nesquehonite cannot be expected to persist in the repository environment.

In the laboratory experiments conducted by SNL, the conversion of the hydromagnesite to magnesite was not observed. However, other laboratory results reported in the scientific literature and observations of natural occurrences of magnesium carbonate minerals and provide some qualitative information on rates of formation that are applicable to the repository environment.

Magnesite has also been observed to form relatively rapidly in solutions at temperatures greater than 60°C (Usdowski, 1994, p. 348-350; Sayles and Fife, 1973, p. 87,89). Elevated temperatures provide the requisite energy needed for dehydration of the  $Mg^{+2}$  ion and formation of the crystal structures of dolomite and magnesite. Davies and Bubela (1973, p. 290) observed the conversion of nesquehonite to protohydromagnesite and hydromagnesite in a matter of days to weeks in experiments conducted at 52°C and magnesium carbonate solutions. The conversion of the nesquehonite to protohydromagnesite under liquid-saturated conditions was typified by a change in morphology from needles to "curved-flake like masses" (Davies and Bubela, 1973, p. 296). In other experiments conducted at 10 to 28°C in NaCl brine solutions, Davies et al. (1977, p. 188,197) also observed the conversion of nesquehonite to protohydromagnesite, hydromagnesite, and huntite over a time period of about 10 months. Two of the important conclusions that can be reached from the work of Bubela and Davies (1973), that are consistent with the SNL experimental results, are: (1) nesquehonite alters to hydromagnesite through intermediate phases (e.g., protohydromagnesite and dypingite) (Bubela and Davies, 1973, p. 299) and (2) the rate of nesquehonite alteration is rapid, explaining why hydromagnesite is more commonly found in nature than nesquehonite (Bubela and Davies, 1973, p. 289).

In the SNL report of 4/23/97, the rate data for magnesite formation from Usdowski (1994, p. 348-350) for 60 and 180°C and Sayles and Fife (1973, p. 89) for 126°C were used to construct an Arrhenius plot of the effect of temperature on reaction rate. From this Arrhenius plot, the time required for magnesite formation can be estimated to take a few hundred years. This result is similar to those obtained by Usdowski (1994, p. 353) of a time of 600 years for the formation of dolomite at 30°C. The formation of magnesite might be expected to take a comparable amount of time. For instance, assemblages of magnesite plus dolomite have been inferred to form from alteration of aragonite plus hydromagnesite in certain arid, saline, near marine environments, such as sabkhas<sup>1</sup> (Usdowski, 1994, p. 356). Sabkhas bear some similarities in conditions to the repository, although they are probably hotter and wetter than what might be expected in the repository. Other field observations of carbonate mineral occurrences in recent sediments have been used to infer periods of a few hundred to a few thousand years for magnesite and dolomite formation (Graf et al. 1961, p. 221; Irion and Müller, 1968, p. 1309,1310).

The estimates of the rates of magnesium carbonate formation made from experimental results are generally consistent with observations of their occurrence in nature. Overall,

---

<sup>1</sup> Sabkha is a geological term referring to a sedimentation environment, located above the high-tide level (supratidal environment) in arid to semiarid coastal settings. It is characterized by evaporite deposits.

occurrences of nesquehonite are rare and found primarily in young deposits from precipitation from meteoric waters (Fischbeck and Muller, 1971, p. 87; Marschner, 1969, p. 1119). Natural occurrences of hydromagnesite and magnesite are more common and typically found in saline environments, such as the sabkhas, evaporites, and alkaline lake sediments (Irion and Muller, 1968, p. 1309, 1310; Renaut and Long, 1989, p. 239; Stamatakis, 1995, p. B179). A good example of the occurrence of magnesium carbonates is provided by Stamatakis (1995, p. B179-B181), who has described a Quaternary age deposit of hydromagnesite, magnesite, dolomite [ $\text{CaMg}(\text{CO}_3)_2$ ] and huntite [ $\text{Mg}_3\text{Ca}(\text{CO}_3)_4$ ] in northern Greece. The genetic model developed by Stamatakis (1995, p. B183, B184) indicates that the magnesium carbonates formed as magnesium-enriched spring waters, derived from sources in mafic and ultramafic rocks, flowed into an enclosed basin and evaporated. As the solutions became more saline and alkaline with evaporation, the magnesium carbonates were precipitated from solution. It is important to note, however, that while these precipitates included hydromagnesite and magnesite, nesquehonite was not found in the deposit. This finding is consistent with the short-lived nature of nesquehonite in saline environments as a result of its relatively rapid rate of conversion to hydromagnesite and magnesite. This field observation is consistent with the experimental results.

These estimates of conversion rate are confounded by the fact that deposits of hydromagnesite are found in some evaporite basins dated as late Quaternary in age (<23.7 million years) (Stamatakis, 1995), indicating that the hydromagnesite has persisted in a metastable state for a long period with only partial conversion to magnesite and other magnesium carbonates.

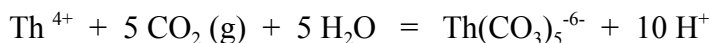
Based on the above discussion, the sequence of events resulting from brine infiltration and reaction with the MgO backfill in the repository may be conceptualized by the following reactions, in order:

1. Rapid reaction (hours to days) between the brine and MgO to produce brucite.
2. Rapid carbonation (hours to days) of the brucite to produce nesquehonite and possibly hydromagnesite.
3. Rapid conversion (days to weeks) of the nesquehonite to hydromagnesite.
4. Slow conversion (hundreds to thousands of years) of the hydromagnesite to magnesite.

The available rate data indicate that some portion, perhaps all, of the hydromagnesite will be converted to magnesite over the 10,000-year period for repository performance. The exact time required for complete conversion has not been established for all chemical conditions. However, the available laboratory and field data clearly indicate that magnesite formation takes from few hundred to, perhaps, a few thousand years. Thus, the early repository conditions can be best represented by the equilibrium between brucite and hydromagnesite. These conditions will eventually evolve to equilibrium between brucite and magnesite. In fact, the Salado Formation contains magnesite in its mineral assemblage, hence its brine is saturated with respect to magnesite solubility (Novak et al. 1996), indicating that conditions conducive to magnesite formation from reactions between brine and the MgO backfill are already present in the repository surroundings. This overall conceptualization is also consistent with the thermodynamic approach used to model the actinide source term, in that solution conditions would be expected to be controlled by the metastable hydromagnesite until it is completely converted to magnesite.

This discussion on the type of magnesium carbonate solid liable to form under the repository conditions may seem academic but is important because of the potential effect on the solution conditions and consequent predictions of actinide solid solubilities. For example, the equilibrium between brucite and nesquehonite would be predicted to buffer the CO<sub>2</sub>(g) partial pressure at 10<sup>-3.8</sup> bars in the Salado Brine (Table 3-1). In comparison, equilibrium for reactions between brucite and the two types of hydromagnesite considered in geochemical modeling calculations yield CO<sub>2</sub>(g) partial pressures of 10<sup>-5.39</sup> to 10<sup>-5.50</sup> atm for the SPC brine. Equilibrium between brucite and magnesite yields a CO<sub>2</sub>(g) partial pressures of 10<sup>-6.92</sup> atm for the SPC brine (see Table 4-8). Hydromagnesite formation produces an intermediate CO<sub>2</sub>(g) partial pressure. Slight differences in pH also occur, depending on the magnesium carbonate considered (Table 4-1). The form of the hydromagnesite, whether Mg<sub>5</sub>(CO<sub>3</sub>)<sub>4</sub>(OH)<sub>2</sub>·4H<sub>2</sub>O or Mg<sub>4</sub>(CO<sub>3</sub>)<sub>3</sub>(OH)<sub>2</sub>·3H<sub>2</sub>O, does not appear to have a major effect on the predicted solution conditions (Table 4-1), hence either may be representative. A similar pattern of results was obtained for the Castile brine. These calculation results show that the partial pressure for CO<sub>2</sub>(g) would be expected to be greatest the case of nesquehonite equilibrium, lowest for magnesite equilibrium, with hydromagnesite at intermediate levels.

For the different CO<sub>2</sub>(g) partial pressures, different solubilities of the actinide solids are obtained in equilibrium modeling calculations. This different solubilities are caused by different levels of formation of aqueous actinide-carbonate complexes by reactions, such as



In general, higher CO<sub>2</sub>(g) partial pressures lead to higher solubilities of actinide solids, depending on the pH and the concentrations of other complexants, because of the formation of carbonate complexes, such as Th(CO<sub>3</sub>)<sub>5</sub><sup>-6</sup>, shown in the above reaction. As a result, the concentrations of actinides calculated for the solubilities of various actinide solids for the elevated CO<sub>2</sub>(g) conditions of nesquehonite equilibrium are greater than the actinide concentrations calculated for hydromagnesite and magnesite equilibrium. Thus, the determination of the magnesium carbonate phase expected under the repository conditions has a direct effect on the actinide source term. The experimental work by Sandia National Laboratories (SNL) [A-93-02, II-A-39] on magnesium carbonate formation has provided valuable information that is relevant to predicting chemical conditions for the repository environment.

Table 3-1. Effects of different magnesium carbonate equilibria with brucite on solution conditions predicted by the FMT model (version 2.2 of FMT, updated version created by SNL in April, 1997, after the CCA).

	SPC Brine (Salado)				ERDA6 Brine (Castile)	
	Hydromagnesite (5424)a	Hydromagnesite (4323)b	Nesquehonite c	Magnesite d	Hydromagnesite (5424)a	Hydromagnesite (4323)b
pH	8.47	8.69	8.69	8.63	9.24	9.24
pmH	9.13	9.37	9.36	9.31	9.90	9.89
log[CO <sub>2</sub> (g)]	-5.31	-5.39	-3.84	-6.89	-5.50	-5.39

- a -  $Mg_5(CO_3)_4(OH)_2 \cdot 4H_2O$
- b -  $Mg_4(CO_3)_3(OH)_2 \cdot 3H_2O$
- c -  $MgCO_3 \cdot 3H_2O$
- d -  $MgCO_3$



## 4.0 FMT Modeling Results

Models and computer codes used in the CCA are required by 40 CFR 194.23(a) to be documented. One method of evaluating the utility of a solubility computer code, including its documentation, is to conduct independent executions of the codes using DOE's database and compare the results to the results obtained by DOE. Such independent runs were undertaken and are discussed below. The purpose of the runs was to verify for EPA that the results obtained were consistent with those submitted to EPA by DOE in their CCA and associated appendices.

An integral component of the actinide source term in the CCA is the FMT (Fracture-Matrix Transport) geochemical model (Babb, 1995; Novak et al. 1996a), which is used to calculate actinide concentrations in WIPP brines based on aqueous speciation and solubility equilibria for the conditions expected in the presence of the MgO backfill. One of the objectives of this report was to reproduce the FMT model calculations following the procedures outlined by Novak et al. (1996a) and (Novak and Moore, 1996).

Actinides can exist in oxidation states ranging from +3 to +6, depending on the specific actinide under consideration and prevailing redox conditions. The FMT model does not include representations of redox processes, hence actinides must be designated as being present entirely in a single oxidation state. The following oxidation states can be expected under reducing conditions (CCA Chapter 6.4.3.5; Appendix SOTERM 4): Thorium will be present in the +4 oxidation state. Americium and curium are expected to be present in the +3 oxidation state. Plutonium is expected to be present as either Pu(+3) or Pu(+4). Uranium is expected to exist in both the +4 and +6 oxidation states; the predominance of which could not be ascertained based on current knowledge or uranium chemistry. Consequently, for the PA, uranium is designated as being present as U(+4) in 50% of the runs and as U(+6) in the other 50%. Likewise, neptunium is expected to be present as either Np(+4) and/or Np(+5), because the designation of a predominant form could be made with complete certainty for the repository conditions.

The thermodynamic database for the FMT model contains information for three actinides oxidation states, i.e., Am(III), Th(IV), and Np(V). The solubilities predicted for the Th(IV) solids were used in the CCA also to represent soluble U(IV), Np(IV), and Pu(IV), an approach referred to in Appendix SOTERM as the oxidation state analogy. This approach is reasonable in that it is recognized that actinides with the same oxidation state have similar chemical properties (Allard, 1981; Allard et. al., 1980; Jensen, 1980).

Also, ThO<sub>2</sub>(am), which was used to represent Th(+4), is generally expected to be more soluble than solid forms of U(+4), Np(+4), and Pu(+4), that might be expected to form under repository conditions (Felmy et al. 1996; Novak and Moore, 1996; Novak et al. 1996a, Novak et al. 1996b), making it a conservative choice as the basis for the +4 actinide analogy. The FMT model contains no data for U(+6), hence it was estimated by an alternative method (see Section 5 of this report).

The FMT verification runs were initiated during a visit to Sandia National Laboratory on Jan. 20-23, 1997, for details of the review see Appendix A of the Technical Support Document to Section 194.23: Models and Computer Codes (A-93-02, V-B-6). The initial runs focused on verifying the results documented in the CCA for predicted actinide concentrations. The version of

the FMT model (version 2.0) and associated database used for these CCA runs was found to calculate incorrect results for some conditions as discussed below. Consequently, on April 24, 1997, an updated version of the FMT model (version 2.2) and associated databases was made available for use by Sandia National Laboratory (Novak, 1997). Based on this chronology, the results of the FMT verification results are discussed below in two sections, one for the version 2.0 and associated thermodynamic database used for the CCA and one for the updated version 2.2 and associated thermodynamic databases (Novak, 1997). The model versions and associated databases used for the different sets of FMT runs are listed in Table 4-1.

#### 4.1 Verification Results for the CCA

The documentation used to review the FMT computer code is found in docket A-93-02, II-G-3, Volume 6. This information consist of the FMT User's Manual, the Implementation Document, the Requirements document and Verification and Validation Plan, and the Validation Document. These documents discuss the theoretical background of the computer code, the nine functional requirements for the FMT computer code, the nine verification and validation test to be done, and the results of the test performed. See A-93-02, V-B-6, Appendix A for a complete discussion of the FMT computer code review.

It is important to note that during EPA's January 1997 visit to Sandia National Laboratory to use the FMT model on the Sandia National Laboratory computer system, it was not clear which thermodynamic database had been used for the CCA calculations. The database has been continuously revised and improved since the CCA was issued as new data have become available. After discussions with Sandia National Laboratory personnel, a database named FMT\_HMW\_345\_960501FANG.CHEMDAT was recommended for EPA's use in verification runs. Based on the date indicated in the file name, i.e., 960501, this database was assumed to be representative of that used for the CCA. The version of FMT was FMT\_FMT2P0\_PA96.EXE.

The starting brine compositions for the FMT verification runs were taken from Table SOTERM-1 in Appendix SOTERM of the CCA. In this table, Brine A is analogous to the SPC or Salado brine in the FMT model runs according to Novak and Moore (1996). The ERDA6 brine is representative of the Castile formation brine.

The FMT runs were conducted in a series of steps to reproduce those described in the available documentation. These steps are:

1. Brine compositions provided in Table SOTERM-1 were converted to molal concentration units and equilibrated. The SPC brine was initially over saturated with  $\text{MgCO}_3$ , hence the chemical potential for this solid was set to +999 kcal/mol in the thermodynamic database to prevent its formation in the preliminary runs and automatic modification of the carbonate concentration. This change was necessary to reproduce the FMT results. The ERDA6 brine was initially over saturated with calcite. This condition was allowed to occur as indicated in Table 2a of Novak and Moore (1996).
2. The brines were equilibrated with the solubilities of halite and anhydrite. These solids are present in the salt formations in the repository.

3. Actinides were added in solid forms as  $\text{AmOHCO}_3(\text{s})$ ,  $\text{ThO}_2(\text{am})$ , and  $\text{KnpO}_2\text{CO}_3 \cdot 2\text{H}_2\text{O}(\text{s})$  and the solutions were equilibrated with their solubilities.
4. The brines were brought into equilibrium with  $\text{Mg}(\text{OH})_2(\text{s})$  and  $\text{MgCO}_3(\text{s})$  solubilities to represent the potential effects of the MgO backfill on the chemical conditions. In this step for the SPC brine, the chemical potential for  $\text{MgCO}_3(\text{s})$ , which was artificially set to +999 kcal/mol in Step 1, was restored to its original value.

The results from these runs for the SPC brine (Brine A or Salado) are shown in Tables 4-2 and 4-3. There are differences in the results for Steps 1 to 3. However, it is the final one, Step 4, that is meaningful to verification. For Step 4, the calculated brine composition is very similar to that obtained by Novak and Moore (1996). The results for the actinides are also close to those obtained by Novak and Moore (1996). There is a slight difference in the concentration calculated for Am(III) ( $4.39\text{e-}07$  vs.  $6.67\text{e-}07$  molal). The reason for this small difference is not clear. It may be a result of different thermodynamic data for the hydrolyzed Am(III) species (see Table 4-3) in the database used for the verification runs compared to those used for the CCA runs or, possibly, very small differences in the brine composition between those obtained here and by Novak and Moore (1996).

Results for the ERDA6 (Castile) brine also show good agreement for the major brine species, Th(IV), and Np(V) (Table 4-4). However, a small difference was observed for the total Am(III) concentration, similar to that observed for the SPC brine. An inspection of the individual species concentrations indicates that the results differ primarily for the hydrolysis species,  $\text{AmOH}^{+2}$ ,  $\text{Am}(\text{OH})_2^+$ , and  $\text{Am}(\text{OH})_3$  (Table 4-5). This observation implies that there may be differences in the thermodynamic data for the hydrolysis species used in these verification runs compared to those used by Novak and Moore (1996). The small discrepancies in the computed concentrations for Am(III) are most likely indicative of different thermodynamic data for various aqueous species present in the database used for the verification runs compared to those used in the CCA runs.

#### 4.2 Effects of Magnesium Carbonates on Actinide Concentrations Predicted by the CCA Version of the FMT Model

At the time the CCA was prepared, experiments on the hydrolysis and carbonation reactions involving the MgO backfill had not been done. Consequently, the predictions for the actinide source term were made assuming that equilibrium between magnesite and brucite would control the pH and  $\text{CO}_2(\text{g})$  partial pressure. Experimental results (A-93-02, II-A-39) however, have indicated that hydrated magnesium carbonates (hydromagnesite and nesquehonite) may also form under the expected repository conditions. As a result of these studies, a series of runs were conducted with the CCA version of the FMT model to evaluate the effects of different hydrated magnesium carbonates on predicted actinide concentrations. The effects were considered to be potentially significant because of the importance of dissolved carbonate for affecting actinide aqueous speciation.

To perform these runs, a line of data on the stoichiometry and chemical potential of hydromagnesite ( $\text{DG}_{\text{r}25\text{C}/\text{RT}} = -2365.6$  for  $\text{Mg}_5(\text{CO}_3)_4(\text{OH})_2 \cdot 4\text{H}_2\text{O}$ ) was inserted into FMT thermodynamic database (file: FMT\_HMW\_345\_960501FANG.CHEMDAT). A value for nesquehonite ( $\text{DG}_{\text{r}25\text{C}/\text{RT}} = -685.4$ ) was already in the database. The chemical potential for magnesite was set to +999 to prevent its formation. Then, using the results from Step 3 of the

verification runs described above for the CCA version of the model as a starting point, separate model runs were made specifying equilibria for brucite/hydromagnesite and brucite/nesquehonite. This procedure was followed for both the SPC (representing Salado brine) and ERDA6 brines (representing Castile brine).

Results from runs with the CCA version of FMT indicated that the pH would be lowered and  $\text{CO}_2(\text{g})$  partial pressure increased for equilibria with the hydrated magnesium carbonate phases compared to magnesite (Tables 4-6 and 4-7). As a result, the predicted concentrations of Th(IV) increased to very high concentrations compared to the case of brucite/magnesite equilibria. Inspection of the speciation results indicate that the increase in Th(IV) is primarily the result of the formation of  $\text{Th}(\text{CO}_3)_5-6$  under the higher  $\text{CO}_2(\text{g})$  partial pressures present at equilibrium for brucite/hydromagnesite and brucite/nesquehonite.

The calculated concentrations of Np(V) under conditions of brucite/nesquehonite equilibria also increased substantially relative to the brucite/magnesite case, reaching highest concentrations in the case of the SPC brine (Table 4-6). This increase appears to be caused by increased carbonate complexation of Np(V) under the comparatively higher  $\text{CO}_2(\text{g})$  partial pressures calculated for brucite/nesquehonite equilibria.

While nesquehonite is not expected to be a long-lived solid under the expected repository conditions, the unrealistically high concentrations for Th(IV) predicted in its presence indicated the presence of unrepresentative constants for certain aqueous species in the FMT thermodynamic database. In particular, the formation of  $\text{Th}(\text{CO}_3)_5-6$  was over predicted, resulting in Th(IV) concentrations over 0.1 molal under conditions of brucite/nesquehonite equilibria (Table 4-6).

Independent of this study, Craig Novak of Sandia National Laboratories (A-93-02, II-G-33) also obtained unrealistically high concentrations for Th(IV) and Np(V) as part of his continued testing of the CCA version of the FMT model. Subsequently, he modified the ion interaction parameters for  $\text{Cl}^-$  and  $\text{Th}(\text{CO}_3)_5-6$  and for the triplets  $\text{Na}^+$  and  $\text{Cl}^-$  and  $\text{Th}(\text{CO}_3)_5-6$  based on values recently derived by Andy Felmy at Pacific Northwest Laboratory from his solubility experiments for the Th(IV)-Cl-CO<sub>3</sub>-2-HCO<sub>3</sub>--H<sub>2</sub>O system (Felmy et al. 1996). Novak also revised the ion interaction parameters for  $\text{Na}^+$  and  $\text{K}^+$  with the Np(V) species,  $\text{NpO}_2\text{CO}_3^-$ ,  $\text{NpO}_2(\text{CO}_3)_2-3$ , and  $\text{NpO}_2(\text{CO}_3)_3-5$  based on available experimental data and modeling studies (Novak et al. 1996b; Novak et al. 1996c). These changes to the thermodynamic database for FMT were completed in April, 1997 (Novak, 1997), and were made available for use by EPA (see discussion in following section).

#### 4.3 Effects of Magnesium Carbonates on Actinide Concentrations Predicted by the Updated Version of the FMT Model

The runs described above in Sections 4.1 and 4.2 were repeated with the updated version of the FMT model and associated databases in April, 1997 and thereafter because of the obvious errors in some of the predicted actinide concentrations. When the updates were made, Novak (1997) created three different thermodynamic databases:

- FMT\_970407\_HYMAG5424.CHEMDAT, includes hydromagnesite  $[\text{Mg}_5(\text{CO}_3)_4(\text{OH})_2 \cdot 4\text{H}_2\text{O}]$  as the primary magnesium carbonate allowed to form

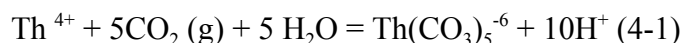
whereas dolomite, magnesite, calcite, aragonite, pirssonite, and gaylussite formation are all disabled.

- FMT\_970407\_HYMAG4323.CHEMDAT, includes hydromagnesite  $[\text{Mg}_4(\text{CO}_3)_3(\text{OH})_2 \cdot 3\text{H}_2\text{O}]$  as the primary magnesium carbonate allowed to form whereas dolomite, magnesite, calcite, aragonite, pirssonite, and gaylussite formation are all disabled.
- FMT\_970407\_NESQ.CHEMDAT, includes nesquehonite  $[\text{MgCO}_3 \cdot 3\text{H}_2\text{O}]$  as the primary magnesium carbonate allowed to form whereas dolomite, magnesite, calcite, aragonite, pirssonite, gaylussite, hydromagnesite, and labile salt formation are all disabled. The disabling of the formation of solids in these files is done by setting their chemical potentials to a high positive value (i.e., +999.99) so that they never enter in to the equilibrium assemblage.

A fourth thermodynamic file was created from FMT\_970407\_NESQ.CHEMDAT by resetting the chemical potentials for dolomite, magnesite, calcite, aragonite, pirssonite, and gaylussite to their original values. This file was named FMT\_970407\_MAGNESITE.CHEMDAT and was used to make runs for conditions of brucite/magnesite equilibrium for comparison with the results from the runs with the hydrated magnesium carbonates.

These four thermodynamic databases were used with FMT to calculate actinide concentrations under conditions of equilibria with brucite, the different magnesium carbonates, accessory solids, and actinide solids (Tables 4-8 and 4-9). Results using both the SPC and ERDA6 brines show that the predicted concentrations for Th(IV) are significantly lower with the updated database than those obtained with the CCA version of FMT for both hydromagnesite and nesquehonite (compare Table 4-8 to 4-6 and Table 4-9 to 4-7). Additionally, good agreement between the results obtained here and those provided by Novak (1997) was achieved (Tables 4-8 and 4-9). Some small differences (less than 5%) occurred but these appear to be reflective of differences in round-off errors or small differences in the starting brine composition, rather than procedural errors or major inconsistencies in thermodynamic databases.

The results also show that Th(IV) concentrations are predicted to be highest under conditions of equilibrium with brucite and nesquehonite, as was found for the CCA version of the FMT model (Tables 4-8 and 4-9). The higher Th(IV) concentrations are a result of increased formation of  $\text{Th}(\text{CO}_3)_5$ -6, i.e.,



under the higher partial pressure of  $\text{CO}_2(\text{g})$  produced by brucite/nesquehonite equilibrium. However, the predicted concentrations are 100 times lower than what was obtained with the CCA version of FMT (see Tables 4-6 and 4-7), making them more believable in consideration of Th(IV) chemistry (Felmy et al., 1996).

The results with the updated version of the FMT database also show that the form of the hydromagnesite, either  $\text{Mg}_5(\text{CO}_3)_4(\text{OH})_2 \cdot 4\text{H}_2\text{O}$  or  $\text{Mg}_4(\text{CO}_3)_3(\text{OH})_2 \cdot 3\text{H}_2\text{O}$ , used in the equilibrium calculations has little impact on the predicted actinide concentrations for both brines (Tables 4-8

and 4-9). Both stoichiometries for hydromagnesite have been reported in the literature (Novak, 1997). Tables 4-8 and 4-9 include the solubility values (for the Salado and Castile brines) used in the PAVT (also see the Technical Support Document for Section 23: Parameter Justification Report, A-93-02, V-B-14). Note that the values as calculated are in molal, whereas the values reported in the CCA are in moles per liter.

In summary, the results of the FMT model can, for the most part, be verified by independent modeling runs following the methodologies provided in support documents to the CCA. Small differences in calculated actinide concentrations were observed but are not considered significant. Most importantly, errors in the FMT thermodynamic database used for calculations presented in the CCA have been corrected and result in more realistic predictions of actinide concentrations for the range of possible conditions that might be expected for equilibria with different magnesium carbonates. EPA's review indicates that the actinide solubilities calculated by FMT and used in the CCA performance assessment appear to be higher than what would be expected in the repository.

Table 4-1. Versions of CHEMDAT databases and FMT executable files used for modeling runs. Pertinent files can be found on the WIPP Alpha Cluster at Sandia National Laboratories in directory EPA:[ROOT.LEEARY.CCA] for January, 1997 runs and EPA:[ROOT.LEEARY.497] for the April, 1997 runs.

Model Runs	FMT Executable Files	CHEMDAT (a) Database
CCA Comparison Runs (1/97)	FMT_FMT2P0_PA96.EXE	HMW_345_960501FANG.CHEMDAT
Post-CCA Comparison Runs (4/97)	FMT_FMT2P0_PA96_2.EXE	HMW_970407_HMAG5424.CHEMDAT (b)
		HMW_970407_HMAG4323.CHEMDAT(c)
		HMW_970407_NESQ.CHEMDAT (d)
		HMW_970407_MAGNESITE.CHEMDAT (e)

- a - Database for thermodynamic constants used by FMT .
- b - Database with hydromagnesite [ $\text{Mg}_5(\text{CO}_3)_4(\text{OH})_2 \cdot 4\text{H}_2\text{O}$ ]
- c - Database with hydromagnesite [ $\text{Mg}_4(\text{CO}_3)_3(\text{OH})_2 \cdot 3\text{H}_2\text{O}$ ]
- d - Database with nesquehonite [ $\text{MgCO}_3 \cdot 3\text{H}_2\text{O}$ ]
- e - Database with magnesite [ $\text{MgCO}_3$ ]

Table 4-2. Comparison of FMT results provided by Novak and Moore (1996) for the CCA to those obtained in the verification runs for the SPC brine (Salado formation). Concentrations in molal.

Element	Step 1		Step 2		Step 3		Step 4	
	Novaka	Verif.	Novakb	Verif.	Novakc	Verif.	Novakd	Verif.
Hydrogen	1.11E+02	1.11E+02	1.11E+02	1.11E+02	1.11E+02	1.11E+02	1.11E+02	1.11E+02
Oxygen	5.58E+01	5.58E+01	5.58E+01	5.58E+01	5.58E+01	5.58E+01	5.59E+01	5.59E+01
Sodium	2.06E+00	2.06E+00	2.90E+00	2.90E+00	2.90E+00	2.90E+00	4.69E+00	4.69E+00
Potassium	8.65E-01	8.66E-01	8.65E-01	8.66E-01	8.65E-01	8.68E-01	1.05E+00	1.05E+00
Magnesium	1.62E+00	1.62E+00	1.62E+00	1.62E+00	1.62E+00	1.62E+00	5.09E-01	5.09E-01
Calcium	2.25E-02	2.25E-02	3.00E-02	3.00E-02	3.05E-02	3.04E-02	3.31E-02	3.31E-02
Chlorine	6.10E+00	6.11E+00	6.95E+00	6.95E+00	6.95E+00	6.95E+00	6.67E+00	6.67E+00
Sulfur	4.49E-02	4.49E-02	5.25E-02	5.24E-02	5.29E-02	5.28E-02	6.02E-02	6.02E-02
Carbon	1.12E-02	1.11E-02	1.12E-02	1.11E-02	1.15E-02	1.52E-02	4.08E-05	4.10E-05
Boron	2.25E-02	2.25E-02	2.25E-02	2.25E-02	2.25E-02	2.25E-02	2.72E-02	2.73E-02
Bromine	1.12E-02	1.12E-02	1.12E-02	1.12E-02	1.12E-02	1.12E-02	1.36E-02	1.36E-02
Th(IV)	0	0	0	0	4.37E-04	3.05E-03	4.98E-09	5.01E-06
Am(III)	0	0	0	0	2.57E-04	1.91E-03	4.39E-07	6.67E-07
Np(V)	0	0	0	0	1.78E-05	2.21E-03	2.64E-06	2.63E-06
pH	3.59	6.06	3.48	6.61	4.97	6.74	8.69	8.69
pmH	4.11	6.59	4.14	5.95	5.63	6.08	9.37	9.37
Charge	1.78E-15	1.09E-16	-8.14E-16	1.75E-15	-1.66E-15	-6.96E-16	-8.17E-16	1.25E-17
Equilibria		halite anhydrite	halite anhydrite AmOHCO3(s) ) ThO2(am) KNpO2CO3. 2H2O(s)	halite anhydrite AmOHCO3(s) ) ThO2(am) KNpO2CO3. 2H2O(s) brucite magnesite				
File Name (e)	SPC	SPC_TAB2B_ 1CARB	SPC_HA	SPC_ TAB2B_ 2CARB	SPC_HA_An	SPC_ TAB2B_ 3CARB	SPC_HA_An _Mg	SPC_ TAB2B_ 4CARB

- a - Database with hydromagnesite  $[Mg_5(CO_3)_4(OH)_2 \cdot 4H_2O]$
- b - Database with hydromagnesite  $[Mg_4(CO_3)_3(OH)_2 \cdot 3H_2O]$
- c - Database with nesquehonite  $[MgCO_3 \cdot 3H_2O]$
- d - Database with magnesite  $[MgCO_3]$
- e- Directory: EPA:[ROOT.LEEARY.CCA]



Table 4-3. Aqueous species concentrations for actinides calculated for the SPC brine (Salado formation) for the CCA from Novak and Moore (1996) and the verification run for Step 4. Concentrations in molal.

Aqueous Species	Novak and Moore (1996)a	Verification (b), Step 4
Th+4	0	0
Th(SO4)20	1.18E-20	0
Th(SO4)3-2	8.47E-20	8.44E-20
Th(OH)3CO3-	4.78E-10	4.78E-10
Th(CO3)5-6	4.98E-06	5.01E-06
Th(OH)40	1.22E-09	1.22E-09
Total	4.98E-06	5.01E-09
Am+3	3.22E-09	3.22E-09
AmCO3+	2.88E-10	2.88E-10
Am(CO3)2-	2.11E-13	2.11E-13
Am(CO3)3-3	3.73E-14	3.73E-14
AmOH+2	3.81E-06	1.53E-09
Am(OH)2+	5.69E-07	6.61E-07
Am(OH)30	1.26E-10	1.00E-09
Total	4.39E-07	6.67E-07
NpO2+	2.40E-06	2.40E-06
NpO2OH0	1.17E-07	1.17E-07
NpO2(OH)2-	1.77E-10	1.77E-10
NpO2CO3-	1.21E-07	1.21E-07
NpO2(CO3)2-3	1.47E-10	1.47E-10
NpO2(CO3)3-5	5.30E-12	5.30E-12
Total	2.64E-06	2.64E-06

a - Run SPC\_HA\_An\_Mg in Novak and Moore (1996).

b - Verification run SPC\_TAB2B\_4CARB.

Table 4-4. Comparison of FMT results provided by Novak and Moore (1996) for the CCA to those obtained in the verification runs for the ERDA6 brine (Castile formation). Concentrations in molal.

Element	Step 1		Step 2		Step 3		Step 4	
	Novaka	Verif.	Novakb	Verif.	Novakc	Verif.	Novakd	Verif.
Hydrogen	1.11E+02	1.11E+02	1.11E+02	1.11E+02	1.11E+02	1.11E+02	1.11E+02	1.11E+02
Oxygen	5.65E+01	5.65E+01	5.65E+01	5.65E+01	5.65E+01	5.65E+01	5.65E+01	5.65E+01
Sodium	5.63E+00	5.50E+00	6.20E+00	6.20E+00	6.22E+00	6.21E+00	6.20E+00	6.20E+00
Potassium	1.09E-01	1.07E-01	1.09E-01	1.07E-01	1.09E-01	1.07E-01	1.09E-01	1.07E-01
Magnesium	2.14E-02	2.09E-02	2.14E-02	2.09E-02	2.14E-02	2.09E-02	4.43E-02	4.33E-02
Calcium	1.26E-02	1.24E-02	1.05E-02	1.06E-02	1.12E-02	1.14E-02	1.33E-02	1.35E-02
Chlorine	5.40E+00	5.27E+00	5.97E+00	5.87E+00	5.98E+00	5.99E+00	5.97E+00	5.97E+00
Sulfur	1.91E-01	1.87E-01	1.89E-01	1.85E-01	1.89E-01	1.84E-01	1.91E-01	1.87E-01
Carbon	1.71E-02	1.68E-02	1.73E-02	1.69E-02	1.86E-02	1.81E-02	3.15E-05	3.18E-05
Boron	7.09E-02	6.92E-02	7.09E-02	6.92E-02	7.09E-02	6.92E-02	7.08E-02	6.92E-02
Bromine	1.24E-02	1.21E-02	1.24E-02	1.21E-02	1.24E-02	1.21E-02	1.24E-02	1.21E-02
Th(IV)	0	0	0	0	3.88E-03	3.75E-03	6.78E-09	6.91E-09
Am(III)	0	0	0	0	4.49E-04	3.50E-04	4.12E-07	7.37E-08
Np(V)	0	0	0	0	1.74E-04	1.80E-04	2.53E-06	2.56E-06
pH	6.18	6.21	6.16	6.16	5.19	5.19	9.24	9.24
pmH	6.74	6.75	6.81	6.81	5.84	5.84	9.89	9.90
Charge	5.38E-16	-1.49E-16	2.77E-16	-2.31E-16	1.80E-15	-6.67E-16	-1.97E-15	2.07E-15
Equilibria	calcite	calcite halite anhydrite	halite anhydrite AmOHCO3(s) ThO2(am) KNpO2CO3.2 H2O(s)	halite anhydrite AmOHCO3(s) ThO2(am) KNpO2CO3.2 H2O(s) brucite magnesite				
File Name(e)	ERDA6	ERDA6_1	ERDA6_HA	ERDA6_2	ERDA6_HA_A n	ERDA6_3	ERDA6_HA_A n_Mg	ERDA6_4

- a - Database with hydromagnesite  $[\text{Mg}_5(\text{CO}_3)_4(\text{OH})_2 \cdot 4\text{H}_2\text{O}]$
- b - Database with hydromagnesite  $[\text{Mg}_4(\text{CO}_3)_3(\text{OH})_2 \cdot 3\text{H}_2\text{O}]$
- c - Database with nesquehonite  $[\text{MgCO}_3 \cdot 3\text{H}_2\text{O}]$
- d - Database with magnesite  $[\text{MgCO}_3]$
- e- Directory: EPA:[ROOT.LEEARY.CCA]

Table 4-5. Aqueous species concentrations for actinides calculated with the CCA version of FMT for the ERDA6 brine (Castile formation) from Novak and Moore (1996) and the verification run for Step 4. Concentrations in molal.

Aqueous Species	Novak and Moore (1996)a	Verification (b), Step 4
Th+4	0	0
Th(SO4)20	9.33E-22	8.63E-22
Th(SO4)3-2	4.11E-20	3.75E-20
Th(OH)3CO3-	1.79E-09	1.80E-09
Th(CO3)5-6	3.71E-09	3.82E-09
Th(OH)40	1.29E-09	1.29E-09
Total	6.79E-09	6.91E-09
Am+3	7.76E-11	7.58E-11
AmCO3+	7.19E-11	7.12E-11
Am(CO3)2-	7.48E-13	7.54E-13
Am(CO3)3-3	8.70E-13	8.88E-13
AmOH+2	2.69E-07	1.29E-10
Am(OH)2+	1.42E-07	7.24E-08
Am(OH)30	1.26E-10	1.00E-09
Total	4.11E-07	7.36E-08
NpO2+	1.70E-06	1.70E-06
NpO2OH0	2.08E-07	2.11E-07
NpO2(OH)2-	1.04E-09	1.06E-09
NpO2CO3-	6.27E-07	6.43E-07
NpO2(CO3)2-3	1.94E-09	2.02E-09
NpO2(CO3)3-5	2.05E-12	2.19E-12
Total	2.54E-06	2.56E-06

a - Run ERDA6\_HA\_An\_Mg in Novak Moore (1996).

b - Verification run ERDA6\_4.

Table 4-6. Brine composition and actinide concentrations calculated with the CCA version of FMT for different magnesium carbonate equilibria for the SPC brine (Salado formation). Concentrations in molal.

Element	Brucite/Magnesite [MgCO <sub>3</sub> ]	Brucite/Hydromagnesite [Mg <sub>5</sub> (CO <sub>3</sub> ) <sub>4</sub> (OH)2.4H <sub>2</sub> O]	Brucite/Nesquehonite [MgCO <sub>3</sub> .3H <sub>2</sub> O]
Hydrogen	1.11E+02	1.11E+02	1.11E+02
Oxygen	5.59E+01	5.78E+01	5.98E+01
Sodium	4.69E+00	3.81E+00	2.01E+00
Potassium	1.05E+00	9.67E-01	8.78E-01
Magnesium	5.09E-01	1.35E+00	2.66E+00
Calcium	3.31E-02	4.02E-02	1.41E-02
Chlorine	6.67E+00	6.60E+00	6.29E+00
Sulfur	6.02E-02	1.22E-01	4.10E-01
Carbon	4.10E-05	5.59E-01	8.01E-01
Boron	2.73E-02	2.52E-02	2.25E-02
Bromine	1.36E-02	1.25E-02	1.12E-02
Th(IV)	5.01E-06	1.12E-01	9.98E-02
Am(III)	6.67E-07	1.64E-07	2.19E-08
Np(V)	2.63E-06	1.08E-06	9.99E-02
pH	8.69	8.52	8.40
pmH	9.37	9.18	9.02
log [CO <sub>2</sub> ] (bar)	-6.89	-5.63	-4.68
Charge	1.25E-17	7.92E-15	5.74E-15
Equilibria	halite anhydrite AmOHCO <sub>3</sub> (s) ThO <sub>2</sub> (am) KNpO <sub>2</sub> CO <sub>3</sub> .2H <sub>2</sub> O(s) brucite magnesite	halite anhydrite AmOHCO <sub>3</sub> (s) ThO <sub>2</sub> (am) KNpO <sub>2</sub> CO <sub>3</sub> .2H <sub>2</sub> O(s) brucite magnesite calcite Mg-oxychloride	halite anhydrite AmOHCO <sub>3</sub> (s) ThO <sub>2</sub> (am) KNpO <sub>2</sub> CO <sub>3</sub> .2H <sub>2</sub> O(s) brucite magnesite calcite Mg-oxychloride Glauberite Polyhalite
File Name(a)	SPC_TAB2B_4CARB	SPC_TAB2B_4_HYMAG	SPC_TAB2B_4_NESQ

a - Directory: EPA:[ROOT.LEEARY.CCA]

Table 4-7. Brine composition and actinide concentrations calculated with the CCA version of FMT for different magnesium carbonate equilibria for the ERDA6 brine (Castile formation). Concentrations in molal.

Element	Brucite/Magnesite [MgCO <sub>3</sub> ]	Brucite/Hydromagnesite [Mg <sub>5</sub> (CO <sub>3</sub> ) <sub>4</sub> (OH) <sub>2</sub> ·4H <sub>2</sub> O]	Brucite/Nesquehonite [MgCO <sub>3</sub> ·3H <sub>2</sub> O]
Hydrogen	1.11E+02	1.11E+02	1.11E+02
Oxygen	5.65E+01	5.67E+01	5.90E+01
Sodium	6.20E+00	5.64E+00	4.15E+00
Potassium	1.07E-01	1.06E-01	9.67E-02
Magnesium	4.33E-02	3.64E-01	1.57E+00
Calcium	1.35E-02	1.07E-02	3.53E-02
Chlorine	5.97E+00	5.97E+00	6.00E+00
Sulfur	1.87E-01	2.23E-01	2.29E-01
Carbon	3.18E-05	5.39E-03	7.64E-01
Boron	6.92E-02	6.88E-02	6.28E-02
Bromine	1.21E-02	1.20E-02	1.10E-02
Th(IV)	6.91E-09	1.02E-03	1.53E-01
Am(III)	7.37E-08	4.94E-08	5.61E-08
Np(V)	2.56E-06	1.87E-06	1.93E-05
pH	9.24	8.79	8.56
pmH	9.90	9.42	9.15
log [CO <sub>2</sub> ] (atm)	-6.89	-5.65	-5.51
Charge	2.07E-15	2.06E-15	4.63E-15
Equilibria	halite anhydrite AmOHCO <sub>3</sub> (s) ThO <sub>2</sub> (am) KNpO <sub>2</sub> CO <sub>3</sub> ·2H <sub>2</sub> O(s) brucite magnesite	halite anhydrite AmOHCO <sub>3</sub> (s) ThO <sub>2</sub> (am) KNpO <sub>2</sub> CO <sub>3</sub> ·2H <sub>2</sub> O(s) brucite magnesite calcite glauberite	halite anhydrite AmOHCO <sub>3</sub> (s) ThO <sub>2</sub> (am) KNpO <sub>2</sub> CO <sub>3</sub> ·2H <sub>2</sub> O(s) brucite magnesite calcite glauberite
File Name (a)	ERDA_4	ERDA_4_HYMAG	ERDA_4_NESQ

a - Directory: EPA:[ROOT.LEEARY.CCA]

Table 4-8. Brine compositions and actinide concentrations calculated with the updated version of FMT for different magnesium carbonate equilibria for the SPC brine (Salado formation). Concentrations in molal.

Element	Brucite/ Hydromagnesite [Mg <sub>5</sub> (CO <sub>3</sub> ) <sub>4</sub> (OH) <sub>2</sub> .4H 2O]		Brucite/ Hydromagnesite [Mg <sub>4</sub> (CO <sub>3</sub> ) <sub>3</sub> (OH) <sub>2</sub> .3H <sub>2</sub> O]		Brucite/ Nesquehonite [MgCO <sub>3</sub> .3H <sub>2</sub> O]		Brucite/ Magnesite [MgCO <sub>3</sub> ]	
	Novak	Verif.	Novak	Verif.	Novak	Verif.	Novak	Verif.
Hydrogen	1.11E+02	1.11E+02	1.11E+02	1.11E+02	1.11E+02	1.11E+02	not reported	1.11E+02
Oxygen	5.59E+01	5.59E+01	5.59E+01	5.59E+01	5.59E+01	5.59E+01	not reported	5.59E+01
Sodium	4.68E+00	4.69E+00	4.68E+00	4.69E+00	4.66E+00	4.69E+00	not reported	4.69E+00
Potassium	1.07E+00	1.05E+00	1.07E+00	1.05E+00	1.11E+00	1.05E+00	not reported	1.05E+00
Magnesium	5.09E-01	5.09E-01	5.09E-01	5.09E-01	5.30E-01	5.30E-01	not reported	5.09E-01
Calcium	3.29E-02	3.31E-02	3.29E-02	3.31E-02	3.34E-02	3.39E-02	not reported	3.31E-02
Chlorine	6.68E+00	6.67E+00	6.68E+00	6.67E+00	6.69E+00	6.66E+00	not reported	6.67E+00
Sulfur	6.06E-02	6.02E-03	6.06E-02	6.02E-02	6.22E-02	6.10E-02	not reported	6.02E-02
Carbon	4.13E-04	4.13E-04	5.38E-04	5.38E-04	2.26E-02	2.27E-02	not reported	1.59E-05
Boron	2.77E-02	2.73E-02	2.77E-02	2.73E-02	2.88E-02	2.72E-02	not reported	2.73E-02
Bromine	1.39E-02	1.36E-02	1.39E-02	1.36E-02	1.44E-02	1.36E-02	not reported	1.36E-02
Th(IV)	1.37E-08	1.37E-08	1.75E-08	1.75E-08	7.22E-04	7.49E-04	not reported	1.70E-09
Am(III)	1.08E-07	1.06E-08	8.31E-08	8.21E-08	3.64E-07	3.53E-07	not reported	7.02E-07
Np(V)	1.38E-07	1.40E-07	1.23E-07	1.25E-07	1.36E-07	1.45E-07	not reported	1.80E-06
pH	8.69	8.69	8.69	8.69	8.69	8.69	not reported	8.69
pmH	9.37	9.37	9.37	9.37	9.37	9.36	not reported	9.37
CO <sub>2</sub> (g)a	-5.50	-5.50	-5.39	-5.39	-3.84	-3.84	not reported	-6.92
Charge	5.87E-15	5.82E-15	8.97E-15	3.07E-15	1.30E-14	3.72E-15	not reported	4.77E-16

Equilibria	Anhydrite MgOxychloride Brucite Hydromagnesian Halite ThO2(am) AmOHCO3 KNpO2CO3	Anhydrite MgOxychloride Brucite Hydromagnesian Halite ThO2(am) AmOHCO3 KNpO2CO3	Anhydrite MgOxychloride Brucite Nesquehonite Halite ThO2(am) AmOHCO3 KNpO2CO3	Anhydrite Brucite Magnesian Halite ThO2(am) Am(OH)3(s) KNpO2CO3				
File Name	FMT_SPC_HMAG5424_970407_22	SPC_4_MG497a	FMT_SPC_HMAG4323_970407_22	SPC_6_MG497a	FMT_SPC_NESQ_970407_22	SPC_8_MG497a		SPC_10_MG497a

a - Directory: EPA:[ROOT.LEEARY.497]

Table 4-9. Brine compositions and actinide concentrations calculated with the updated version of FMT for different magnesium carbonate equilibria for the ERDA6 brine (Castile formation). Concentrations in molal.

Element	Brucite/ Hydromagnesite $Mg_5(CO_3)_4(OH)_2 \cdot 4H_2O$		Brucite/ Hydromagnesite $Mg_4(CO_3)_3(OH)_2 \cdot 3H_2O$		Brucite/ Nesquehonite $MgCO_3 \cdot 3H_2O$		Brucite/ Magnesite $MgCO_3$	
	Novak	Verif.	Novak	Verif.	Novak	Verif.	Novak	Verif.
Hydrogen	1.11E+02	1.11E+02	1.11E+02	1.11E+02	1.11E+02	1.11E+02	not reported	1.11e+02
Oxygen	5.66E+01	5.65E+01	5.66E+01	5.65E+01	5.67E+01	5.66E+01	not reported	5.65e+01
Sodium	6.20E+00	6.20E+00	6.20E+00	6.20E+00	6.18E+00	6.18E+00	not reported	6.20e+00
Potassium	1.11E-01	1.07E-01	1.11E-01	1.07E-01	1.16E-01	1.06E-01	not reported	1.09e-01
Magnesium	4.57E-02	4.40E-02	4.59E-02	4.42E-02	7.74E-02	7.35E-02	not reported	4.63e-02
Calcium	1.34E-02	1.36E-02	1.34E-02	1.36E-02	1.61E-02	1.64E-02	not reported	1.33e-02
Chlorine	5.97E+00	5.97E+00	5.97E+00	5.97E+00	5.96E+00	5.96E+00	not reported	5.97e+00
Sulfur	1.91E-01	1.87E-01	1.91E-01	1.87E-01	1.93E-01	1.90E-01	not reported	1.91e-01
Carbon	7.77E-04	7.91E-04	1.01E-03	1.03E-03	3.54E-02	3.67E-02	not reported	3.06e-05
Boron	7.21E-02	6.92E-02	7.21E-02	6.92E-02	7.48E-02	6.91E-02	not reported	7.10e-02
Bromine	1.26E-02	1.21E-02	1.26E-02	1.21E-02	1.31E-02	1.21E-02	not reported	1.24e-02
Th(IV)	4.63E-08	4.70E-08	5.98E-08	6.07E-08	1.19E-03	1.30E-03	not reported	3.03e-09
Am(III)	1.45E-08	1.44E-08	1.31E-08	1.31E-08	2.44E-06	2.53E-06	not reported	7.97e-08
Np(V)	5.28E-07	5.50E-07	5.25E-07	5.48E-07	8.92E-07	8.89E-07	not reported	1.89e-06
pH	9.24	9.24	9.23	9.24	9.17	9.18	not reported	9.23
pH	9.89	9.90	9.89	9.89	9.82	9.83	not reported	9.88
CO2(g)a	-5.50	-5.50	-5.39	-5.39	-3.87	-3.87	not reported	-6.91
Charge	1.54E-14	1.55E-15	7.56E-15	4.09E-16	1.62E-15	1.95E-15	not reported	5.55e-16



Equilibria	Anhydrite Brucite Hydromagne site Halite Glauberite ThO2(am) KNpO2CO3 AmOHCO3	Anhydrite Brucite Hydromagnesit e Halite Glauberite ThO2(am) KNpO2CO3 AmOHCO3	Anhydrite Brucite Hydromagnesit e Halite Glauberite ThO2(am) Na3NpO2(CO 3)2 NaAm(CO3)2. 6H2O	Anhydrite Brucite Magnesite Halite Glauberite ThO2(am) Am(OH)3(s) KNpO2CO3				
File Name	FMT_ERDA 6_HMAG54 24_970407_ 22	ERDA6_4_MG 497a	FMT_ERDA6 _HMAG4323 _970407_22	ERDA6_6_MG497a	FMT_ERD A6_NESQ _970407_2 2	ERDA6_8_MG497a		ERDA6_10 _MG497a

a - Directory: EPA:[ROOT.LEEARY.497]

## 5.0 Review of the Uranium(VI) Solubility

The actinides in the +III, +IV, and +V, are calculated with the FMT computer code as described in section 4 of this document. However, the FMT database contains no data for U(+VI), hence it was estimated by an alternative method. That approach was to use a single U(VI) solubility value ( $\sim 1 \times 10^{-5}$  moles/liter) without reference to a solubility-controlling solid phase. This different approach was reviewed to determine if it was appropriate for use in the performance assessment.

### 5.1 Representation of the Uranium(VI) in the Actinide Source Term for the CCA

Appendix SOTERM, Section 3.4.4, indicates that available data for U(VI) are not sufficiently reliable to allow accurate predictions of U(VI) solubility and aqueous speciation with the FMT model in high ionic strength solutions. In particular, a model for U(VI) hydrolysis has not been developed to the extent necessary for application to WIPP brines. As a result, a single concentration of  $8.8 \times 10^{-6}$  molal was selected to represent U(VI) in the actinide source term model<sup>2</sup>. This concentration is based on an assessment by Hobart and Moore (1996) of U(VI) solubility experiments conducted with brines at pH 10 in the absence of CO<sub>2</sub>(g) by Reed et al. (1996). Novak and Moore (A-93-02, II-G-1, CCA Reference 479) present DOE's approach to estimating concentrations for dissolved +VI actinides under WIPP disposal room conditions.

In an interim report of data collected from experiments subsequent to the submission of the CCA, Reed and Wygmans (1997) reported uranium concentrations of  $1.1 \pm 0.2 \times 10^{-8}$  M to  $5.5 \pm 0.5 \times 10^{-7}$  M in their 355 day old experiments using WIPP G-Seep and ERDA-6 brines (with and without carbonate) at pH ranging from 7 to 10. In Docket Reference: A-93-02, II-G-44 (WPO# 45115), Bynum and Wang state that 1997 Reed and Wygmans data show "that over a period of just a few months, uranium (VI) in ERDA-6 brine at pH 10 in the absence of carbonate (i.e. conditions representing the backfilled disposal room) dropped to concentrations of approximately  $5 \times 10^{-7}$  moles per liter. This is approximately 1.5 orders of magnitude less than the solubility of uranium (VI) utilized in the CCA PA." In addition, calculations by SNL staff (A-93-02, II-G-44; WPO# 45115) using a low ionic strength database (with WIPP type brine compositions diluted to make their composition consistent with the database), predict U(VI) solubilities for Castile and Salado type brines between  $10^{-6}$  moles/liter and  $10^{-7.2}$  moles/liter.

The selection of a single concentration for U(VI) is a simple approach and may be conservative but it is based on the following two assumptions that may not be completely valid, i.e.,

1. Experiments conducted in the absence of CO<sub>2</sub>(g) are representative of the repository conditions, and
2. U(VI) speciation cannot be modeled because the stabilities of the hydrolysis species have

---

<sup>2</sup> Note, there is a typographical error in the U(VI) concentration given in the text at the top of page SOTERM-28. The correct value should be:  $8.7 \times 10^{-6}$  molal rather than  $8.8 \times 10^{-5}$  molal to be consistent with the value in Table SOTERM-2.

not been exactly established.

While CO<sub>2</sub>(g) partial pressure in the repository may be low, especially if microbial degradation is minimal, it will not be completely absent. For instance, the FMT calculations described above indicate that CO<sub>2</sub>(g) partial pressures would be predicted to be about 10<sup>-5.5</sup> bar for equilibrium between brucite and hydromagnesite, the hydrous magnesium carbonate EPA expects to be dominant in the repository as described in section 3 of this document. The CO<sub>2</sub>(g) partial pressures could range as high as 10<sup>-3.8</sup> bar in the presence of nesquehonite, but this solid is not expected to persist for long periods (see Tables 4-8 and 4-9). In comparison, the ambient partial pressure of CO<sub>2</sub>(g) in the atmosphere is about 10<sup>-3.5</sup> bar.

The supposition that the stabilities of the U(VI) hydrolysis species are not exactly known is probably true. However, under the conditions expected for the repository, U(VI) hydrolysis species are expected to be subordinate to U(VI) carbonate species. For instance, speciation calculations for conditions of equilibrium with different magnesium carbonate solids and schoepite (UO<sub>3</sub>•2H<sub>2</sub>O), indicate that U(VI) speciation is dominated by UO<sub>2</sub>CO<sub>3</sub>, UO<sub>2</sub>(CO<sub>3</sub>)<sub>2</sub>-2, and UO<sub>2</sub>(CO<sub>3</sub>)<sub>3</sub>-4, with one exception of brucite/magnesite equilibria for the Salado brine (Table 5-1). Schoepite has been suggested as a solubility-controlling solid for U(VI) in aerobic systems with low CO<sub>2</sub>(g) partial pressure (Hobart et al. 1996). Previous speciation calculations of U(VI) speciation in WIPP brines also indicate the predominance of U(VI) carbonate species over hydrolysis species for alkaline conditions (see Figure 5 in Hobart et al. 1996). These calculations imply that precise knowledge of the stabilities of the hydrolysis species is not necessarily needed to model U(VI) speciation under the expected repository conditions because only a small fraction of the total dissolved U(VI) exist as hydrolysis species.

## 5.2 Potential Solubility Controls for Uranium(VI)

Past reviews of U(VI) chemistry have considered schoepite (UO<sub>3</sub> • 2H<sub>2</sub>O) to be a possible controlling phase for U(VI) (Hobart et al. 1996). A comparison of U(VI) concentrations reported by Hobart and Moore (1996) and Reed and Wygmans (1997) to the predicted solubility of schoepite suggests that it may be solubility-controlling under neutral to acidic pH conditions (Figure 5-1). However, under the alkaline pH conditions expected for the brines in the presence of MgO backfill, schoepite solubility greatly overestimates measured U(VI) concentrations. Under these conditions, experimental data from Reed and Wygmans (1997) appear to be approximated by the solubilities of sodium and calcium uranates (Na<sub>2</sub>U<sub>2</sub>O<sub>7</sub> and CaUO<sub>4</sub>) (Figure 5-1). The uranates are substantially less soluble than schoepite and might be expected to form upon interaction with the high concentrations sodium and calcium in the WIPP brines.

However, there are a few caveats regarding the data shown in Figure 5-1 that should be considered. First, the experimental data from Reed and coworkers shown in Figure 6-1 are not entirely adequate for making solubility interpretations because they do not report CO<sub>2</sub>(g) partial pressure or carbonate concentrations. Additionally, the predicted solubility curves were calculated with a low ionic strength model of aqueous speciation and solubility (i.e., the PHREEQC geochemical model, Parkhurst, 1995). Hence, the comparisons in Figure 5-1 should not be over interpreted. Despite these caveats, the experimental data indicate pH-dependent solubilities that are consistent with those predicted for various U(VI) solids. A dependence on CO<sub>2</sub>(g) partial pressure can also be expected.

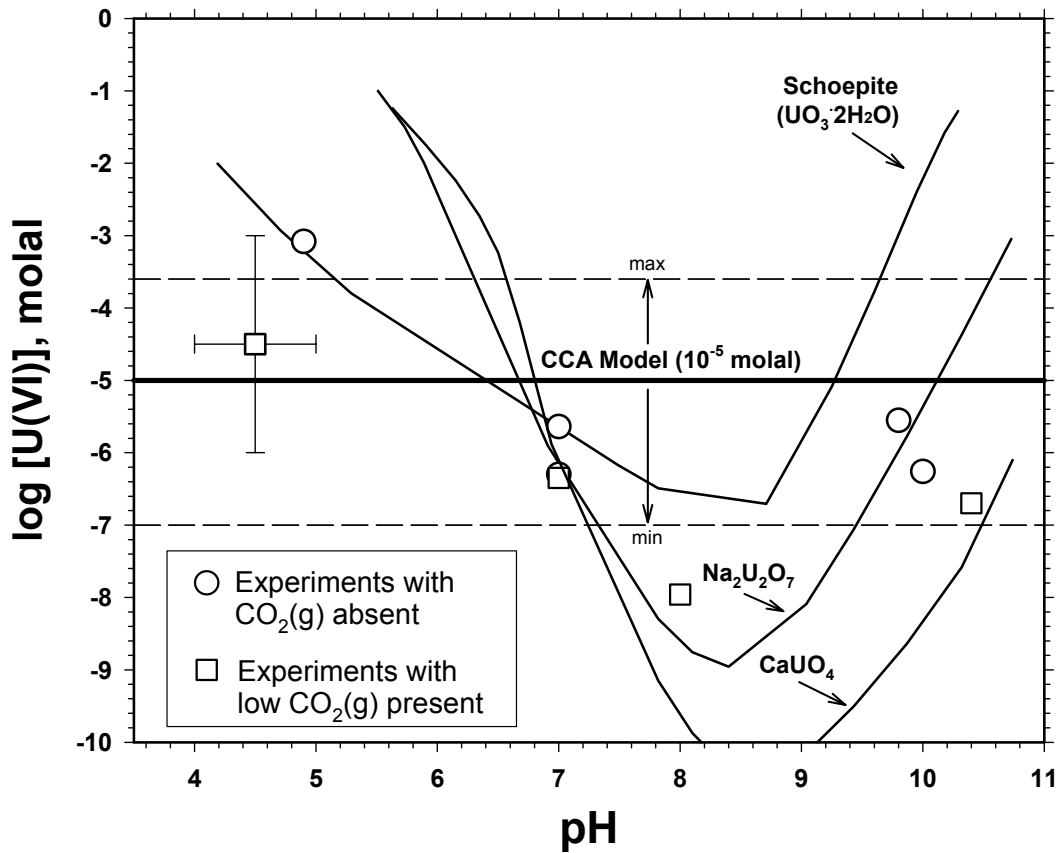
In summary, the single concentration used to represent U(VI) in the actinide source term does not account for any relationship between U(VI) and solution conditions evident in the experimental work or inferred from existing thermodynamic data. However, information presented in 1) Hobart and Moore (1996), 2) Reed and Wygmans (1997), and 3) new calculations (A-93-02, II-G-44; WPO#45115), in combination with the use of uncertainty ranges (discussed in the next section), indicate that the U(VI) solubility values used in CCA calculations are adequate for use in the performance assessment. The U(VI) solubility and uncertainty range used in the CCA appear to capture estimated and experimental U(VI) solubilities that could be expected in the repository.

Table 5-1. Aqueous speciation results for U(VI) in brines equilibrated with brucite and different magnesium carbonates and schoepite (UO<sub>3</sub>.2H<sub>2</sub>O) obtained with the PHREEQC geochemical model and MINTEQ.DAT thermodynamic database (Parkhurst, 1995).

Equilibria	Salado (a)			Castile (a)		
	Magnesite	Hydro-magne site	Nesque- honite	Magnesite	Hydro-magne site	Nesque-ho nite
pH (s.u.)	9.1	9.1	9.1	9.9	9.8	9.8
CO <sub>2</sub> (g) (atm)	-6.7	-5.5	-5.5	-6.7	-5.5	-5.5
Tot U(VI) (molal)	2.1E-08	2.0E-6	2.0E-06	9.6E-07	9.2E-04	9.2E-04
UO <sub>2</sub> (CO <sub>3</sub> ) <sub>3-4</sub> (%)	1.7	69.4	69.4	88.2	98.5	98.5
UO <sub>2</sub> (CO <sub>3</sub> )-2 (%)	11.6	29.4	29.4	11.4	1.5	1.5
UO <sub>2</sub> CO <sub>3</sub> 0 (%)	2	0.3	0.3	0.3	<0.1	<0.1
(UO <sub>2</sub> ) <sub>3</sub> (OH) <sub>5+</sub> (%)	72.9	0.8	0.8	<0.1	<0.1	<0.1
UO <sub>2</sub> OH+ (%)	11.7	0.1	0.1	<0.1	<0.1	<0.1
UO <sub>2</sub> +2 (%)	<0.1	<0.1	<0.1	<0.1	<0.1	<0.1
(UO <sub>2</sub> ) <sub>2</sub> (OH) <sub>2+2</sub> (%)	<0.1	<0.1	<0.1	<0.1	<0.1	<0.1
UO <sub>2</sub> Cl- (%)	<0.1	<0.1	<0.1	<0.1	<0.1	<0.1
UO <sub>2</sub> SO <sub>4</sub> 0 (%)	<0.1	<0.1	<0.1	<0.1	<0.1	<0.1
UO <sub>2</sub> (SO <sub>4</sub> ) <sub>2-2</sub> (%)	<0.1	<0.1	<0.1	<0.1	<0.1	<0.1

a - Salado and Castile brine compositions were taken from Table SOTERM-1 and diluted 10-times for input to PHREEQC to decrease the ionic strength of the solution to increase the accuracy of activity coefficients calculated by PHREEQC.

Figure 5-1. Comparisons of solubilities of U(VI) solids to concentrations reported by Reed and Wygmans (1997) and Reed and Moore (1996) for brines with and without CO<sub>2</sub>(g). Solubility curves were calculated for 25°C and CO<sub>2</sub>(g) partial pressure of 10<sup>-5.5</sup> bar, expected for brucite/hydromagnesite equilibrium in Salado brine.



## 6.0 Actinide Solubility Uncertainty Range

### 6.1 Documentation

In the CCA, DOE uses point estimates for the actinide solubility and has estimated an uncertainty range around the point estimates. In CCA, Appendices SOTERM and PAR, (A-93-02, II-G-1) discussions of the uncertainties in actinide solubilities are provided with references to Bynum (1996a, A-93-02, II-G-1, CCA reference 106). However, this memo only gives a single page that listed log values of uncertainties for FMT modeling simulations with no discussion of what experimental data were used in the error calculations. It does not provide information on the details of the uncertainty calculations.

An additional investigation of the WIPP library by EPA did reveal a more detailed description by Bynum (1996b, WPO41374) in addition to that which was cited in the CCA. This additional report is dated 9-3-96, which postdates the previous oral descriptions provided in a June, 1996 meeting. The description provided in this 9-3-96 report is used as the basis of the discussion in the following section.

### 6.2 Methodology for Defining Uncertainties in Actinide Solid Solubilities

A brief description of the uncertainty calculation and the histogram for the error distribution is provided in Appendix SOTERM (pp. SOTERM 28-29). This description is consistent with that provided in Bynum (1996b). As described by these references, the method involved determining the differences between concentrations calculated by the FMT model and those measured in solubility experiments. The calculated and measured solubilities were then plotted, with the differences between each then approximated by measurement using a ruler. The populations of errors from different comparisons were accumulated and used to generate a cumulative distribution of errors. In some cases, differences between concentrations calculated with the NONLIN model (instead of the FMT model) and experimentally measured concentrations were also used. The NONLIN model has been used to determine equilibrium constants from experimental data using nonlinear regression analysis, and the Pitzer-type parameter database for calculating activity coefficients from Harvie et al. (1980, 1984), Felmy and Weare (1986), and Felmy and Rai (1992). This database is also used in FMT and NONLIN, thus, it is logical to conclude that comparisons from NONLIN calculations should be analogous to those obtained from FMT.

Before conducting the uncertainty analysis, Bynum (1996b) made an assessment of which solubility data were appropriate for inclusion in the uncertainty distribution. As explained by Bynum (1996b), the criteria for inclusion was as follows. If a data set for an actinide oxidation state was determined to be technically deficient or inconsistent, then the whole data set was removed from consideration to avoid making subjective judgments about specific studies. As a result, solubility data for actinides in the +6 oxidation state were thrown out. This decision seems appropriate in view of the fact that the CCA source term was unable to develop a solubility model for U(VI), which is the only hexavalent actinide species expected under WIPP conditions.

Experimental solubility data for +4 actinides were also eliminated from consideration in the uncertainty analysis because as stated in Bynum (1996b): "The data available for the +4 model were

found to have significant problems in the extrapolated regions and were thus determined to be inadequate for use in this analysis.” This statement seems to contradict the discussion of +4 actinides in Appendix SOTERM (page SOTERM-26) where it is implied that data for Th(IV) are available from Felmy et al. (1991), Felmy and Rai (1992), and Felmy et al. (1996), and are adequate for describing ThO<sub>2</sub>(am) solubility and Th(IV) aqueous speciation in brines. The last sentence on page SOTERM-26 indicates that Th(IV) solubility has been measured in WIPP brines, implying that there should be experimental data relevant to determining uncertainties in solubilities according to the criteria of Bynum (1996b). From these statements, it is unclear why the experimental data for Th(IV) were eliminated from consideration in the uncertainty analysis. It is also indicated in Appendix SOTERM that the dissolved Th(IV) solids are more soluble than the other +4 actinides and are used to provide a conservative model of the solubilities of the other +4 actinides [i.e., U(IV), Pu(IV), and Np(IV)]. This statement infers that it would be important to include uncertainties from solubility studies for Th(IV) because it is the model used to represent both U(IV) and Pu(IV).

The exclusion of the +4 and +6 solubility data from consideration left only data for +3 and +5 actinides for the uncertainty analysis (Bynum, 1996b). Using available data, a total of 150 measurements of differences between predicted solubilities and analytically determined actinide concentrations were made by Bynum (1996b). Of this total 104 (69% of 150 total) were from experiments on the solubilities of Nd(III) carbonates [NaNd(CO<sub>3</sub>)<sub>2</sub>.XH<sub>2</sub>O] in brines for which FMT was used to make solubility predictions (Bynum, 1996b). Solubility data for Am(III) in carbonated brines (Runde and Kim, 1994, cited in SOTERM) yielded 35 (23% of 150 total) more measurements for comparison to FMT predictions. Eleven data points (7% of 150 total) were obtained from experiments on Np(V) solubility in carbonated brines, 9 of which were conducted in low ionic strength solutions that may not be representative of brines. Solubility data for Pu(III) solids in brines (e.g., Felmy et al. 1989) were not included in the uncertainty analysis. On page SOTERM-25, it is stated that “... an An(III) model has been parameterized in the Pitzer formalism for the Na, Cl, SO<sub>4</sub>, CO<sub>3</sub>, and PO<sub>4</sub> systems; Pu<sup>+3</sup>-Na<sup>+</sup>-Cl- in Felmy et al. (1989)...” This statement implies that data for Pu(III) solubility must have been available. The reason for their exclusion from the uncertainty analysis is not clear, considering the criteria set forth in Bynum (1996b) that only complete datasets were used or eliminated in their entirety to avoid making subjective judgments.

While the approach used to define uncertainties in the actinide concentrations for the source would appear to provide a reasonable representation of the potential range of error inherent in the FMT model predictions, its implementation is inconsistent. The entire database of uncertainties may be skewed by the prevalence of data for the +3 actinides (93% of the total comparisons), which have the most extensive database of all the actinides (see page SOLTERM-25), and exclusion of data for other oxidation states. Additionally, 69% of the error distribution is derived from studies with Nd(III), which is not an actinide, although its chemical behavior may be argued to provide an analogue for the +3 actinides.

Whether or not data from primarily +3 actinides is representative of actinides in other oxidation states is difficult to assess. More specifically, the question that arises is: How does the best solubility data set [i.e., +3 actinides exclusive of Pu(III)] represent uncertainties for less studied actinides (i.e., +4, +5, and +6 actinides)? It would seem logical that the uncertainties for the +4 and +6 actinides must be larger because less of a basis of knowledge is available to depend upon for



making predictions. However, the same uncertainty range and distribution was used to represent all of the actinides for source term input to the performance assessment.

The questions that have been raised here are concerned primarily with the approach and implementation used to determine uncertainties. However, it should be recognized that, in practice, the method used by Bynum (1996b) resulted in the maximum possible error limits for the data considered, that is from -2 to +1.4 log units about the mean predicted concentrations. Bynum (1996b) could have used a statistical approach to define error limits based on a 90 or 95% confidence interval calculated for the distribution of errors presented in Figure SOTERM-6 and obtained a smaller range of uncertainty. Instead, he conservatively used the maximum range of errors determined from 150 measurements of differences between measured and predicted concentrations. It is not clear that including more data for the other actinide oxidation state would appreciably change this range. EPA thus concludes that the uncertainty range uses a reasonable approach and is appropriate for use in performance assessment.

## 7.0 Influence of Ligands and Complexants on Actinide Migration

Actinide mobility is a broad concept that includes all mechanisms which could lead to actinide migration in the aqueous phase. This includes soluble actinide species, complexation of actinides with other dissolved and thus mobile compounds, and colloidal transport. The discussion in SOTERM on mineral-fragment colloids and intrinsic colloids was found to be reasonable by EPA and was not evaluated further. Complexation of the actinides by organic complexants is discussed in this section.

Complexation by ligands and humic materials was recognized as a potential mechanism at the WIPP which could enhance the mobility of the actinides beyond that predicted by solubility experiments and related solubility modeling (e.g., FMT modeling, discussed in Section 5.0). Ligands are a part of the waste stream planned for disposal at WIPP and microbial degradation of the waste cellulose could generate humic materials (see Section 9.0). DOE also recognized this phenomenon as a potential problem and addressed the issue in Appendix SOTERM, which presented the results from some limited experimentation conducted by DOE. The intent of that experimentation was to bound the effect of complexants and ligands under repository-relevant conditions (Appendix BIR, II-G-1, Volumes III-V). Therefore, the purpose of this review was to determine whether DOE appropriately characterized organic ligands and humic materials on their potential to increase the mobilities of actinides and to evaluate DOE's approaches for representing such processes. EPA's conclusion is that the role of organic ligands will not increase actinide mobility. It would be expected that humic materials increase actinide mobility in a freshwater system, however EPA believes that humic materials will coagulate and settle out in the repository brine. There are, however, uncertainties in DOE's characterization of humic materials.

In order to conduct an objective evaluation of the potential effects which ligands and complexants may have on the Actinide Source Term, the following were reviewed:

- the fundamental chemical phenomena related to aqueous complexation of metals by ligands and humic materials;
- literature specifically tailored to nuclear-waste disposal with an emphasis on salt repositories<sup>3</sup>; and
- sections in Appendix SOTERM dealing with ligands and complexants.

The review, presented below, focused on the fundamental complexation principals and incorporated information gleaned from the available literature.

### 7.1 Introduction to Complexation Chemistry

---

<sup>3</sup>While the complexation of radionuclides has received some research attention over the past several decades, available information was found to be sparse and salt-specific papers were rare.

Complexation (or coordination) chemistry is a broad term referring to the attachment of negative atoms or molecules (anions), neutral polar molecules, or even positive molecules such as amines (e.g.,  $\text{NH}_2\text{NH}_3^+$ ) to cations (often transition-metal cations). Small, highly charged cations generally form the strongest, and hence most stable, complexes. The transition metals are particularly adept at forming such complex compounds. The complexing groups are called ligands. The nonmetallic atom within the ligand that is attached directly to the cation is called the donor atom because it is providing the electron pair needed to form a bond with the cation. The bonds formed are considered to be intermediate in nature between a covalent and an electrostatic bond. Large molecules having multiple functional groups, such as humic and fulvic acid, can also assimilate cations through analogous complexation bonding.

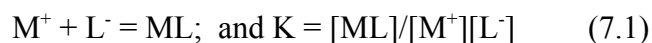
The simplest system, ligands, will be discussed first. This will be followed by a discussion of the more complex chemistry of humic materials (complex ligands) as metal complexants. Finally, a discussion of literature relative to modeling ligand and humic complexation behavior in the environment will be presented.

### 7.1.1 Ligands.

Most anions, such as  $\text{Cl}^-$ ,  $\text{HCO}_3^-$ ,  $\text{CO}_3^{2-}$ ,  $\text{F}^-$ ,  $\text{SO}_4^{2-}$ ,  $\text{NO}_3^-$ , and  $\text{OH}^-$  are examples of inorganic ligands which commonly form complexes with cations in aqueous solutions. Depending on the solution conditions, the stability of the complex may be greater than the stability of either the bare cation or the bare anion. This leads to the formation of an aqueous complex. Numerous geochemical texts discuss the chemistry of these complexes in detail, as well as their implication to the mobilities of cations in natural aqueous systems (Garrels & Christ, 1965; Sawyer & McCarty, 1978; Krauskopf, 1979; Stumm & Morgan, 1981; Dragun, 1988). In fact, complexation chemistry plays a key role in the aqueous behavior of many elements and compounds under natural aqueous conditions.

Organic ligands which attach to the cation at more than one location (by different atoms within the structure of the ligand) are called chelating groups and the complex thus formed is called a chelate. Many synthetic compounds, such as EDTA (ethylenediaminetetraacetic acid) form chelates. EDTA is used in chemical separation processes (Bowen & Gibbons, 1963). DTPA (diethylenetriamine-pentaacetic acid), a similar synthetic compound, has been used to flush metal contaminants (including radionuclides) from humans (Raymond, et.al, 1982). Citrate is an example of a natural organic compound which forms chelates with metal ions using its three carboxylic acid groups. It is used in various chemical processes to sequester aqueous metal cations (Merck Index, 1989).

Sawyer & McCarty (1978) and Dragun (1988) discuss the equilibrium relationships between cations and ligands. For simple 1:1 complexes, the following general reaction is used for the complex formation:



where:  $\text{M}^+$  = the metal cation;  $\text{L}^-$  = the ligand;

$K$  = the equilibrium constant for the reaction; and  
[ ] refer to activities of the dissolved species.

When multiple ligands sequentially attach to the cation, an equilibrium constant can be generated for each successive reaction. Because it is useful to have one equilibrium constant for a series of reactions, the stability constant  $\beta$  is used to represent the overall reactions at equilibrium. Sawyer & McCarty (1978) show that  $\beta$  is equivalent to  $K$  for 1:1 reactions ( $\beta_1 = K_1$ ). However, for the step wise addition of further ligands (1:2, 1:3, etc.),  $\beta_2 = K_1K_2$ ,  $\beta_3 = K_1K_2K_3$ , etc. Because stability constants are based on the ratio of the product activities over the reactant activities, larger  $\beta$  values are associated with more stable complexes. The  $\beta$  values are used to determine the relative stability of various (and often competing) complexation reactions. Therefore, comparison of  $\beta$  values between competing reactions provides an indication of which reaction will dominate an aqueous solution under specific conditions.

Stumm & Morgan (1981) point out that the formation of complexes between metal cations and ligands, as shown in equation 8.1, is in principal no different than the neutralization of acids with bases. Further, the precipitation of a metal cation, often as a hydroxide or oxide solid, is simply an exchange reaction where coordinated water molecules are preferentially exchanged for a ligand.

Stumm & Morgan (1981) state that complexing species (ligands) will tend to increase the apparent solubility of otherwise insoluble metal salts. What is actually happening is that the soluble complex provides an aqueous sink for the metal cations. The intrinsic solubility of the solid phase has not changed but the stabilities of its soluble species are increased by the formation of complexes with the ligands. In essence, the formation of metal-ligand complexes sequester the metal cation into the aqueous phase. Thus, the dissolution reaction continues in an effort to achieve equilibrium between the solid phase and the aqueous phase. Because of the complication brought about by complexing ligands present in solutions, Stumm & Morgan suggest that all significant chemical species and all likely reactions and equilibria potentially available to a solid phase in an aqueous setting need to be considered when predicting a metal's aqueous behavior. In particular, they note that "the smaller the solubility product, the stronger the tendency to form soluble associates". Ligands can form metal buffers in solution analogous to pH buffers for acids and bases.

Dragun (1988) offers the following five general reaction categories for how ligands affect the adsorption of cations on soil surfaces:

- 1) The ligand has a relatively low affinity for both the cation and the soil surfaces. The net result is that the ligand has little effect on the cation's adsorption. The ligand will migrate with the flowing water. The cation's mobility is dependent almost entirely on its  $K_d^4$ . The  $Cl^-$  anion is an example of such a "spectator" ligand.

---

<sup>4</sup>  $K_d$  is a partitioning, or sorption, coefficient defined as the ratio of the cation's concentration in the solid phase to its concentration in the aqueous phase.

- 2) The ligand and the cation form a strong complex which is, in turn, adsorbed onto soil particles. The net result is that the aqueous mobility of both the ligand and the cation are retarded because their complex prefers to be adsorbed. The hydroxide anion is a example of a ligand which promotes this type of behavior.
- 3) The ligand and the cation form a strong complex but that complex has a low affinity for adsorption onto the soil particles. The net result is that the complex migrates with the flowing ground water. EDTA complexed with metal contaminants is an example of this type of behavior.
- 4) The ligand is strongly adsorbed by the soil but it does not complex strongly with the cation. The net result is that the ligand's migration in the ground water is retarded but the cation migrates with the ground water. High molecular weight natural organic compounds tend to sorb strongly onto soil surfaces (e.g., humic compounds such as humic and fulvic acid, discussed later). Examples of the situation described here is fulvic acid in the presence of Zn, Mn and Ca.
- 5) The ligand is strongly adsorbed by the soil and has a strong affinity for the cation. The net result is that the both the ligand's and the cation's migration in the ground water are retarded relative to the flow of the ground water. Examples of the situation described here is fulvic acid in the presence of Fe and Cu. This differs from 2) in that the ligand is first strongly adsorbed, rather than the ligand-metal complex. It then complexes with the cation.

These five general reactions demonstrate various complexing mechanisms of ligands with metals which can influence the mobility of the metals. In some cases, ligands enhance metal mobility and in other cases, they can retard mobility. For example, humic materials (discussed later) can retard metal migration under certain circumstances, such as when the humic molecule itself is attached to an immobile mineral surface. Clearly, the nature of the stability constants for the ligand-metal complexes, coupled with aqueous conditions, will dictate a metal ion's relative mobility compared to the rate of water flow.

#### 7.1.2 Humic Materials.

In addition to inorganic ligands and chelating ligands, there exists a broad class of complexants which are naturally occurring but which can't be classified as simple ligands. These complexants are the humic substances, which can be found in soils, ground waters, and surface waters. They can have a profound influence of the mobility of trace metal contaminants in freshwater systems.

Stumm & Morgan (1981) provide a comprehensive review of humic and related substances in natural aqueous environments. The transformation of biogenic substances (such as vegetative matter) in soil, water, and sediment produces the first class of degradation products, humic materials. Under ideal conditions, further transformation leads to coal, oil, and finally, graphite. However, our interest for this report lies with humic substances because of their predicted production in the WIPP by microbial degradation of cellulose (paper, etc.). This phenomenon is discussed in Section 8. Humic substances are thought to comprise most of the naturally occurring soluble organic matter found in the environment. Consequently, understanding their geochemistry

is important to predicting the mobility of various contaminants.

Stumm & Morgan (1981) describe humic substances as consisting of organic polymers with molecular weights ranging from 300 to 30,000. These substances contain functional groups such as aliphatic hydroxyl groups (alcohols), aromatic hydroxyl groups (phenols), and organic acids (carboxylic acids). These functional groups account for most of the complexation chemistry of humic substances observed in the environment. This includes the ability to form chelates. Humic substances are composed of three fractions:

- 1) humic acid is composed of high molecular weight polymers soluble in alkaline solutions but which will precipitate in acid solutions;
- 2) fulvic acid is composed of lower molecular weight compounds, is soluble over the entire natural pH range, and contains more functional groups than humic substances; and
- 3) humin, which is a fraction that is insoluble in either acidic or basic solutions, and thus is not further discussed.

Humic and fulvic acid are known to concentrate and transport toxic metals in vadose water, ground water, and surface water systems of low ionic strengths. They also have a strong tendency to adsorb onto clay surfaces, hydrous oxide surfaces, as well as other mineral surfaces. Their carboxylic acid groups are particularly able to form chelates with metal cations. Both humic acid and fulvic acid are generally soluble under alkaline conditions. However, they are known to precipitate in the presence of  $\text{Ca}^{2+}$  and  $\text{Mg}^{2+}$ . Humic substances exist in solutions as mostly colloids but  $\text{Ca}^{2+}$  and  $\text{Mg}^{2+}$  tend to coagulate the colloids and ferric oxide tends to stabilize them. River waters rich in humic substances lose these materials upon entering the ocean. This effect is thought to be due primarily with the tendency of  $\text{Ca}^{2+}$  and  $\text{Mg}^{2+}$  to coordinate with carboxyl and hydroxyl functional groups which causes the colloids to coagulate and settle out of solution. This same effect will likely occur in the WIPP should brine inundation occur.

The presence of iron (as metal wastes) and  $\text{Mg}^{2+}$  (as MgO backfill) in the WIPP will make ferric oxides and  $\text{Mg}^{2+}$  available for interaction with humic materials. Whether the humic colloids are precipitated by the  $\text{Mg}^{2+}$  or stabilized by the ferric oxide is uncertain, although the expected reducing conditions of the repository could limit the stabilizing effect of ferric oxide.

### 7.1.3 Interpreting and Modeling the Metal-Complexing Effects of Ligands and Humic Materials.

This section provides a brief review of several textbooks which address the intricacies of interpreting and modeling metal complexes with ligands and humic materials. Some general trends in metal complexation are discussed which are useful for understanding actinide complexation at the WIPP.

The behavior of complexes in natural waters is discussed in detail by Stumm & Morgan (1981). They claim that organic ligands commonly encountered in the environment are able to form “moderately stable complexes with most multivalent cations”. They also suggest that EDTA is not a representative model for organometallic complexes normally found in seawater. They show that, considering only a simple system,  $\text{Ca}^{2+}$  will out-compete  $\text{Fe}^{3+}$  in the presence of a strong complex former such as EDTA because the Ca-EDTA complex is so strong. However, when citrate is the chelating ligand,  $\text{Ca}^{2+}$  is not as dominant. It is further emphasized that in nature, where the aqueous system is likely to be much more complex than laboratory conditions, consideration must be given to the impact of a full suite of available ligands and competing cations if realistic transport predictions are to be achieved. It is noteworthy that no ligand or complexant has been found that is completely specific for one cation. Clearly, competition for complexant sites will occur in any natural aqueous system.

Stumm & Morgan (1981) state that in order to understand natural aqueous systems, the dominant solution variables must be defined. These variables include “major cations, oxidation-reduction status, acid-base components, minor ions, complexing components, and adsorbing surfaces”. In order to model a natural aqueous system using these defined variables, they recommend a systematic approach to evaluate the relative importance of the various components and to establish the aqueous system’s stability. This approach includes evaluating the simple interactions of the major components with the rest of the system followed by the complex interactions of the minor components. They introduce the concept of multimetal, multiligand models to achieve this goal. The type of questions to be answered by the modeling include metal-ion speciation variation with the addition of ligands; the effect of pH change on free metal concentrations; the effect of metal-adsorbing particles on metal-ion speciation; the competition between metal-adsorbing particles and soluble ligands for the metal cations; and the chemical speciation resulting from anoxic conditions.

Stumm & Morgan (1981) summarize their discussion of the difficulty of modeling aqueous systems by describing the complicated network of interactions between metals,  $\text{H}^+$ , and ligands. They state on page 394 that:

“because each cation interacts and equilibrates with all ligands and each ligand similarly equilibrates with all cations, the free concentration of metal ions and the distribution of both cations and ligands depend on the total concentrations of all the other constituents of the system [70,71]. The addition of Fe(III) (or of any other metal) to a water medium, for example, in a productivity experiment, produces significant reverberations in the interdependent “web” of metals and ligands and may lead to a redistribution of all trace metals (hence an observed change in productivity is not necessarily caused by a change in

the availability of Fe to the cell)".

Dragun (1988) states that, generally, the affinities of cations for humic compounds decrease in the order trivalent cations > divalent cations > monovalent cations. He further notes that while fulvic acids are soluble over most of the pH range for natural systems, metal cations can form water insoluble metal-fulvic complexes which precipitate. A fulvic acid to metal ratio > 2 generally promotes the formation of soluble complexes although trivalent and divalent metals tend to form insoluble complexes over the pH range of 5-7.

Forstner & Wittmann (1981) discuss the ability of organic compounds in water to influence the distribution of metal cations in the following ways:

- 1) complexing metals and increasing their aqueous concentrations;
- 2) affecting the distribution between oxidized and reduced forms of the metals;
- 3) reducing metal toxicity to aquatic life by sequestering the metal;
- 4) affecting the distribution of metals between the aqueous phase and suspended solid phases; and
- 5) affecting the stability of colloids containing the metals.

Consistent with Dragun (1988), Forstner & Wittmann also noted that fulvic acid was particularly important to the migration of heavy metals owing to its lower molecular weight, greater number of functional groups, and higher solubility compared to humic acid.

#### 7.1.4 Summary.

In summary, the intent of this section is to show that the chemistry of low temperature, dilute, aqueous systems containing metals, ligands, and complexants under typical natural conditions can be very complicated.

### 7.2 Importance of Ligands and Complexants to WIPP Actinide Mobility

Within the background context presented in Section 7.1, the literature review was expanded to include information more directly relevant to WIPP repository conditions. The result of that review is presented in this section.

Numerous DOE reports and documents are available which predict that the chemistry of a brine-invaded WIPP repository will be complicated (e.g., Brush, 1990; Brush, 1995; Novak, et. al, 1995; Pepenguth, et. al, 1996; SNL, 1996; and USDOE, 1996a). Because a mobile actinide source term can only occur under aqueous conditions, the presence of brine is required before actinide solid phases can dissolve and become mobile, ligands can complex actinides and cause them to be mobile, microbes can cause cellulosic degradation to form humic materials, or gases can be generated. While human intrusion by drilling may bring brine to the repository, it will be a brief event compared to the 10,000-year life of the repository.



Much of the geochemistry and microbiology of the WIPP site relies on the presence of an aqueous phase to promote potential reactions which could lead to formation of a mobile actinide source within the repository. Therefore, in order to evaluate work completed by DOE supporting the source-term predictions, EPA has assumed that brine will be present and that it will be commingled with the waste during much of the repository's performance period.

As discussed in Section 7.1, it should be understood that ligands and natural humic complexing agents can complex with actinides, transition metals, and alkaline-earth elements (primarily divalent cations of calcium and magnesium) and raise their mobile aqueous concentrations above that predicted by dissolution of their individual solubility-controlling solid phases. This does not cause a change in the intrinsic solubility of the solid phases, but the complexing agents act as a mobile aqueous sink for the cations which allows for progressively more solid phase dissolution with increased complexing agent availability. Thus, the mobile actinide concentration is increased.

Both the ligands and humic complexants will be available in the repository brine for reaction with actinides, alkaline earth elements, and transition metals depending on their various aqueous concentrations (soluble plus colloidal concentrations). The concentrations of actinides in brines is dependant upon all possible reactions of all the alkaline-earth and metal ions and actinide species with all of the ligands and humic materials, which will determine the mobile concentration of each ion and each actinide species. The discussion which follows is a brief review of the literature regarding the complexation of divalent cations and actinides by these complexing agents. The purpose of the literature review is to provide background information on complexation phenomena so that the evaluation of SOTERM, discussed later, can be more easily understood. Sections 7.2.1 and 7.2.2 first provide brief descriptions of the sources of ligands and humic materials, respectively, in the WIPP.

#### 7.2.1 Organic Ligands.

DOE has defined an inventory for synthetic ligands (such as EDTA) and natural ligands (such as acetate, oxalate, lactate, or citrate). These compounds were used during chemical processing and are included as waste with the other TRU wastes. Consequently, they are expected to be present in the TRU waste brought to the WIPP (Appendix BIR, II-G-1, Volumes III-V). Appendix SOTERM provides a summary of that inventory amount (in grams) in Table SOTERM-4 for the ligands acetate, oxalate, citrate, and EDTA. This table also includes potential concentrations of these ligands in an inundated repository. These four ligands form aqueous complexes with actinides potentially increasing actinide mobility, depending on concentrations and conditions. Thus, knowledge of their behavior may be important to establishing actinide mobility under WIPP disposal conditions. However, as DOE correctly states in SOTERM, alkaline-earth and transition metal ions will be available to compete with the actinides for complexation with the ligands.

Other organic waste compounds will also likely be part of the materials disposed at WIPP. These compounds could include RCRA wastes (as defined in 40 CFR 261) but there is no reason to disagree with DOE's contention that the impact of such RCRA wastes on actinide mobility will be negligible compared to the impact of the ligands mentioned above (see Bynum [1997a] for additional details on DOE's position).

### 7.2.2 Humic Materials.

In addition to the presence of chemical processing ligands, two sources for humic materials are also expected to be included with the wastes. One is disposed soils and the other is the cellulosics component of the waste. The soil contains some naturally occurring humic substances as part of its organic fraction. In one DOE test plan (Papenguth and Behl, 1996), this was considered to be the main source. However, SOTERM recognized that the main source for humic materials would more likely be microbial degradation of waste cellulosics, rather than soil.

Providing that brine is present, the microbial fauna will likely degrade the cellulosics and produce humic materials, carbon dioxide gas, and methane gas as byproducts. Because the amount of cellulosic material in the repository is expected to be high, there is a potential for a relatively large supply of complexing humic materials (humic and fulvic acids) to be available for complexing the aqueous actinide species and metal cations. However, humic and fulvic acids tend to form colloids in brine that would be expected to coagulate and settle out of solution (Hounslow, 1995).

### 7.2.3 Transition Metal Complexation.

Nowack, et al. (1997) investigated the influence of both natural and anthropogenic ligands on the aqueous transport of metals. They evaluated the effect of EDTA on the remobilization of metals during the infiltration of surface water from a river to the ground water. Metals such as Zn, Cu, and Ni and the alkaline-earth element Ca were successful in dislodging Fe(III) from EDTA at pH values >7 as the Fe(III)-EDTA complex flowed through an infiltration path contaminated with heavy-metals. With pH values <7, the Fe(III)-EDTA complex was stable and exchange by heavy metals was less likely. Thus, pH can strongly influence competition of metals for ligand complexation sites.

Choppin and Shanbhag (1981) studied the complexation of calcium by humic acid using a solvent extraction procedure (in a low pH, relatively low ionic strength solution). They found that the binding constant increased over an order of magnitude when the pH was increased from 3.9 to 5.5 in 0.1 M NaClO<sub>4</sub>. Log b varied from 2.25 to 3.9 over this pH range. They also confirmed that only a 1:1 complex was formed under these conditions. While not directly relevant to the WIPP conditions, it does show that calcium can be bound by humic acid.

It should be understood that such studies are often conducted under acidic conditions because actinide concentrations (solubility driven concentrations) are usually higher than those found in alkaline solutions. Solubilities of actinide solids are generally low in the WIPP alkaline solutions (see Section 4). Thus, due to relatively high analytical detection limits available to the experimenter, practical considerations often dictate that the experiments be conducted in acidic solutions. This has been a problem for the WIPP studies where acidic laboratory conditions do not represent expected alkaline repository conditions. DOE has argued that acidic conditions are more

conservative than alkaline conditions owing to these generally higher solubility concentrations of actinides in acidic solutions.

Schnitzer & Skinner (1967) measured the fulvic-acid stability constants for the divalent cations of Pb, Ni, Mn, Co, Ca, and Mg in low ionic strength solutions. Log stability constants varied from 1.23 to 3.47 at pH 3.5 and 2.09 to 6.13 at pH 5.0 for this suite of cations. This indicated that higher pH values lead to higher stability constants consistent with the observations of Choppin and Shanbhag (1981). At pH 3.5, the decreasing order of the stability constants was Ni>Pb>Co>Ca>Mn>Mg. At pH 5.0, the decreasing order of the stability constants was Pb>Ni>Mn≈Co>Ca>Mg. Under these conditions, the heavy metals generally showed consistently higher stability constants than the transition metals, with Mn being anomalous.

The importance of transition metal complexation is that available transition metal cations, while mostly divalent, could still successfully compete with multivalent actinide species for humic-material binding sites, thus rendering the humic materials unavailable for binding with, and thus potentially mobilizing, the actinides. The competition between transition metals and actinides is dependent on their relative concentrations, their relative abilities to bind with the humic materials (the relative strength [higher  $b$  values] of their complexes), and other confounding reaction mechanisms, such as the formation of ternary complexes discussed in Section 7.2.4. Appendix SOTERM introduced the competition concept and provided some limited data to show that the binding sites on the humic materials would be overwhelmed by the availability of relatively high concentrations of transition metals compared to actinide concentrations. This issue is developed in more detail below.

#### 7.2.4 Actinide Complexation

Studies have been completed that address the binding of actinide elements by humic materials. Kim & Sekine (1991) investigated the complexation of Np(V) with humic acid in 0.1 M NaClO<sub>4</sub> over the pH range of 6-9 where the NpO<sub>2</sub><sup>+</sup> ion is unhydrolyzed. The humic acid was extracted from Gorleben groundwater (of low ionic strength). They reported that only a 1:1 complex was observed. Consistent with the reports discussed above, log  $b$  values increased systematically with pH (2.28 at pH 6 to 3.10 at pH 9). The authors point out that the NpO<sub>2</sub><sup>+</sup> ion has a relatively low complexation constant with humic acid compared to other actinides, in the range of the divalent calcium cation. While the ionic strength of the aqueous solution is much lower than WIPP brines, at least this study approached the high pH conditions expected at the MgO-backfilled WIPP.

Rao & Choppin (1995) investigated the pH dependence of ligand binding constants with Np(V) over the pH range of 4.5-7.5 in 0.1 M NaClO<sub>4</sub> at 25°C. They did not find a pH dependency for binding of this actinide under the experimental conditions utilized. The log  $b$  values varied from 2.15 to 2.44 over this pH range for humic materials having different sources and molecular weights. They suggested that Np(V) probably only forms a 1:1 complex with the humic molecules' carboxyl groups.

Choppin and Nash (1980) investigated the complexation of Th(IV) with both humic and fulvic acids. The authors observed high complex stability and indicate that two types of binding

sites are present for Th(IV) on these organic acids. They calculated the  $[ThHu]/[Th] \approx 4 \times 10^{10}$  and suggest that without the availability of competing ligands, such as carbonate and hydroxide anions, Th(IV) would be complexed completely by humic materials.

Under WIPP conditions, inorganic and organic ligands may be available to compete with humic materials for complexation with the actinides. In addition, numerous transition-metal cations may be available to compete with the actinides for these complexant's binding sites. While the humic materials may or may not themselves be mobile, transition metals may replace the actinides at humic binding sites. This would, in effect, "force" the actinides into the brine phase, because the actinides would no longer be sequestered by the humic materials and precipitated. The resultant actinide aqueous concentration will be controlled by the actinide solid phase or by the availability of other inorganic and organic ligands. Because of the numerous possible reactions available, the WIPP actinide source-term experimentation and modeling efforts must be able to predict actinide mobility under such chemically competitive conditions and take into account the impact of various complexation mechanisms, such as the formation of ternary complexes.

### 7.3 Evaluation of SOTERM Relative to Ligands and Humic Materials

Two segments of DOE's CCA Appendix SOTERM (1996) are discussed below. Section SOTERM.5 is titled "The Role of Organic Ligands". Section SOTERM.6 is titled "Mobile Colloidal Actinide Source Term". This later section contains subsection SOTERM.6.3.3 titled "Humic Substances". Only the subsection will be discussed herein.

#### 7.3.1 Ligands.

Section SOTERM.5 briefly discusses the potential impact which four key ligands (acetate, citrate, oxalate, and EDTA), which are expected to be present in the WIPP wastes, could have on actinide mobility. It was stated that these ligands could increase the dissolved actinide concentrations in the brine. Consequently, DOE performed an analysis of the "effect of organic liquids" on actinide mobility. It is assumed that "liquids" is a typographic error and that "ligands" was intended. The discussion was limited to these four ligands because the authors claim that due to the expected competition from multivalent metal cations, which are also expected to be present in the waste, these organic ligands "will not be available to complex the actinides and thus will not impact dissolved actinide concentrations in the WIPP". Interestingly, the metals chosen for study ( $Fe^{2+}$ ,  $Ni^{2+}$ ,  $Cr^{2+}$ ,  $Mn^{2+}$ ,  $V^{2+}$ ,  $Cu^{2+}$ , and  $Pb^{2+}$ ) are all divalent, as shown in Table SOTERM-7, rather than being multivalent. Further,  $Cr^{2+}$  and  $V^{2+}$  are metastable in aqueous conditions whereas  $Cr^{3+}$  and  $V^{3+}$  would be expected to be stable. Because repository conditions will probably be reducing,  $Cu^+$  is likely be present instead of  $Cu^{2+}$ .

The text states that reactions with organic ligands and actinides generally form 1:1 complexes and, contrary to Hummel (1995), no mention of ternary complexes is offered. DOE defines the apparent stability constant  $b$  in a manner consistent with that presented in Section 7.1 of this report.

DOE states in SOTERM that "about 60 organic compounds" could be included in the WIPP wastes but based on screening studies at Florida State University, only ten of these compounds were considered to have the potential of enhancing actinide concentrations in the brine. Further work

narrowed the study candidates to five compounds. The selection of the four ligands included in Appendix SOTERM was based on the fact that they are expected to be present in the waste, along with others, and that they are the only water soluble compounds present in “significant quantities” such that they may have an impact on actinide mobility. As stated in Section 7.2.1, EPA found no compelling reason to disagree with DOE’s logic to select only these four ligands for actinide source-term evaluation.

Table SOTERM-4 provides an estimate for the repository inventory of these four compounds. Also shown are their concentrations, based on dividing their inventory quantities by the repository’s brine volume. This volume was chosen by DOE to be the least amount which could credibly cause transport of waste materials from the repository. The order of decreasing predicted repository concentration shown in Table SOTERM-4 is citrate > acetate > oxalate > EDTA with the following estimated concentrations:  $1.1 \times 10^{-3}$  m acetate,  $4.7 \times 10^{-4}$  m oxalate,  $7.4 \times 10^{-3}$  m citrate,  $4.2 \times 10^{-6}$  m EDTA. The calculations of the effects of organic chemicals on the aqueous speciation of actinides were based on these calculated organic concentrations.

DOE states in SOTERM that the apparent stability constants for organic ligand-actinide complexation ( $\beta$  values) were determined at Florida State University. WIPP document WPO-35307 (1996) describes the source of the  $\beta$  values tabulated in Table SOTERM-5. Comparison of the Table SOTERM-5 log  $\beta$  values with the log  $\beta$  versus NaCl molality plots showed significant differences. For example, Table SOTERM-5 values for  $\text{Am}^{3+}$  complexed with citrate were -4.84 to -5.9 (log values). Reading the WPO-35307 plots provided log values of -10.1 to -10.2--a difference of 4-5 orders of magnitude. However, subsequent discussions with Sandia National Laboratories staff (Robert Moore) indicated that the WPO-35307 plots had several errors. Sandia provided EPA with a revised document (Moore, 1996) which corrected the errors. Therefore, EPA concluded that the values in Table SOTERM-5 accurately represented the Florida State University experimental results.

The authors of SOTERM state that “complexation constants” (apparent stability constants  $\beta$ ) for each ligand-actinide combination (no Pu values are shown in Table SOTERM-5) were determined with the Pitzer formulation for high ionic strength solutions using the NONLIN computer code. These results were added to the FMT code and calculations were performed to “evaluate competition among complexing sites”. The authors further state that Florida State University experimentally determined the log  $\beta$  values under high molal solutions of NaCl (3-5m) for Mg complexed by acetate, oxalate, citrate, and EDTA in order to include the effects of the Mg backfill material in the competition calculations. With these data, the output from the FMT code was said to have calculated the equilibrium solubility (aqueous concentration) of the actinides under repository conditions.

To further demonstrate that there was competition for ligand sites by aqueous species other than actinides or  $\text{Mg}^{2+}$ , the authors discuss the sources for transition metals that could be available to the repository brines. Corroded iron and steel in the waste are said to contribute Fe, Ni, Cr, V, and Mn to the brine. Further, Pb is expected to be a waste component. Literature sources for log  $\beta$  values determined for  $\text{Fe}^{2+}$ ,  $\text{Ni}^{2+}$ ,  $\text{Cr}^{2+}$ ,  $\text{Mn}^{2+}$ ,  $\text{V}^{2+}$ ,  $\text{Cu}^{2+}$ , and  $\text{Pb}^{2+}$  are shown in Table SOTERM-7 for EDTA. Fewer of these metals’  $\beta$  values are variously listed for citrate, oxalate, and acetate. All of the data are from experiments using low ionic strength solutions so that the relevance to the WIPP repository conditions is uncertain.

In order to try and assess the impact that these divalent metal cations might have on available ligand adsorption sites, competition calculations (not experiments) were conducted for conditions of low ionic strength NaCl solutions (not brines) containing EDTA (as a test case owing to its known strong complexation affinities [high  $\beta$  values] for transition metals) and saturated with iron hydroxide (presumed to be ferrous iron hydroxide,  $\text{Fe}(\text{OH})_2$ , based on listing  $\text{Fe}^{2+}$  in the Table SOTERM-7 and showing  $\text{Fe}^{2+}$  in the  $\beta$  equations on page SOTERM-40), nickel hydroxide, and MgO. The results of the calculations are claimed to show that 99.8 percent of the EDTA is complexed with Ni. The claim is also made that both Ni and Fe have relative high solubility under high ionic strength conditions compared to low ionic-strength conditions. DOE states that the calculations demonstrate the ability of Ni to cause EDTA to be “unavailable for complexation with the actinides and rendering complexation of actinides by organic ligands inconsequential”.

The approach of using scoping equilibrium calculations is a good start to developing the transition metal-actinide competition issue further. However, the text states that a Ni concentration of  $3.65 \times 10^{-4}$  molal was used in these calculations. In contrast, Savage (1995) provides a thorough review of Ni geochemistry in the context of its expected behavior in the environment of a nuclear waste repository. He reviews the literature on Ni geochemistry and concludes, based on numerous observations of natural Ni concentrations in surface and ground waters, that the expected concentration of Ni in the environment should be  $<10^{-8}$  molal. Even in areas with hyperalkaline springs and ophiolitic rocks high in Ni, the Ni concentration in the associated waters is on the order of  $2 \times 10^{-8}$  molal. It is possible that in an artificial environment with corroding Ni steels that Ni concentrations could be higher, but DOE does not provide experimental evidence supporting this possibility.

Hummel (1993) investigated the effect of organic ligand complexation of radionuclides in cement pore water where pH values exceeded 11. He found that for EDTA complexes with transition metals and radionuclides, Ca-organic or metal-hydroxy complexes were able to prevent EDTA, NTA, citrate, or oxalate from influencing radionuclide speciation. Because the conditions were similar to those expected for the WIPP, this report supports DOE’s contention that ligands will have a negligible affect on actinide mobilization in the WIPP.

To gain insight into the potential for ligand-enhance actinide solubility, EPA performed a modeling exercise with EDTA and thorium to estimate the effect of EDTA on the brine concentration of thorium (using the solid phase  $\text{ThO}_2[\text{am}]$ ). The result of that modeling exercise is presented in the following section. These results tend to support DOE’s contention that ligands probably will not cause significant enhancement of actinide mobility under WIPP disposal conditions, at least for EDTA complexing with thorium.

### 7.3.1.1 Effects of EDTA on ThO<sub>2</sub>(am) Solubility

Organic ligands have the potential to affect the solubilities of actinide solids in the repository through the formation of aqueous complexes with dissolved actinides. In Appendix SOTERM of the CCA, these effects are discounted because the organic compounds are expected to be present in low concentrations and hypothesized to be consumed by complexation reactions with other soluble ions (i.e., iron, nickel, calcium, magnesium, sodium, etc.) that will be present in much greater concentrations in the brines than the actinides.

To explore this hypothesis, the effects of EDTA on the solubility of ThO<sub>2</sub>(am) were examined by EPA as a test case. EDTA was chosen among the organic ligands because it has the strongest tendency to complex metals, including the actinides (see Table SOTERM-5 in the CCA); hence, it is expected to be the organic ligand most likely to have an effect on the predicted solubilities of actinide solids. Table 7-1, below, shows the relative stability constants for the four major ligands and illustrates that EDTA has the highest affinity for complexation of the four:

Table 7-1

Organic Complex	log Stability Constant	Organic Ligand (m)	Th(IV) (m)	Product $\beta[\text{Th(IV)}][\text{EDTA}]$
Th(IV)-EDTA	16.25	$4.2 \times 10^{-6}$	$1 \times 10^{-8}$	747
Th(IV)-acetate	3.93	$1.1 \times 10^{-3}$	$1 \times 10^{-8}$	$9.7 \times 10^{-8}$
Th(IV)-oxalate	7.26	$4.7 \times 10^{-4}$	$1 \times 10^{-8}$	$8.6 \times 10^{-5}$
Th(IV)-citrate	9.75	$7.4 \times 10^{-3}$	$1 \times 10^{-8}$	0.4

As shown by these calculations, the affinity for Th(IV) to form an organic complex with EDTA is about 3 orders of greater than for citrate, which has the next highest affinity. Consequently, it is appropriate to use the Th(IV)-EDTA complex for any bounding calculations to assess the effects of organic ligands on the aqueous speciation of the actinides and solubilities of the actinide solids for the brine solutions expected to infiltrate into the repository over time. There is no reason to consider the other organic ligands (i.e., acetate, oxalate, and citrate) because their potential to complex the actinides is so much less than EDTA.

To assess the effects of EDTA to complex Th(IV) in a brine solution, DOE conducted a series of speciation calculations, considering the probable concentrations of major solutes (e.g., Mg<sup>2+</sup>) and metals (e.g., Fe<sup>2+</sup>, Ni<sup>2+</sup>) expected to be present in the brines and also known to form complexes with EDTA. These calculations are described on pages SOTERM-40 to 41 in Appendix SOTERM of the CCA. The calculation results indicated that only 3% of the EDTA was complexed with EDTA. The remainder of the EDTA was tied up with Mg<sup>2+</sup>, Fe<sup>2+</sup>, and Ni<sup>2+</sup>. This finding indicates that the even for the organic complex with the highest potential to form an organic complex [i.e., Th(IV)-EDTA] very little of that organic complex will actually be present because of

the vast majority of the EDTA will form complexes with other ions present in much higher concentrations than the actinides.

In EPA's review of the actinide source term, an independent calculation of the potential effects of EDTA on the solubility of  $\text{ThO}_2(\text{am})$  was conducted to determine whether the calculations were sensitive to the EDTA concentration. The solid,  $\text{ThO}_2(\text{am})$ , was used because it is expected to control the Th(IV) concentrations in the repository environment based on experimental investigations and FMT model calculations (Novak and Moore, 1996; Novak et al. 1996; 1997). Also, as noted above, among the actinides, aqueous Th(IV) has the highest tendency to be complexed by EDTA. Based on these factors, the EDTA-Th(IV)-brine system should provide the greatest possibility for an organic ligand to affect the prediction of the solubility of an actinide solid.

The solid,  $\text{ThO}_2(\text{am})$ , was also chosen for EPA's test case because it is expected to control the Th(IV) concentrations in the repository environment based on experimental investigations (Felmy et al. 1991; 1996) and FMT model calculations (Novak and Moore, 1996; Novak et al. 1996a; 1997). Also, among the actinides, aqueous Th(IV) also has the highest tendency to be complexed by EDTA (Table 7-1). Based on these factors, the EDTA-Th(IV)-brine system should provide the greatest possibility for an organic ligand to affect the prediction of the solubility of an actinide solid.

The PHREEQC geochemical model (version 1.5) (Parkhurst, 1995) was used for the solubility calculations. PHREEQC is a well established model that has been used for a variety of problems in aqueous geochemistry for a number of years. It also has the capability to use the MINTEQA2 database of equilibrium constants developed by the EPA (Allison et al. 1990), which includes a number of reactions involving EDTA (Table 7-2). This database was augmented with the Th(IV) species in Table 7-2, for which equilibrium constants were calculated from the chemical potentials provided in the FMT database (Novak, 1997).

The formulations for activity coefficients incorporated in PHREEQC are not representative of high ionic strength solutions, hence the  $\text{ThO}_2(\text{am})$  solubility calculations were performed for the SPC brine diluted 10 times (Table 7-3). Although this solution composition may not be exactly representative of the repository environment, the resulting calculations still provide a reasonable approximation of the effects of EDTA concentration on  $\text{ThO}_2(\text{am})$  solubility. Additionally, the solubility calculations were conducted for a constant  $\text{CO}_2(\text{g})$  partial pressure of  $10^{-5.5}$  bars, which is the level expected for equilibrium between brucite [ $\text{Mg}(\text{OH})_2$ ] and hydromagnesite [ $\text{Mg}_5(\text{CO}_3)_4(\text{OH})_2 \cdot 4\text{H}_2\text{O}$ ] resulting from reactions between the MgO backfill and SPC brine (see Sections 3 and 4). The maximum EDTA concentrations expected for the repository are estimated at about  $4.2 \times 10^{-6}$  m (see Table SOTERM-4 in the CCA). Thus, the  $\text{ThO}_2(\text{am})$  solubility calculations were conducted for an EDTA concentration range of  $4.2 \times 10^{-6}$  m to  $4.2 \times 10^{-2}$  m.

The results of the solubility calculations for  $\text{ThO}_2(\text{am})$  indicate that the effect of EDTA is negligible at concentrations less than about  $4.2 \times 10^{-4}$  m (Figure 8-1), which is 100 times the concentration estimated for the inundated repository. For example, at the estimated EDTA concentration of  $4.2 \times 10^{-6}$  m, Th(IV) levels were not different from solutions without EDTA over the pH range of about 3 to 11. At an EDTA concentration  $4.2 \times 10^{-2}$  m, which is 10,000 times the level estimated for the repository, an increase in Th(IV) concentrations is predicted for pH less than



about 7.5 (Figure 8-1). At higher pH, the EDTA has no substantial effect on ThO<sub>2</sub>(am) solubility because aqueous Th(IV) speciation is dominated by hydroxyl, carbonate, and sulfate complexes rather than EDTA complexes. The EDTA is predicted to be present primarily as complexes with Ca<sup>+2</sup> and Mg<sup>+2</sup> under alkaline conditions.

Also shown in Figure 7-1, are the concentrations of Th(IV) predicted by the FMT code for the SPC and ERDA-6 brines for similar conditions (from Tables 4-8 and 4-9). The FMT-predicted Th(IV) concentrations fall close to the line predicted by the PHREEQC model, indicating that PHREEQC provides a reasonable approximation of ThO<sub>2</sub>(am) solubility for the brines for the conditions considered. Based on the results of these calculations for Th(IV) and EDTA, and understanding that the EDTA-Th analysis is a conservative assessment of actinide-organic ligand behavior, the organic ligands are not expected to have an appreciable effect on the solubilities of actinide solids at the concentrations estimated for the repository. At higher concentrations, organic ligands may affect actinide solubilities, but at least for EDTA, concentrations 100 times greater than the estimated concentration are required and the effect is limited to neutral to acidic conditions not expected in the presence of the MgO backfill.

Table 7-1. Reactions involving EDTA in the MINTEQA2 version of the PHREEQC database relevant to calculations of ThO<sub>2</sub>(am) solubility in SPC (Salado) brine.

Reaction	log K (25°C)	Source
H+ + EDTA-4 = HEDTA-3	9.96	MINTEQA2
2H+ + EDTA-4 = H2EDTA-2	16.21	MINTEQA2
3H+ + EDTA-4 = H3EDTA-	18.86	MINTEQA2
4H+ + EDTA-4 = H4EDTA0	20.93	MINTEQA2
5H+ + EDTA-4 = H5EDTA+	23.46	MINTEQA2
Ca+2 + EDTA-4 = CaEDTA-2	12.4	MINTEQA2
Ca+2 + EDTA-4 + H+ = CaHEDTA-	16	MINTEQA2
K+ + EDTA-4 = KEDTA-3	1.7	MINTEQA2
Mg+2 + EDTA-4 = MgEDTA-2	10.6	MINTEQA2
Mg+2 + EDTA-4 + H+ = MgHEDTA-	15.1	MINTEQA2
Na+ + EDTA-4 = NaEDTA-3	2.5	MINTEQA2
Th+4 + 4H2O = Th(OH)40 + 4H+	-19.17	FMT
Th+4 + 5CO3-2 = Th(CO3)5-6	27.13	FMT
Th+4 + 3H2O + CO3-2 = Th(OH)3CO3- + 3H+	-3.73	FMT
Th+4 + 2SO4-2 = Th(SO4)20	11.63	FMT
Th+4 + 3SO4-2 = Th(SO4)3-2	12.46	FMT
ThO2(am) + 4H+ = Th+4 + 2H2O	10.5	FMT

Th+4 + EDTA-4 = ThEDTA0	15.56-16.94a	Table SOLTERM-5
Am+3 + EDTA-4 = AmEDTA- b	13.76-15.1	Table SOLTERM-5
NpO2+ + EDTA-4 = NpO2EDTA-3 b	5.45-6.7	Table SOLTERM-5
UO2+2 + EDTA-4 = UO2EDTA-2 b	10.75-12.16	Table SOLTERM-5

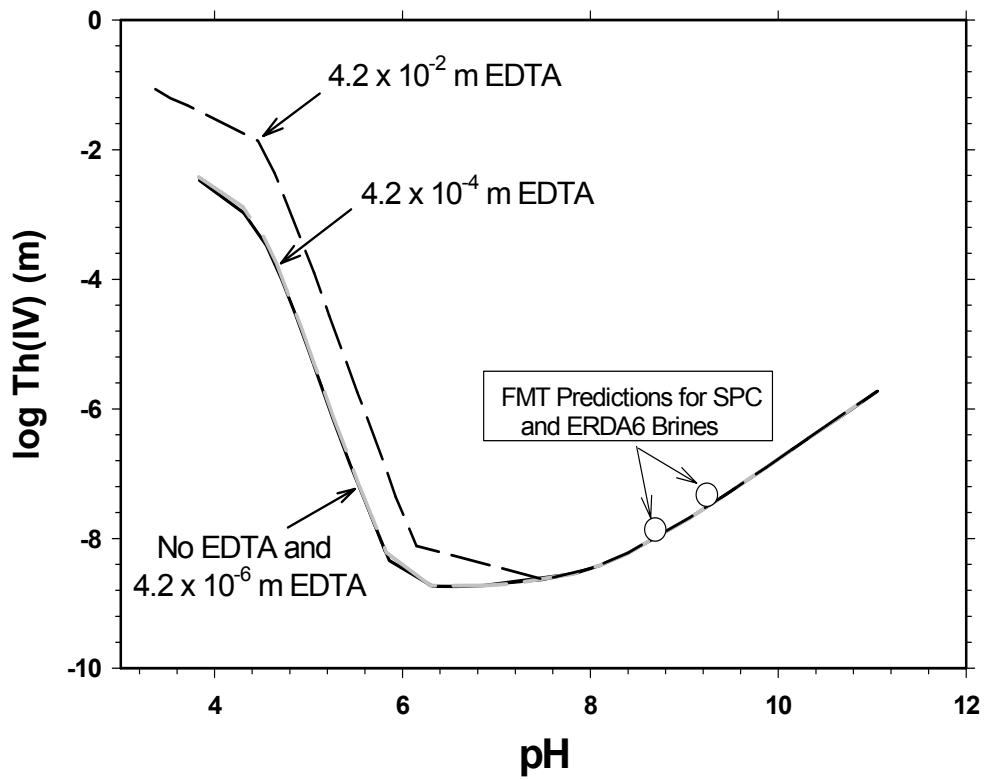
a - log K = 16.94 used in PHREEQC runs on ThO<sub>2</sub>(am) solubility.

b - Shown for comparison, but not included in PHREEQC runs on ThO<sub>2</sub>(am) solubility.

Table 7-2. Solution composition used for PHREEQC calculations of the effects of EDTA on ThO<sub>2</sub>(am) solubility.

Analyte	Concentration (molal)
Na	0.183
K	0.077
Mg	0.144
Ca	0.002
Cl	0.535
SO <sub>4</sub>	0.004
B	0.002
log [CO <sub>2</sub> (g)] (bars)	-5.5
EDTA	0-0.042

Figure 7-1. Solubility of  $\text{ThO}_2(\text{am})$  with pH at 25(C in SPC brine diluted 10 times predicted with the PHREEQC model for a range of EDTA concentrations.



### 7.3.2 Humic Materials.

Section SOTERM.6.3.3 provides an introduction to the chemistry of humic materials and discusses the potential impact of this group of natural organic compounds on actinide mobility under WIPP conditions. The authors state that waste soil could introduce humic materials but that a greater source is probably microbial degradation of waste cellulose. Generally, it was stated that the solubility of humic materials generated in the repository would control their ability to mobilize actinides. Once their solubility is determined, establishing the ability of these substances to bind with actinides in solution is needed to assess their overall potential impact on actinide mobility.

Solubility experiments for five humic substances performed at Sandia National Laboratories were said to have been completed from both the undersaturated and the over saturated directions in brines variously containing  $\text{Ca}^{2+}$  and  $\text{Mg}^{2+}$ , in addition to the NaCl brine matrix. While the concentration of  $\text{Na}^+$  had little effect on humic substance solubility,  $\text{Ca}^{2+}$  and  $\text{Mg}^{2+}$  had a greater effect, that being a decrease in solubility. The results of these experiments provided a solubility range for humic acid of 1.5 mg/L to 2.0 mg/L in NaCl brines with  $\text{Ca}^{2+}$  and  $\text{Mg}^{2+}$  concentrations >10mM.

The SOTERM discussion describing DOE's determination of the aqueous concentration of humic materials expected under WIPP conditions is confusing. It is stated on page SOTERM-59, as mentioned above, that the "solubility" was measured at Sandia. This implies, by the general chemical definition of solubility, that the solubility values provided refer to the concentration of dissolved, ionized humic molecules (they "become molecularly or ionically dispersed in the solvent to form a true solution" [Lewis, 1993]). SOTERM variously describes the humic-actinide association as the mobile fraction, the soluble fraction, and the humic-bound colloidal actinides. Humic solubility is referred to as "the concentration of reactive humic substance in the aqueous phase" (page SOTERM-58). Because the aqueous chemistry of dissolved, colloidal, and suspended (mobile, but larger than colloidal particles) humic materials can differ, it is important to define what form of humic materials the "solubility" value (2.0 mg/l) used in SOTERM refers. To clarify this issue, DOE provided a memo describing the origin of the "solubility" value used in SOTERM (Bynum, 1997b). This value resulted from a simple experiment where known quantities of humic materials were added to a WIPP brine solution, shaken, and allowed to settle for several days. Brine was then pipetted from the upper portion of the container and analyzed for humic material concentration. The result of the analysis provided values between 1.5 mg/l and 2.0 mg/l. The higher value was selected for DOE's calculations.

It is clear that "solubility" values thus obtained refer to an approximation of the "mobile" fraction which includes the dissolved fraction, colloidal fraction, and suspended fraction. Thus, the 2.0 mg/l value can be accepted as conservative (i.e., it bounds the high concentration value) if it is assumed that the value will not increase over the repository's 10,000-year regulatory lifetime and that actinide binding constants are the same for all three fractions. Further, relatively low mobile concentrations of humic and fulvic acids are expected in the brines owing to their tendency to flocculate and precipitate in such high ionic-strength solutions (Hounslow, 1995). This is consistent with the mobile concentration value.

Florida State University determined site binding capacity for two of the humic acids and

obtained literature values for the one fulvic acid used. Values ranged from 1.5-9.5 meq OH<sup>-</sup>/g. Binding capacity provides some insight to the potential number of active binding sites per mass of humic substance available to aqueous species. Higher values indicate that the substance has more binding sites than materials with lower values. It should be understood that actinide binding may be different than OH<sup>-</sup> binding on these molecules (i.e., species specificity for certain binding sites). Loading the humic materials with WIPP-appropriate actinide species, instead of OH<sup>-</sup>, may result in different binding capacities, although it is not certain that they would be higher than the values obtained for OH<sup>-</sup>.

Florida State University was then said to have performed binding studies of Am<sup>3+</sup> and UO<sub>2</sub><sup>2+</sup> with the two humic acid and one fulvic acid substances. The studies were done in brine solutions at low pH (4.8-6) and without MgO backfill material present although the authors still claim that the results should provide conditions leading to maximum uptake of these two actinides by the humic substances. They also claim that the Mg<sup>2+</sup> from the MgO backfill will successfully compete with the actinides, although this is contrary to much of the discussion provided in Section 7.2.2. Table SOTERM-11 provides the results of the experiments at pH 6 and in a NaCl brine with a concentration of 6 molal. Log β values (including β<sub>1</sub> and β<sub>2</sub> values) for all of the experiments ranged from 4.6-10.46. These are relatively high values compared to acetate, citrate, and oxalate values but generally lower than EDTA values.

Based on the Florida State University results, the Appendix SOTERM authors state that the consistency in the log β results for Am<sup>3+</sup> and UO<sub>2</sub><sup>2+</sup> and the lack of a NaCl concentration effect justifies the use of published stability constants for the other actinides. Appendix SOTERM refers to the work of Choppin & Nash (1980) where the stability constants for Th(IV) complexed with several humic and fulvic acids were studied in NaCl media at low pH (3.95-5.03). Log β values for these experiments were reported between 9.7 and 13.2. Although Appendix SOTERM stated that no direct experimental evidence for this was found Appendix SOTERM speculated that stability constants under high pH conditions would be less due to competition from hydrolysis reactions. EPA believes that it is reasonable to assume that that stability constants under high pH conditions would be less. Other published stability constants were used for Np species but none could be found for Pu. Hence, the oxidation state analogy argument was used for the other actinides, as summarized in Table SOTERM-12.

In terms of competition for humic substance binding sites by Ca<sup>2+</sup> and Mg<sup>2+</sup>, the authors state that no stability constants for these divalent cations could be found at basic pH values. They used acidic values from the literature for experiments conducted only under low ionic strength solutions. Because the literature values were obtained at conditions far removed from expected WIPP conditions, the impact of Ca<sup>2+</sup> and Mg<sup>2+</sup> as competitors with actinides for humic substance binding sites is still not well established. Moreover, no consideration for the role of transition metals as competitors with actinides was presented, as was done for ligands. Analogous to ligands, any such competition is expected to reduce the overall mobility of actinides as humic colloids under repository conditions (assuming that immobile humic materials do not play a significant role in actinide retardation).

Based on a somewhat incomplete WIPP-relevant data base and a number of assumptions, the authors of Appendix SOTERM calculated proportionality constants for humic-associated

actinides compared to dissolved actinides (PHUMCIM for Castile brine and PHUMSIM for Salado brine). A maximum concentration for humic-associated actinides was also determined (CAPHUM). These constants were used in an apparent series of calculations which appear to lead to a final concentration of mobile actinides. However, the approach seems to have been based on numerous overlapping assumptions such that the final outcome is not entirely convincing. DOE does attempt to interject a note of assurance by stating (Appendix SOTERM 6.3.3.2) that “Uncertainties due to analytical precision are small compared to uncertainties in knowledge of the dominant humic substance type, site binding densities, and actinide solubilities. The proportionality factor approach coupled with the actinide solubility model uncertainty results in an adequate representation of the uncertainty in the concentration of actinides bound by mobile humic substances.”

In Appendix SOTERM, Section 6.3.3, the derivation of the parameters relevant to the effects of humic substances on actinide concentrations is described. The concentration of an actinide complexed with humics [AnHS] is obtained from a mass balance expression that includes the concentration of humic complexed with calcium and magnesium, dissolved actinide concentration, and uncomplexed humic concentration (see Equations 6-16 to 6-20 in Appendix SOTERM). The proportionality constant (parameter names PHUMCIM and PHUMSIM) is determined from the ratio of [AnHS] to the dissolved actinide concentration, where the dissolved actinide concentration is derived from solubility calculations.

In Table SOTERM-14, the proportionality constants for the +4 actinides (i.e., Th(IV), U(IV), Np(IV), and Pu(IV)) have a value of 6.3, indicating that the proportion of actinide present as humic complexes is 6.3 times the dissolved or, in this case, uncomplexed concentration. Proportionality constants for other oxidation states are smaller. Consequently, in the calculation of the actinide(IV) source terms, the dissolved actinide concentrations are multiplied by a factor of 6.3 to account for the amount that might be present as humic complexes. However, this concentration cannot be greater than  $1.1 \times 10^{-5}$  molar, which is the theoretical maximum concentration that could be complexed by a typical humic substance at a maximum solubility of 2 mg/L and site binding capacity of 5.56 meq/L OH<sup>-</sup> per gram.

EPA finds that this calculation is relatively conservative and potentially bounding in that the formation of other inorganic complexes of the actinides, such as hydrolysis and carbonate species are not considered in the derivation of the proportionality constants. Complexation of actinides by these species would theoretically reduce the concentrations of actinides in humic complexes, and reduce the proportionality constants. It also implies that humic substances have the potential to affect actinide solubilities and they should be considered in calculations of actinide solid solubilities. DOE does include humics in the calculation of the actinide source term using the equation (Appendix SOTERM 7.2): Total Mobile Actinides = Dissolved + Humic colloids + Microbial colloids + Mineral colloids + Intrinsic colloids.

Arguments for CAPMIN tend to be more convincing than for PHUMCIM and PHUMSIM, probably because it is a simpler concept. It uses the measured (near-WIPP conditions) mobile-fraction concentration of humic substances and the highest site binding capacity for fulvic acid (albeit for OH<sup>-</sup>, rather than actinides) to calculate a maximum humic-associated actinide concentration of  $1.1 \times 10^{-5}$  M. The authors state that this maximum concentration is conservative because all the actinides will be competing for the existing “pool” of humic substances. While true for the potentially enormous mass of humic materials available in the repository (compared to the

actinide concentration), it does not account for the possible species specificity of certain binding sites. That is, not all of the actinides may be competing for the same binding sites.

## 7.4 Conclusions

Organic ligands and humic substances are expected to be part of the waste inventory in the WIPP repository. Both types of organic compounds are known to combine chemically with the actinides, as well as other solutes, and thus provide the potential to increase actinide mobilities beyond what would be expected from only inorganic chemical processes.

Based on the information presented in Appendix SOTERM, DOE has developed a hypothesis for its conclusions concerning the role that both waste ligands and humic materials may play in the mobilization of WIPP-disposed actinide elements under brine-inundated, disposal conditions. The mechanisms postulated came primarily from fundamental physiochemical principles, existing literature references, and chemical equilibrium model calculations.

### 7.4.1 Ligands

The effects of organic ligands, such as EDTA, citrate, acetate, and oxalate are not expected to play a major role in affecting the mobilities of actinides because their complexation chemistries are dominated under the expected alkaline pH conditions by major solutes, such as Ca and Mg, that are present in high concentrations in WIPP brines. Metals, such as Fe and Ni, may also form strong complexes with these ligands, reducing the amount available for complexing actinides. This assumption was validated primarily on model calculations of chemical equilibrium. EPA concludes that while there are uncertainties, the basis for explaining the behavior of organic ligands is reasonably well established for use in performance assessment.

### 7.4.2 Humic Materials

Based on EPA's review of the literature, the mechanisms for complexation of humic materials with metals under environmental conditions has not been well established by the scientific community. However, some guidance for understanding this phenomenon for metals and actinides was found. In particular, Hummel (1995) presents a particularly detailed discussion of likely mechanisms to be expected and demonstrates that nuclear repository environments represent a complicated arena for the interaction of radionuclides, humic materials, organic and inorganic anions, other metal cations, and solid surfaces. Hummel suggests that without realistic, reliable, and experimentally verified models, no credit can be taken for competition by transition metal and divalent cations with actinide species for available complexant bindings sites. In contrast to Hummel's very conservative approach, DOE discussed in SOTERM that Ca and Mg would compete with actinides for binding sites on humic materials but they took no credit for the likely competition from the transition metals.

DOE's assumptions of 1:1 complexes between humic materials and actinides probably provides a valid first approximation of humic-actinide behavior in the WIPP. It may even provide a conservative model of actinide mobility, although their approach is probably simplified (e.g., the concept of ternary complexes was not introduced). Given the current limitations in the



development of models in the literature for humic complexation of metals (including actinides), DOE has reasonably addressed the issue in SOTERM, albeit mainly conceptually. Because humic materials are unlikely to cause excessive actinide mobility under WIPP conditions based on the arguments in SOTERM and EPA's literature review, the incorporation of humic materials in the performance assessment is adequate, although not without uncertainties.

#### 7.4.3 General Conclusions

DOE has assembled in SOTERM a relatively consistent and probably conservative model for the potential enhancement of actinide mobilization by ligands and humic materials. In many instances, they have taken no credit for mechanisms, such as adsorption within the repository, which would be expected to significantly limit actinide migration. Generally, the experimental work performed by DOE to date, as presented in the Appendix SOTERM document, has only limited repository-relevant results to support the WIPP actinide source term model.

In summary, DOE's overall approach to understanding the impact of organic ligands and humic materials on the actinide source term appears to be reasonable for use in performance assessment. In addition, EPA's sensitivity analysis (Technical Support Document for Section 194.23: Sensitivity Analysis, A-93-02, V-B-13) indicates that humic materials have minimal effect on solubilities.

## 8.0 Microbial Effects

Microbiological issues that are important to a review of the Actinide Source Term in DOE's WIPP CCA fall into two categories: the potential magnitude of microbially-mediated radionuclide mobilization and the potential for, and rate of, microbial gas generation. This section is a critique of methods used by DOE to infer Performance Assessment (PA) modeling parameters in these two subject areas. PA calculations using microbially-mediated gas-generation and microbial accumulation parameters are the principle microbially-based evidence submitted to EPA by DOE for demonstrating that the WIPP repository will comply with disposal standards, as set forth in 40 CFR Part 194 and 40 CFR 191.13. The primary source of the information reviewed was the CCA and associated appendices.

In the CCA, PA parameters are either constant values or distributions of possible values with specified maxima, minima and distribution functions. A Latin hypercube sampling program is used to select values of the distributed parameters for input to PA modeling runs. In the CCA, Appendix PAR, microbial parameters associated with radionuclide mobilization are specified as constants, while gas generation parameters are sampled according to uniform or delta distributions (retabulated herein as Tables 8-1 and 8-2).

The evaluation of microbial issues begins with a consideration of the types of microbes likely to grow in the WIPP repository and our general lack of knowledge about their properties. The two remaining sections are evaluations of parameter for microbial gas generation and development for microbially-mediated actinide transport. EPA finds that:

- 1) DOE's approach to address the probability of gas generation is adequate for use in performance assessment although there are uncertainties in future microbial populations.
- 2) DOE's simplified formulation of microbial actinide accumulation in the CCA is appropriate given our knowledge of expected microbial populations.
- 3) The experiments used as support to estimate actinide binding parameters have uncertainties associated with them due to limited data and projection to future populations. EPA recognizes the uncertainties associated with the parameterization of PROPMIC and CAPMIC, however, EPA finds that the approach used in the CCA reasonable given the data and the need to use existing populations to extrapolate to future populations.

### 8.1 Microbes in the WIPP repository.

The WIPP repository is 655 m (2150 feet) underground in a >200 million-year-old crystallized salt deposit (CCA, p. 2-36). Brine occurs as small intergranular and intragranular pockets within the Salado Formation with dissolved salt concentrations up to 8M. MgO added as backfill during waste emplacement will buffer the system over a range of pmH values between 9.13 and 9.9.

To live in this extreme environment, microorganisms require biochemical adaptations that prevent osmotic loss of intracellular water. Some microbial species are known which adapt to

extremely hypersaline conditions by producing intracellular, organic osmolytes or by accumulating large concentrations of intracellular  $K^+$  ions. Additional adaptive characteristics of extreme halophiles (extremophiles tolerant of high salt concentrations) include cell walls with unusually high proportions of acidic amino acids and intracellular proteins with low proportions of hydrophobic amino acids (Madigan et al. 1997). Species adapted to high pH, hypersaline environments have been identified in cultures from soda lakes.

Most organisms inhabiting the concentrated salt environment are members of the domain Archaea, an evolutionary group distantly related to both the Bacteria and Eukarya. A history of the discovery of Archaea and investigations into their role in the ecology of the biosphere have recently been reviewed (Morell 1997, Pace 1997). Some Bacteria and eukaryotic algae, brine shrimp and brine flies are also found in hypersaline environments (Madigan et al. 1997). Historically, microbiological studies have focused on members of the domain Bacteria. Although current research is adding to our knowledge of microbial diversity, the Archaea are today a highly undercharacterized group. DOE has identified one such microbial culture from the WIPP site, WIPP-1A. DOE used this culture in determining the microbial related parameters PROPMIC and CAPMIC.

A number of important microbial community properties are difficult to estimate due to the currently embryonic state of environmental microbiology. Even culturable species are underdescribed, as is demonstrated by the many new taxa described annually in the microbiological literature. Thus, the likelihood is that cultured microorganisms from the WIPP site may be less than ideal models for the microbial community in situ; microbes at the WIPP site are predominantly uncharacterized and currently uncharacterizable, at least with respect to variables such as metabolite production rates. Also, it is generally difficult to estimate the rate and extent of slow processes with very long timelines by extrapolation from short term model studies. Thus, there is high uncertainty of the applicability of current culture studies to the calculation of future metabolic rates and microbially-mediated actinide mobilization.

## 8.2 Microbial Gas Generation.

### 8.2.1 Probability of gas generation.

Carbon dioxide,  $N_2O$ ,  $N_2$ ,  $H_2S$ ,  $H_2$  and methane gasses are potential products from the microbial degradation of organic materials in WIPP wastes. However, it is difficult to predict whether these gasses will actually be generated. Among the variables affecting the probability of gas production is the presence or absence of microbes with the ability to mineralize WIPP organic wastes (mainly cellulose) directly to  $CO_2$ , rather than to intermediate breakdown products. The presence of microbes such as denitrifiers, sulfate reducers, methanogens and hydrogen producers which are able to survive under repository conditions also affect the potential for gas generation. Other factors that may limit gas generation include the concentrations of nutrient and toxic compounds and limitations imposed by temperature, salinity, Eh, pH and the availability of electron acceptors. These factors determine whether microbes which are present can form sustainable populations.

The WIPP environment will undergo significant shifts in pH, Eh, and water content after the

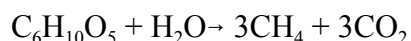
site is sealed, at which time it will become relatively inaccessible to exogenous microbes. It is therefore possible that microbes capable of producing gasses under long-term repository conditions might not be present at the time of closure. These microbes could also be absent from inoculating brines entering the repository. If both these possibilities occurred, then transformations otherwise thermodynamically and physiologically feasible would nonetheless fail to occur. On the other hand, Winogradsky demonstrated in the 1940's that microorganisms with a wide diversity of capabilities are present in many inhospitable environments, and can be wakened from quiescent states by introduction of the appropriate conditions (Winogradsky 1949). It is therefore difficult to predict with confidence whether microorganisms transforming WIPP organics into CO<sub>2</sub>, N<sub>2</sub>O, N<sub>2</sub>, H<sub>2</sub>S, H<sub>2</sub>, and/or methane will be present.

Combining the uncertainty of inoculation with the possibility that chemical and physical conditions at the WIPP may or may not promote substantial growth, leads to high uncertainty in predicting gas generation. Brush (1995) arrived at a similar assessment, concluding that "although significant microbial gas production is possible, it is by no means certain."

### 8.2.2 Amount of CO<sub>2</sub> predicted in the WIPP.

CO<sub>2</sub>, which is the product of complete degradation of organic compounds by microorganisms, may be produced in amounts varying from zero to an upper limit determined by the total carbon in the inventory of organic materials. DOE plans to use MgO backfill in the repository and reactions with CO<sub>2</sub> will sequester CO<sub>2</sub> in the repository.

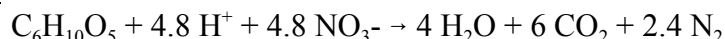
Appendix SOTERM predicts that the major microbial carbon-degrading pathway in the WIPP will be methanogenesis:



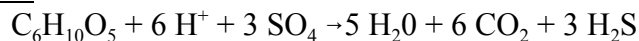
This chemical equation is an alternative to the hydrogen reduction of CO<sub>2</sub> most typically used to illustrate methanogenesis (4 H<sub>2</sub> + CO<sub>2</sub> → CH<sub>4</sub> + 2 H<sub>2</sub>O). Since any CO<sub>2</sub> evolved in the WIPP is likely to be precipitated by reactions with MgO, methanogenesis must proceed via this alternative pathway which is mediated by methanol, methylamine, acetate and/or other organic intermediates. Only a small number of organisms are known to carry out the methanol, methylamine and acetate reductions. Nonetheless, conversion of acetate to methane appears to be an ecologically significant process, occurring in sewage digestors and in anoxic freshwaters where competition from sulfate reducers is not significant (Madigan et al. 1997).

Other anaerobic pathways contributing to destruction of organic materials in the WIPP will be denitrification and sulfate reduction.

#### denitrification:



sulfate reduction:



DOE determined that there will be approximately  $1 \times 10^9$  moles of organic carbon in the repository. Based on the predominance of methanogenesis, which produces only about 0.5 mole  $\text{CO}_2$  per mole carbon in cellulose, this would result in a maximum of  $5 \times 10^8$  moles of  $\text{CO}_2$  being formed by methanogenesis (A-93-02, II-A-39).

The backfill plan for the WIPP in the CCA envisions approximately  $2 \times 10^9$  moles of MgO added to the repository, approximately two-fold greater than the organic carbon to be emplaced. In addition, excess MgO will compensate for inhomogeneities in  $\text{CO}_2$  production and moisture distribution, which may otherwise allow  $\text{CO}_2$  to accumulate in pockets where organic content is high and available MgO has been consumed.

### 8.2.3 Rate of $\text{CO}_2$ production.

Experiments using the cultured strain WIPP-1A have been used to estimate the rate of WIPP organic carbon mineralization as between 0.3 and 0.02 mol C/kg organic material/yr ( $6.3 \times 10^{-10}$  to  $9.5 \times 10^{-9}$  mol C/kg organic materials per second, Table 8-2). Since this cultured strain may not be representative of the microbial community which will dominate the WIPP after closure, this rate estimate must be considered only approximate. However, microbial mineralization rates do not vary among strains as much as, say, microbial metal accumulation parameters. Also, the maximum measured rate was determined under conditions of nutrient repletion, far more favorable for microbial growth than expected conditions at the WIPP (Francis and Gillow 1994). Therefore,  $\text{CO}_2$  production rates estimated from these experiments are likely to be conservative overestimates of possible  $\text{CO}_2$  production rates in the WIPP repository.

With the addition of MgO backfill to the WIPP plan, estimated rates of  $\text{CO}_2$  production are not likely to be of significant concern. Recent experimental work has indicated that MgO is converted to hydrated magnesium carbonates in a matter of days to weeks, although much longer periods are required to reach chemical equilibrium (see Section 4.0). The relatively rapid formation of metastable hydrated magnesium carbonates should limit the buildup of  $\text{CO}_2$  from microbial processes.

## 8.2 Microbial Factors Influencing Actinide Migration in Flowing Brines and Groundwaters.

### 8.2.1 Background

Microbes can influence the mobility of radionuclides in three ways: by altering pH and Eh, by releasing organic ligands, and by accumulation on or within their cell walls.

### 8.2.1.1 pH and Redox Potential.

Actinide solubility is dependent upon the pH and redox potential of the solvent (Section 4.0). In general, low pH and oxidizing conditions promote the dissolution of radionuclides, increasing their mobility in migrating brines while high pH and reducing conditions generally lower actinide mobility. Microbial degradation of organic compounds generates CO<sub>2</sub> and consumes electron acceptors. This lowers the pH of aqueous solutions but also creates low redox potential (reducing) conditions as oxygen and other electron acceptors are depleted. Thus, some consequences of microbial activity are to promote actinide mobility while others decrease actinide mobility. In addition, carbonate ions generated by microbial metabolism influence the speciation of dissolved actinides, generally increasing their solubility.

In the WIPP, pH, redox potential, and carbonate ion concentrations will be controlled by abiotic factors. MgO backfill will sequester CO<sub>2</sub> and ensure high pH, while large amounts of ferrous iron and limited oxygen will ensure reducing conditions after site closure.

### 8.2.1.2 Organic Ligands of Microbial Origin.

Microbes produce three types of molecules which may form complexes with actinides in solution:

- Macromolecules produced by partial degradation of cellulose, rubbers and plastics, or by cell lysis.
- Simple organic compounds exuded as products of microbial metabolism.
- Siderophores and specific metal binding proteins secreted in response to excess or insufficiency of toxic or essential metals; little is known about siderophores but they could increase actinide solubilities (Birch and Bachofen, 1990).

Relatively little is known about the influence of these materials on the mobilization of metals, including actinides. The metal complexation capacity of an organic molecule is dependent upon its concentration, overall structure and number of functional groups, as well as pH, redox potential, ionic strength and metal concentrations in the medium (reviewed by Birch and Bachofen, 1990).

#### 8.2.1.2.1 High Molecular Weight Compounds.

High molecular weight compounds produced from cellulose or cell lysis (disruption of cellular integrity) are similar to environmental humic acids. Binding of actinides to humic and fulvic acids is discussed in Section 8. Under various experimental conditions, humics have been observed to bind Am and Th, though not Pu (Fisher et al. 1983, Miekeley and Kuchler 1987, Nash and Choppin 1980, Sibley et al. 1984).

By definition, humic acids are sparingly soluble in 2M NaOH, and it is likely that humic-like cellulose degradation products will precipitate under conditions expected at the WIPP. For undisturbed repository scenarios cellulose degradation products are unlikely to increase actinide

concentrations in the aqueous phase.

#### 8.2.1.2.2 Low Molecular Weight Compounds

Chemical modeling suggests that at pH 10 the complexation capacity of most low molecular weight organic acids (except citrate) is negligible (Campbell and Tessier 1984).

Lactate, citrate and acetate are generally preferred over cellulose as microbial growth substrates. However, some organisms are unable to degrade them, and some release them as products of their metabolism. In the current model of microbial communities, producers and consumers of such intermediate breakdown products typically coexist and maintain the compounds at steady state concentrations in the environment. Consistent with this working hypothesis, small molecules such as amino acids are found at measurable levels in the ocean environment, and the same is probably true for other small metabolites.

In the case of the WIPP, the uncertainty of inoculation with any particular type of microorganism suggests that microbes which degrade citrate or other actinide-binding small molecules could be absent. If microbes that thrive in anoxic, hypersaline, basic conditions while degrading low molecular weight actinide-binding molecules are absent, concentrations of these small molecules may build up. On the other hand, as the brines migrate to environments inhabited by other microbial communities, these small molecules are likely to be degraded. Low molecular weight metabolites could increase actinide mobilization for scenarios in which WIPP brines are brought to the Culebra or directly to the surface.

#### 8.2.1.3 Metal accumulation by microorganisms.

Like other biological materials, microbes can accumulate actinides and other metals by sorption or precipitation at their cell surfaces, or as dense, intracellular inclusions. Volesky (1994) states that the ability to concentrate metals varies over several orders of magnitude, with some organisms sorbing very little (amount unspecified) and others accumulating >30% of their dry weight in metal.

As with gas generation, significant actinide accumulation by microorganisms is possible, but by no means certain. However, the possibility exists that colloidal microbes carrying bound radionuclides will significantly increase levels of radionuclides able to migrate in brines.

Microorganisms can accumulate metals as extracellular deposits by several mechanisms. Some sulfate reducers form extracellular sulfide deposits which can contain large amounts of metals (Kelly et al. 1979), and microbial communities accumulating Mn, Fe, Ni and Cu may deposit iron oxide extracellularly (Ferris et al. 1989). The fungus *Rhizopus arrhizus* can precipitate large amounts of uranylhydroxide within its microcrystalline cell wall (Tsezos and Volesky 1982a). Similarly, metal-resistant strains of *Citrobacter* precipitate Cd, Pb, Cu and U as insoluble metal phosphates on the cell surface. This phenomenon is associated with an extracellular phosphatase (Macaskie and Dean 1984, 1987). Extracellular metal deposition is not, however, invariably dependent upon cellular metabolism. Volesky (1994) observed "microcrystalline uranium-containing fibrils accumulated first around the cell and eventually penetrating inside while the surrounding layer still grows" for suspensions of killed *Saccharomyces cerevisiae*. It is

important to note that experiments with WIPP-1A, a halophilic archaean isolated from the WIPP site, show extracellular deposition of crystalline Pu in association with phosphorus and other elements (Strietelmeier et al. 1996). These experiments demonstrated that halophilic microbes present at the WIPP can accumulate actinides by extracellular deposition of crystalline metal.

Intracellular metal deposits have been reported for cyanobacteria, bacteria, algae, protozoa and fungi after exposure to radionuclides and other heavy metals (Bonhomme et al. 1980, Gadd and Griffiths 1978, Wood and Wang 1983, Strandberg et al. 1981). Many of these electron dense intracellular deposits are of unknown composition. Others have been shown to contain metallothioneins, which are low molecular weight metal binding proteins induced by exposure to metals (reviewed by Gadd 1990). Metallothioneins are thought to function in detoxification and also the storage and regulation of intracellular metal ion concentrations. Intracellular transport of metals is in some cases inhibited by metabolic inhibitors. In others, metals are accumulated by both living and dead organisms (Volesky 1994). In several algae, bacteria and yeasts, metals accumulated intracellularly may greatly exceed amounts taken up by surface adsorption (Gadd 1989, Kelly et al. 1979).

Metal accumulation by a variety of microorganisms has been evaluated using biosorption equilibrium isotherms (Tsezos and Volesky, 1981, 1982a, b, Volesky 1990). For these experiments, initial metal concentrations were kept constant while the microbial biomass in each sample was varied. In most cases, metal uptake (in mg per gram biomass) versus equilibrium solution metal concentrations (in mg per liter) followed curves that could be approximated by either Langmuir or Freundlich model equations.

### 8.3.2 DOE Modeling of Microbial Actinide Binding for WIPP PA.

#### 8.3.2.1 Appropriateness of mathematical models.

PA modeling for the WIPP CCA considers microbial actinide accumulation according to a simplified model. According to the model, each radionuclide is distributed between microbially-bound and aqueous phases according to a proportionality constant (PROPMIC), with a maximum (CAPMIC) value representing saturation binding capacity of the colloidal microbe population. Considering the large uncertainty in the identities and properties of microbes that will grow in the WIPP, it seems reasonable to adopt these simple and tractable mathematics which can be used to approximate more complex and realistic binding functions such as those observed by Tsezos and Volesky (1981).

While the mathematical functions used to model microbial actinide mobilization are adequately conceived, the same cannot be said for experiments performed by BNL and LANL researchers to determine the microbial actinide binding parameters.



### 8.3.2.2 Experimental determination of PROPMIC binding constants.

8.3.2.2.1 Number of model organisms. DOE experiments to determine PROPMIC values examined binding properties of two microbial cultures, one of which (archaeal strain WIPP-1A) was chosen as the model organism. Experiments examining only one cultured microbial strain is unlikely to have the same binding properties as the microbial population which may grow in the WIPP. However, the strain used is indigenous to the Salado brine.

8.3.2.2.2 pH conditions. All DOE experiments to measure microbial actinide binding parameters were performed using model brines designed to mimic in situ conditions in the present-day WIPP environment, without MgO backfill. These experiments do not reflect high pH conditions expected in the WIPP after closure. Salado brine has a pH of 5 to 7 versus the pH of 9 expected after closure with MgO backfill.

8.3.2.2.3 Microbial growth phase. Experiments performed at BNL and LANL to determine microbial actinide binding parameters were based on a concept of microbial growth that more accurately describes laboratory batch cultures than natural populations (Appendix SOTERM, section 6.3.4).

Natural microbial communities are more complex than pure cultures, and much current research aims to determine the growth phase of microbial cells in situ (e.g. Karner and Fuhrman, 1997). The prevailing "microbial loop" hypothesis explains that, although microbial numbers remain remarkably constant over time, cells in natural populations are not in a non-metabolizing state like stationary phase (Azam et al. 1983). Instead, microbial populations are in an overall steady-state in which bacterial and archaeal cells are cropped (consumed) by predatory microbes (ciliates, flagellates, and perhaps bacteria and archaea) and viruses. The remaining population grows steadily to maintain constant cell density. Within the population, it is likely that some cells are adapted to the prevailing conditions and are growing logarithmically, while others are growing slowly, dormant, or dying. Thus, it is not clear which growth phase is appropriately tested in experiments to estimate microbial binding constants for natural populations. The experiments described in SOTERM focus exclusively on cultures in stationary phase.

8.3.2.2.4 Experimental sampling protocol. A curious aspect of the BNL and LANL microbial binding constant experiments is that actinide binding was measured using only suspended cells in unmixed, stationary phase cultures. The proportionality constant for each actinide was determined from floating cells in the culture medium as the molar ratio of actinide retained on a 0.4  $\mu\text{m}$  filter (after passing through a 10  $\mu\text{m}$  filter) to actinide passing through a 0.04  $\mu\text{m}$  filter. The researchers did not assess proportionality constants obtained from whole cultures processed in the same way, and did not evaluate whether constants obtained from the suspended cells were conservative compared to whole culture proportionality constants.

The rationale stated for using the suspended microbes in these experiments is that these represent the "mobile fraction" of microorganisms, important for transport considerations. As stated in SOTERM, "Results of the experiments showed that the mobile concentration of microbes was a couple orders-of-magnitude less than the total concentration of microbes." If the entire culture had been used to measure binding constants, it is likely that the binding constants would be "a couple orders-of-magnitude" greater. EPA recognizes that the binding constant calculations did

not address the entire population of microbes that may be present in the WIPP disposal system. The approach used by DOE, however, takes into account those microbes that would presumably be mobile and for which the binding constant must be determined. This approach is reasonable, and presents a more realistic interpretation because it includes that mobile fraction which would be expected to affect transport. EPA recognizes that the fraction which settled out of the fluid column could bind with - and therefore reduce - actinides available for transport.

8.3.2.2.5 Accuracy of DOE binding proportion values. Papenguth (1996) indicates that the actinide-binding proportionality factors derived from WIPP-1A data are "coupled with a plus or minus one order-of-magnitude uncertainty in the concentration of actinide solubilities [which] results in a plus or minus one order-of-magnitude uncertainty in the concentration of actinides bound by mobile microbes." Since it is possible that microbes won't survive, or least thrive, in the WIPP, EPA believes that this uncertainty range is adequate for performance assessment.

8.3.2.3 Determination of CAPMIC cap values. PA calculations apply the microbial actinide binding proportionality constants over the range of dissolved actinide concentrations until "cap" values for maximum microbially-bound actinides are reached. The microbial cap value is "defined as the actinide concentration in molarity at which no growth was observed" for the WIPP-1A culture (Papenguth 1996). The WIPP-1A culture is from the Salado and EPA concludes that it is the best available estimate of future populations. In addition, EPA finds it is reasonable to define the microbial cap value based on no observed growth.

## 8.4 Conclusions

Microbial populations may affect the mobility of actinides in the WIPP repository in numerous ways, including metabolic alteration of brine pH and redox potential, production of soluble organic ligands, and mobilization of actinides bound to mobile (colloidal) microbes. To model the future behavior of the WIPP, DOE researchers have attempted to determine parameters to describe some of these processes. While there are uncertainties with microbial binding proportion (PROPMIC) parameters and **in the assumptions used to generate** maximum concentrations of microbially-bound actinides (CAPMIC parameters), EPA finds that DOE's approach addresses microbial affects on actinide mobility and it is adequate for use in performance assessment. Other potential microbial effects, such as alteration of pH, redox potential and generation of CO<sub>2</sub> gas appear to be inconsequential under WIPP conditions.

Table 8-1. Microbial Parameters for Performance Assessment: Constant Parameters

<u>ID#</u>	<u>Material</u>	<u>Material Description</u>	<u>Parameter</u>	<u>Parameter Description</u>	<u>Distribution Type</u>	<u>Units</u>	<u>Value</u>	<u>WPO#</u>
3447	AM	Americium	CAPMIC	Maximum concentration of actinide on microbe colloids	CONSTANT	mol/l	1.00E+00	37712
3311	AM	Americium	PROPMIC	Moles of actinide mobilized on microbe colloids per moles dissolved	CONSTANT	mol/mol	3.60E+00	36858
3313	NP	Neptunium	CAPMIC	Maximum concentration of actinide on microbe colliode	CONSTANT	mol/l	2.70E-03	36860
3314	NP	Neptunium	PROPMIC	Moles of actinide mobilize on microbe colloids per moles dissolved	CONSTANT	mol/mol	1.20E+01	36861
3315	PU	Plutonium	CAPMIC	Maximum concentration of actinide on microbe colloids	CONSTANT	mol/mol	6.80E-05	36862
3317	PU	Plutonium	PROPMIC	Moles of actinide mobilized on microbe colliods per moles dissolved	CONSTANT	mol/mol	3.00E-01	36864
3318	TH	Thorium	CAPMIC	Maximum concentration of actinide on microbe colloids	CONSTANT	mol/l	1.90E-03	36865
3320	TH	Thorium	PROPMIC	per mole of actinide mobilized on microbe colloids moles dissolved	CONSTANT	mol/mol	3.10E-00	36867
3308	U	Uranium	CAPMIC	Maximum concentration of actinide on microbe colloids	CONSTANT	mol/l	2.10E-03	36855
3307	U	Uranium	PROPMIC	Moles of actinide mobilized on microbe colloids per moles dissolved	CONSTANT	mol/mol	2.10E-03	36856

Table 8-2. Microbial Parameters for Performance Assessment: Sampled Parameters

<u>LHS #</u>	<u>ID#</u>	<u>Material</u>	<u>Material Description</u>	<u>Parameter</u>	<u>Parameter Description</u>	<u>Distribution Type</u>	<u>Units</u>	<u>Mean</u>	<u>Median</u>	<u>Low</u>	<u>High</u>	<u>Std. Deviation</u>	<u>WPO#</u>
2	2823	WAS_ARE A	Waste emplacement area and waste	PROBDEG	Prob. of plastics & rubber biodegradation in event of significant microbial gas generation	DELTA	NONE	n.a.	n.a.	0	2	n.a.	34881
(2)	2824	REPOSIT	Repository regions outside of Panel region	PROBDEG	Prob. of plastics & rubber biodegradation in event of microbial gas generation	DELTA	None	n.a.	n.a.	0	2	n.a.	33264
3	657	WAS_ARE A	Waste emplacement area and waste	GRATMICI	Biodegradation rate, inundated conditions	UNIFORM	mol/kg*s	4.915E-09	4.915E-09	3.1710E-10	9.51E-09	0	34928
(3)	2128	RRPOSIT	Repository regions outside of Panel region	GRATMICI	Gas production rate, microbial, inundated rate	UNIFORM	mol/k*s	4.915E-09	4.915E-09	3.1710E-10	9.51E-09	0	33235
4	656	WAS_ARE A	Waste emplacement area and waste	GRATMICH	Gas production rate, microbial, humid conditions relative to inundated rate	UNIFORM	mol/k*s	6.342E-10	6.342E-10	0	1.27E-09	0	34923
(4)	2127	REPOSIT	Repository regions outside of Panel region	GRATMICH	Gas production rate, microbial, humid conditions relative to inundated rate	UNIFORM	mol/k*s	6.342E10	6.342E-10	0	1.27E-09	0	33234
5	2994	CELLULS	Cellulose	FBETA	Factor beta for microbial reaction rates	UNIFORM	NONE	5.000E-01	5.00E-01	0	1.000	00.29	31826

## 9.0 Conclusions and Key Issues

Actinides can exist in oxidation states ranging from +3 to +6, depending on the specific actinide under consideration and prevailing redox conditions. After closure, the repository is expected to become anoxic relatively rapidly. The assumption of reducing conditions after closure is reasonable because of the interaction of the iron and brine. DOE presents the experimental and chemical reasoning for the determination of the specific oxidation states for each actinide expected to be predominant in the repository and identifies the expected oxidation states for thorium, uranium, neptunium, americium, curium, and plutonium.

The addition of magnesium oxide backfill to the disposal system will buffer solubilities and sequester CO<sub>2</sub> from microbial respiration, if microbes survive in the repository environment. DOE's determination of which magnesium carbonate mineral phase will dominate the repository was investigated and EPA believes that metastable, hydrated magnesium carbonate phases (probably hydromagnesite) are more likely to be present than magnesite, as suggested by DOE in Appendix SOTERM. This is important because these hydrated phases can be shown to change the actinide solubilities from that modeled in the CCA performance assessment (PA). The presence of the hydromagnesite acts to reduce the solubility while the short-lived nesquehonite phase increases actinide solubility. EPA believes that hydromagnesite will be the metastable hydrated magnesium carbonate phase and nesquehonite will be an intermediate phase. The presence of hydromagnesite rather than magnesite reduces, from the values used in the CCA, the expected actinide solubilities of the +III, +IV, and +V actinide oxidation states.

The Fracture-Matrix Transport (FMT) geochemical model was reviewed and EPA determined that the thermodynamic model was appropriate for calculating the actinide solubilities of the +III, +IV, and +V actinide oxidation states. It was concluded that by following the methodologies documented in the CCA, the results provided in the CCA can be verified. This was determined after errors in the database were discovered, communicated to DOE, corrected by DOE, and the runs redone by EPA.

In contrast to the +III, +IV, and +V actinide oxidation states, the FMT thermodynamic database contains no data for uranium (+VI) so its solubility was estimated by an alternative method. EPA believes that the evidence provided by DOE in the CCA and in supplemental information indicates that the CCA uranium (+VI) solubility values are adequate for use in the performance assessment.

In the CCA, DOE uses point estimates for the actinide solubility and has estimated an uncertainty range around the point estimates. The uncertainty range developed by DOE used data from 150 measurements of differences between measured and predicted concentrations to develop an uncertainty range that adequately captures actinide uncertainty.

Complexation by ligands and humic materials could enhance the mobility of the actinides beyond that predicted by solubility experiments and related solubility modeling. EPA reviewed DOE's documentation and conducted independent calculations and concludes that while organic ligands will be present, they are not expected to have appreciable effect on actinide solubilities. A

review of DOE's presentation of humic materials finds that there are uncertainties associated with DOE's characterization of humic materials, but EPA believes that humic materials are unlikely to cause excessive actinide mobility under WIPP conditions. EPA concludes that the incorporation of the humic materials is adequate for performance assessment, although not without uncertainties.

Microbiological issues that are important to a review of the Actinide Source Term in DOE's WIPP CCA fall into two categories: the potential magnitude of microbially-mediated radionuclide mobilization and the potential for, and rate of, microbial gas generation. EPA finds that, even though there are uncertainties with DOE's characterization of microbial issues, DOE's approach in the performance assessment is reasonable relative to gas generation and actinide microbial binding parameters. EPA believes that DOE's overall approach to determining microbial binding parameters encompasses a number of uncertainties; however, these uncertainties are mitigated when taken into the broader context of PA. That is, performance assessment assumes the presence of microbes that may in fact not be present, and although DOE's calculated values are somewhat uncertain, they are based upon conceptualizations and simplifications appropriate for PA.

Although there were uncertainties in DOE's characterization of some issues, EPA has concluded that generally the technical approach used by DOE for establishing the actinide source term was scientifically valid.

## 10.0 References

- A-93-02, V-B-13, Technical Support Document for Section 194.23: Sensitivity Analysis Report.
- A-93-02, V-B-6, Technical Support Document for Section 194.23: Models and Computer Codes.
- A-93-02, II-G-3, QA packages for 13 PA Codes, Supplemental Information Supporting the DOE/WIPP Compliance Certification Application, Volume 6-- FMT Quality Assurance Package.
- A-93-02, II-A-39, Chemical Conditions Model: Results of the MgO Backfill Efficacy Investigation.
- A-93-02, V-B-5, Technical Support Document: Overview of Major Performance Assessment Issues.
- A-93-02, V-B-14, Technical Support Document for Section 194.23: Parameter Justification Report.
- A-93-02, II-G-44, Bynum, R. V. and Y. Wang (1997). "U(VI) Solubility Calculation Performance of Uranium (VI) Solubility Predictions for EPA, WPO#45115.
- A-93-02, II-G-33, April 21, 1997 memorandum from Craig F. Novak to R. Vann Bynum "Calculation of Actinide Solubilities in WIPP SPC and ERDA6 Brines Under MgO Backfill Scenarios Containing Nesquehonite or Hydromagnesite as the MgO-CO<sub>3</sub> Solubility-limiting Phase". WPO 46124.
- Allard, B. (1981) Solubilities of actinides in neutral or basic solutions. In Actinides in Perspective, (Norman M. Edelstein, Ed.) Pergamon Press, New York, pp. 553-580.
- Allard, B., H. Kipatsi, and J. O. Liljenzin (1980) Expected species of uranium, neptunium, and plutonium in neutral aqueous solutions. *J. Inorg. Nucl. Chem.* 42, 1015-1027.
- Allison, J. D., D. S. Brown, and K. J. Novo-Gradec, (1990). MINTEQA2/PRODEFA2, A Geochemical Assessment Model for Environmental Systems: Version 3.0 User's Guide. EPA/600/3-91/021. Environmental Research Laboratory, Office of Research and Development, U.S. Environmental Protection Agency, Athens, Georgia.
- Azam, F., T. Fenchel, J.G. Field, J.S. Gray, L.A. Meyer-Reil, and F. Thingstad, (1983). The ecological role of water-column microbes in the sea. *Mar. Ecol. Prog. Ser.* 10:157-263.
- Babb, S. C. (1995) WIPP PA User's Manual for FMT, Version 2.0, Document Version 1.00, WPO#28119, Sandia National Laboratories, Albuquerque, New Mexico.
- Birch, L. and Bachofen, R. (1990). Complexing agents from microorganisms. *Experientia* 46:827-834.
- Bonhomme, A., Quintana, C. and Duraud, M. (1980). Electron microprobe analysis of zinc incorporation into rumen protozoa. *J. Protozool.* 27:491-497.

- Bowen, H. J. M. and D. Gibbons (1963)., Radioactivation Analysis, Oxford Press.
- Brookins, D.G. (1988) Eh-pH Diagrams for Geochemistry. Springer-Verlag, Berlin.
- Brush, L. H. (1990). “Test Plan for Laboratory and Modeling Studies of Repository and Radionuclide Chemistry for the Waste Isolation Pilot Plant”, Sandia National Laboratories Report SAND90-0266., CCA Reference No. 91.
- Brush, L. H. (17 March 1995). “Systems Prioritization Method--Iteration 2 Baseline Position Paper: Gas Generation in the Waste Isolation Pilot Plant”, Sandia National Laboratories Report (WPO 30052).Brush, L.H. (1995). CCA Reference No. 92
- Bynum, R. V. (1996a). “Update of Uncertainty Range and Distribution for Actinide Solubilities to be Used in CCA NUTS Calculation”, Memo to M. S. Tierney and C. Stockman, dated May 23, 1996, WPO37791, A-93-02, II-G-1, CCA Ref. No.106.
- Bynum, R. V. (1996b). “Analysis to Estimate the Uncertainty for Predicted Actinide Solubilities”, WBS 1.1.10.1.1, Rev. 0, effective date 9/3/96, WPO41374.
- Bynum, R. V. (1997a). “Clarification of Waste Components Which May Impact the Actinide Source Term”, Memo to File, dated 2 September 1997, WPO31162.
- Bynum, R. V. (1997b). “Clarification of Humic Solubilities in CCA Appendix SOTERM”, Memo to Hans Papenguth, dated 16 September 1997, WPO35855.
- Campbell, P.G.C. and Tessier, A. (1984). Determination of the complexation capacity of natural waters using metal solubilisation techniques. *Dev. Biogeochem* 1:67-81.
- Choppin, G. R. (1991) Redox speciation of plutonium in natural waters. *J. Radioanalytical and Nucl. Chem., Articles*, 147, 109-116.
- Choppin, G. R. & P. M. Shanbhag (1981), “Binding of Calcium by Humic Acid”, in the Journal of Inorganic and Nuclear Chemistry, Vol. 43, PP 921-922.
- Davies, P. J. and B. Bubela (1973) The transformation of nesquehonite into hydromagnesite. *Chemical Geology* 12, 289-300.DOE/CAO, 1996.
- Davies, P. J., B. Bubela, and J. Ferguson (1977) Simulation of carbonate diagenetic processes: Formation of dolomite, huntite, and monohydrocalcite by the reactions between nesquehonite and brine. *Chemical Geology* 19, 187-214.
- Doner, H. E. and W. C. Lynn (1977) Carbonate, Halide, Sulfate, and Sulfide Minerals, in *Minerals in Soil Environments* (J. B. Dixon and S. B. Weed, Eds.) Soil Sci. Soc. Am., Madison, Wisconsin, pp. 75-98.Dragun, J., The Soil Chemistry of Hazardous Materials, Hazardous and Materials Control Research Institute, Silver Spring, MD, 1988.
- Dragun, James, 1988, The Soil Chemistry of Hazardous Materials, Hazardous Materials Control



Research Institute, (University of Colorado, Boulder, TD878.D72).

Felmy, A. R. and J. H. Weare (1986), "The Prediction of Borate Mineral Equilibria in Natural Waters, Applications to Searles Lake, California", in *Geochim. Cosmochim. Acta* 50, 2771-2783, WPO30421.

Felmy, A. R., D. Rai, J. A. Schramke, and J. L. Ryan (1989), "The solubility of plutonium hydroxide in dilute solutions and in high-ionic-strength brines", in *Radiochimica Acta* 48, 29-35.

Felmy, A. R., D. Rai, and M. J. Mason (1990), "The Solubility of  $\text{AmOHCO}_3(\text{c})$  and the Aqueous Thermodynamics of the System  $\text{Na}^+\text{-H}^+\text{-CO}_3\text{-OH-H}_2\text{O}$ ", in *Radiochimica Acta*, 55, 177-185.

Felmy, A. R., D. Rai, and M. J. Mason (1991) The Solubility of Hydrus Thorium(IV) Oxide in Chloride Media: Development of an Aqueous Ion-Interaction Model. *Radiochimica Acta* 55, 177-185 WPO 40225.

Felmy, A. R. and D. Rai (1992), "An Aqueous Thermodynamic Model for High Valence 4:2 Electrolyte  $\text{Th}^{+4}\text{-SO}_4$  in the system  $\text{Na}^+\text{-K}^+\text{-Li}^+\text{-NH}_4^+\text{-SO}_4\text{-2-HSO}_4\text{-H}_2\text{O}$  to High Concentrations", in *J. Solution Chem.* 21, 407-423, WPO40224.

Felmy, A. R., D. Rai, S. M. Sterner, M. J. Mason N. J. Hess, and S. D. Conradson (1996) Thermodynamic Models for Highly Charged Aqueous Species: The Solubility of Th(IV) Hydrus Oxide in Concentrated  $\text{NaHCO}_3$  and  $\text{Na}_2\text{CO}_3$  Solutions. In preparation. Copy on file in the Sandia WIPP Central Files. A:1.1.10.1.1: TO: QA: Inorganic (IV) Actinide Thermodynamic Data, WPO40226, 8/14/96.

Ferris, F.G., Schultze, S., Witten, T.C., Fyfe, W.S. and Beveridge, T.J. (1989). Metal interactions with microbial biofilms in acidic and neutral pH environments. *Appl. Environ. Microbiol.* 55:1249-1257.

Fischbeck, R. and G. Muller (1971) Monohydrocalcite, hydromagnesite, nesquehonite, dolomite, aragonite, and calcite in speleotherms of the Frankische Schweiz, Western Germany. *Contributions Mineralogy and Petrology* 33, 87-92.

Fisher, N.S., Bjerregaard, P. and Huynh-Ngoc, L. (1983). Interactions of marine plankton with transuranic elements 2. Influence of dissolved organic compounds on americium and plutonium accumulation in a diatom. *Mar. Chem.* 13:45-56.

Forstner, U. & Wittmann, G. T. W. (1981), Metal Pollution in the Aquatic Environment, Springer-Verlag, New York.

Francis, A.J. and Gillow, J.B. (1994). Effects of microbial processes on gas generation under expected WIPP repository conditions: progress report through 1992. SAND93-7036, Sandia National Laboratories, Albuquerque, NM. CCA Ref. No. 256.

Gadd, G.M. (1989). In *Biotechnology -- A Comprehensive Treatise*, Vol. 6b (H.-J. Rehm and G. Reed, eds). VCH Verlagsgesellschaft, Weinheim.

Gadd, G.M. (1990). Metal tolerance. In *Microbiology of Extreme Environments* (C. Edwards, ed).

McGraw Hill, pp. 178-210.

Gadd, G.M. and Griffiths, A.J. (1978). Microorganisms and heavy metal toxicity. *Microbial Ecol.* 4:303-317.

Garrels, R. M. & Christ, C. L. (1965), Solutions, Minerals and Equilibria, Freeman, Copper & Co., San Francisco, CA.

Graf, D. L., A. J. Eardley, and N. F. Schimp (1961) A preliminary report on magnesium carbonate formation in glacial Lake Bonneville. *The Journal of Geology*, 69, 219-223.

Harvie, C. E., N. Moller, and J. H. Weare (1980) The Prediction of Mineral Solubilities in Natural Waters, The Na-K-Mg-Ca-Cl-SO<sub>4</sub>-H<sub>2</sub>O System from Zero to High Concentrations at 25°C. *Geochim. Cosmochim. Acta* 44, 981-997.

Harvie, C. E., N. Moller, and J. H. Weare (1984) The Prediction of Mineral Solubilities in Natural Waters, The Na-K-Mg-Ca-H-Cl-SO<sub>4</sub>-OH-HCO<sub>3</sub>-CO<sub>2</sub>-H<sub>2</sub>O System from to High Ionic Strengths. *Geochim. Cosmochim. Acta* 48, 723-751 WPO30422.

Hobart, D. E. and R. C. Moore (1996) Analysis of Uranium(VI) Solubility Data for WIPP Performance Assessment WBS 1.1.10.1. (WPO 39856).

Hobart, D. E., C. J. Bruton, F. J. Millero, I. M. Chou, K. M. Trauth, and R. Anderson (1996) Estimates of the Solubilities of Waste Element Radionuclides in Waste Isolation Pilot Plant Brines: A Report by the Expert Panel on the Source Term. SAND96-0098, Sandia National Laboratories, Albuquerque, New Mexico.

Hounslow, Arthur W. 1995, Water Quality Data, Analysis and Interpretation. CRC Press, Lewis Publishers.

Hummel, W. (1993), "Organic Complexation of Radionuclides in Cement Pore Water: A Case Study" Paul Scherrer Institut Report TM-41-93-03, PES-93-617, WPO 47516. Villigen, PSI, Switzerland.

Hummel, W. (1995), "Competition of Other Complexes: Theoretical Aspects", in Binding Models Concerning Natural Organic Substances in Performance Assessment, Proceedings of an NEA Workshop held 14-16 September 1994 in Bad Zurzach, Switzerland, published by the Nuclear Energy Agency-Organization for Economic Co-operation and Development, Series on Safety Assessment of Radioactive Waste Repositories, Paris, France, pp. 215-222.

Irion, G. and G. Mueller (1968) Huntite, dolomite, magnesite, and polyhalite of Recent age from Tuz Golu, Turkey. *Nature* 220, 1309-1310.

Jensen, B. S. (1980) The geochemistry of radionuclides with long-half lives: Their expected migration behavior. Report Riso-R=430, Riso National Laboratory, DK-4000, Roskilde, Denmark.

Karner, M. and Fuhrman, J.A. (1997). Determination of active marine bacterioplankton: a comparison of universal 16S rRNA probes, autoradiography, and nucleoid staining. *Appl. Environ. Microbiol.*

63:1208-1213.

Kelly, D.P., Norris, P.R. and Brierley, C.L. (1979). Microbiological methods for the extraction and recovery of metals. In *Microbial Technology, Current State, Future Prospects* (A.T. Bull, D.C. Ellwood and C. Ratledge, eds). Cambridge Univ. Press, pp. 263-308.

Kim, J. I. & T. Sekine (1991), "Complexation of Neptunium (V) with Humic Acid", in *Radiochimica Acta*, Vol. 55, pp. 187-192.

Krauskopf, K. B. (1979) *Introduction to Geochemistry*, 2nd Ed., McGraw-Hill.

Lewis, R. J., Sr. (1993), *Hawley's Condensed Chemical Dictionary*, Twelfth Edition, Van Nostrand Reinhold.

Lippman, F. (1973) *Sedimentary Carbonate Minerals*, Springer-Verlag, New York.

Lovley, D.R., Coates, J.D., Blunt-Harris, E.L., Phillips, E.J.P. and Woodward, J.C. (1996). Humic substances as electron acceptors for microbial respiration. *Nature* 382:445-448.

Macaskie, L.E. and Dean, A.C.R. (1984). Cadmium accumulation by a *Citrobacter* sp. *J. Gen. Microbiol.* 130:53-62.

Macaskie, L.E. and Dean, A.C.R. (1987). Use of immobilized biofilm of *Citrobacter* sp. for the removal of uranium and lead from aqueous flows. *Enzyme Microb. Technol.* 9:2-4.

Madigan, M.T., Martinko, J.M. and Parker, J. (1997). *Brock Biology of Microorganisms*, eighth edition. Prentice Hall. 986pp.

Mackenzie, F. T., W. D. Bischoff, F. C. Bishop, M. Loijens, J. Schoonmaker, and R. Wollast (1983) *Magnesian Calcites: Low-Temperature Occurrence, Solubility, and Solid-Solution Behavior*, in *Reviews in Mineralogy, Volume 11, Carbonates: Mineralogy and Chemistry* (R. J. Reeder, Ed.) Mineral. Soc. Am., Washington, D.C., pp. 97-144.

Marschner, H. (1969) Hydrocalcite ( $\text{CaCO}_3 \cdot \text{H}_2\text{O}$ ) and nesquehonite ( $\text{MgCO}_3 \cdot \text{H}_2\text{O}$ ) in carbonate scales. *Science* 165, 1119-1121.

Merck Index, 11th Edition (1989) Merck & Co., Inc., CCA Ref. No. 98.

Miekeley, N. and Kuchler, I.L. (1987). Interactions between thorium and humic compounds in surface waters. *Inorgan. Chim. Acta* 140:315-319.

Moore, R.C., 1996, Model parameters for Deprotonation of Lactic Acid, Citric Acid, Oxalic Acid, and EDTA and Complexion of Acetate, Lactate, Citrate, Oxalate, and EDTA with  $Mg^{+2}$ ,  $NpO_2^+$ ,  $AM^{3+}$ ,  $Th^{4+}$  and  $UO_2^{2+}$  in NaCl Media. Memorandum to C.F. Novak, (copy on file in the Sandia WIPP central files A:1.1.1.1.4: TD: QA; WPO 35307) (Reference No. 443).

Morell, V. (1997). Microbiology's scarred revolutionary. *Science* 276:699-702.

Morse, J. W. and F. T. Mackenzie (1990) *Geochemistry of Sedimentary Carbonates*, Elsevier, Amsterdam.

Nash, K. L. & G. R. Choppin (1980), "Interaction of Humic and Fulvic Acid with Th(IV)", in the *Journal of Inorganic and Nuclear Chemistry*, Vol. 42, pp. 1045-1050.

Novak, C. F., N. J. Dhooge, H. W. Papenguth, and R. F. Weiner (1995) "Systems Prioritization Method--Interaction 2 Baseline Position Paper: Actinide Source Term" Sandia National Laboratories Report, dated 31 March 1995, WPO 28742.

Novak, C. F. and R. C. Moore (1996) "Estimates of Dissolved Concentrations for +III, +IV, +V, and +VI Actinides in a Salado and a Castile Brine under Anticipated Repository Conditions." Memo to M. D. Siegel, March 28, 1996, Sandia National Laboratories, Albuquerque, New Mexico, CCA Ref. No. 479.

Novak, C. F., R. C. Moore, and R. V. Bynum (1996a) Prediction of Dissolved Actinide Concentrations in Concentrated Electrolyte Solutions: A Conceptual Model and Model Results for the Waste Isolation Pilot Plant (WIPP). In Proceedings of the 1996 International Conference on Deep Geological Disposal of Radioactive Waste, Canadian Nuclear Society, Toronto, Canada (ISSN No: 0-919784-44-5). CCA Ref. No. 481.

Novak, C. F., I. Al Mahamid, K. A. Becraft, S. A. Carpenter, N. Hakem, and T. Prussin (1996b) Measurement and Thermodynamic Modeling of Np(V) Solubility in Dilute through Concentrated  $K_2CO_3$  Media. SAND96-1604J, Sandia National Laboratories, Albuquerque, New Mexico, WPO 44290.

Novak, C. F., H. Nitsche, H. B. Silber, K. Roberts, Ph.C. Torreto, T. Prussin, K. Becraft, S. A. Carpenter, D. E. Hobart, and I. Al Mahamid (1996c) Neptunium (V) and neptunium(VI) solubilities in synthetic brines of interest to the Waste Isolation Pilot Plant (WIPP). *Radiochim. Acta* 74, 31-36.

Novak, C. F. (1997) Calculation of Actinide Solubilities in WIPP SPC and ERDA6 Brines under MgO Backfill Scenarios Containing Either Nesquehonite or Hydromagnesite as the  $Mg-CO_3$  Solubility-Limiting Phase. Memo to R. Vann Bynum, dated April 21, 1997, Sandia National Laboratories, Albuquerque, New Mexico. WPO 46124.

Nowack, B., H. Xue, & L. Sigg (1997), "Influence of Natural and Anthropogenic Ligands on Metal Transport during Infiltration of River Water to Groundwater", in *Environmental Science and Technology*, Vol. 31, pp. 866-872.

Pace, N.R. (1997). A molecular view of microbial diversity and the biosphere. *Science* 276:734-740.

- Parkhurst, D. L. (1995) User's Guide to PHREEQC - A Computer Program for Speciation, Reaction-Path, Advective-Transport, and Inverse Geochemical Calculations, Water-Resources Invest. Rep. 95-4227, U.S. Geol. Survey, Lakewood, Colorado.
- Papenguth, W.H. (1996). Rationale for definition of parameter values for microbes. Title 40 CFR Part 191 Compliance Certification Application for the Waste Isolation Pilot Plant, Appendix WCA (DOE/CAO draft 2184), Attachment A.
- Papenguth, H. W. & Yugal K. Behl (16 January 1996) "Test Plan for Evaluation of Colloidal-Facilitated Actinide Transport at the Waste Isolation Pilot Plant", Sandia National Laboratories Waste Isolation Pilot Plant Test Plan TP-96-01. WPO 31337. CCA Ref. No. 496.
- Rai, D., A. R. Felmy, S. M. Sterner, D. A. Moore, M. J. Mason, and C. J. Novak (1997) The solubility of Th(IV) and U(IV) hydrous oxides in concentrated NaCl and MgCl<sub>2</sub> solutions. *Radiochimica Acta* 79, 239-247.
- Rai, D., A. R. Felmy, and J. L. Ryan (1990) Uranium(IV) hydrolysis constants and solubility product of UO<sub>2</sub>•xH<sub>2</sub>O(am). *Inorganic Chemistry*, 29, 260-264.
- Rai, D., J. L. Swanson, and J. L. Ryan (1987) Solubility of NpO<sub>2</sub>•xH<sub>2</sub>O in the presence of Cu(I)/Cu(II) redox buffer. *Radiochimica Acta* 42, 35-41.
- Rai, D. and J. L. Ryan (1985) Neptunium(IV) hydrous oxide solubility under reducing and carbonate conditions. *Inorg. Chem.* 24, 247-251.
- Rai, D., R.J. Serne, and J. L. Swanson (1980) Solution species of plutonium in the environment. *J. Environ. Qual.* 9, 417-420.
- Rao, L. & G. R. Choppin (1995), "Thermodynamic Study of the Complexation of Neptunium(V) with Humic Acids", in *Radiochimica Acta*, Vol. 68, pp. 87-95.
- Raymond, K. N., M. J. Kappel, V. L. Pecoraro, W. R. Harris, C. J. Carrano, F. L. Weigl, and P. W. Durbin, (1982), "Specific Sequestering Agents for Actinide Ions", in *Actinides in Perspective*, Ed. N. M. Edelstein, Pergamon Press, pp 491-507.
- Reed, D. T., D. G. Wygmans, and M. K. Richmann (1996) Stability of Pu(VI), Np(VI), and U(VI) in Simulated WIPP Brine. Argonne National Laboratory Interim Report (cited by Hobart and Moore, 1996). WPO 35197.
- Reed, D. T. and D. G. Wygmans (1997) Actinide stability/solubility in simulated WIPP brines. Interim Report 3/21/97, Actinide Speciation and Chemistry Group, Chemical Technology Group, Argonne National Laboratory, Argonne, Illinois. WPO 44625.

- Renaut, R. W. and P. R. Long (1989) Sedimentology of the saline lakes of the Cariboo Plateau, Interior British Columbia, Canada. *Sedimentary Geology* 64, 239-264.
- Runde, W. and J. I. Kim (1994) Untersuchungen der Übertragbarkeit von Labordaten natürliche Verhältnisse. Chemisches Verhalten von drei- und fünfwertigem Americium in salinen NaCl-Lösungen. Report RCM-01094, Munich: Institut für Radiochemie, Technische Universität München. (Available as report DE 95752244 from National Technical Information Service, 555 Port Royal Road, Springfield, Virginia 22161.)
- Sandia National Laboratories Report (1996) "Control of the Chemical Environment Through Implementation of an MgO Backfill Material", WIPP RCRA Part B Permit Application, DOE/WIPP 91-005, Rev. 6, dated 8 April 1996.
- Savage, D. (1995), "The Geochemical Behaviour of Nickel in the Repository Environment", in Material Research Society Symposium Proceedings, Vol. 353, published by the Materials Research Society, pp. 1159-1166.
- Sawyer, C. N. & McCarthy, P. L. (1978), Chemistry for Environmental Engineering, 3rd Edition, McGraw Hill, New York, NY.
- Sayles, F. L. and W. S. Fyfe (1973). "The crystallization of magnesite from aqueous solutions. *Geochim. Cosmochim. Acta* 37, 87-99.
- Schnitzer, M. & S.I.M. Skinner (1967), "Organo-Metallic Interactions in Soils: 7. Solubility Constants of Pb<sup>++-</sup>, Ni<sup>++-</sup>, Mn<sup>++-</sup>, Co<sup>++-</sup>, Ca<sup>++-</sup>, and Mg<sup>++-</sup>-Fulvic Acid Complexes", in *Soil Science*, Vol. 103, #4, pp. 247-252.
- Scott, M. J. and J. J. Morgan (1991) Energetics and conservative properties of redox systems. In *Chemical Modeling of Aqueous Systems, II* (D. C. Melchior and R. L. Bassett, Eds.) ACS Symp Ser. 416, Am. Chem. Soc., Washington, D.C., 368-367.
- Sibley, T.H., Clayton, J.R., Wurtz, E.A., Sanchez, A.L. and Alberts, J.J. (1984). Effects of dissolved organic compounds on the adsorption of transuranic elements. *Devl. Biogeochem.* 1:289-300.
- Silva, R. J. and H. Nitsche (1995) Actinide environmental chemistry. *Radiochimica Acta* 70/71, 377-396.
- Stamatakis, M. G. (1995) Occurrence and genesis of huntite-hydromagnesite assemblages, Kozani, Greece - important new white filters and extenders. *Trans. Instn. Min. Metall., Sect. B: Appl. Earth Sci.*, 104, B179-B186.
- Strandberg, G.W., Shumate, S.E. II and Parrott, J.R. Jr. (1981). Microbial cells as biosorbants for heavy metals: accumulation of uranium by *Saccharomyces cerevisiae* and *Pseudomonas aeruginosa*.. *Appl. Environ. Microbiol.* 41:237-245.

- Strietelmeier, B.A., Sebring, R.J., Gillow, J.B., Dodge, C.J., Pansoy-Hjelvik, M.E., Kraus, S.M., Leonard, P.A., Triay, I.R., Francis, A.J. and Papenguth, H.W. (1996). Plutonium interaction with a bacterial strain isolated from the waste isolation pilot plant (WIPP) environment. Div. Environ. Chem. Preprints Extended Abstr. 36:46-47.
- Stumm, W. and J. J. Morgan (1996) *Aquatic Chemistry, Third Edition*, John Wiley & Sons, New York.
- Tsezos, M. and Volesky, B. (1981). Biosorption of uranium and thorium. *Biotechnol. Bioeng.* 23:583-604.
- Tsezos, M. and Volesky, B. (1982a). The mechanism of uranium biosorption by *Rhizopus arrhizus*. *Biotechnol. Bioeng.* 24:385-401.
- Tsezos, M. and Volesky, B. (1982b). The mechanism of thorium biosorption by *Rhizopus arrhizus*. *Biotechnol. Bioeng.* 24:955-969.
- U. S. Department of Energy (1996a) "Title 40 CFR Part 191 Compliance Certification Application for the Waste Isolation Pilot Plant, Appendix SOTERM", DOE/CAO 1996-2184, October 1996.
- U.S. Department of Energy (1998), Letter from George Dials to Mary Kruger, DOE Response to EEG Comments of 12/31/97, dated Feb.24, 1998. Docket A-93-02, IV-G-34.
- Usdowski, E. (1989) Synthesis of dolomite and magnesite at 60°C in the system  $\text{Ca}^{+2}\text{-Mg}^{+2}\text{-CO}_3\text{-2-Cl--H}_2\text{O}$ . *Naturwissenschaften* 76, 374-375.
- Usdowski, E. (1994) Synthesis of dolomite and geochemical implications. In *Dolomites: Volume in Honor of Dolomieu* (B. Purser, M. Tucker, and D. Zenger, Eds.) Special Publication No. 21 of the International Association of Sedimentologists, Blackwell Scientific Publications, Boston.
- Volesky, B. (1990). Removal and recovery of heavy metals by biosorption. In: *Biosorption of Heavy Metals* (B. Volesky, ed). CRC Press, pp. 7-43.
- Volesky, B. (1994). Advances in biosorption of metals: selection of biomass types. *FEMS Microbiol. Rev.* 14:291-302.
- Weiner, R.F. (1996) Oxidation State Distribution in the WIPP. Presentation at Technical Exchange Meeting on June 27, 1996, Sandia National Laboratory, Albuquerque, New Mexico.
- Winogradsky, S. (1949). *Microbiologie du sol, problems et methodes*. Barneoud Freres, France.
- Wood, J.M. and Wang, H.K. (1983). Microbial resistance to heavy metals. *Environ. Sci. Technol.* 17:582-590.